# SV40 CHROMATIN STRUCTURE IN INTACT CELLS AND VIRUS PARTICLES AS PROBED BY PSORALEN PHOTOADDITION

by

Gordon W. Robinson

A DISSERTATION

Presented to the Department of Biochemistry
and the Graduate Division
of the
Oregon Health Sciences University
in partial fulfillment of
the requirements for the degree of

Doctor of Philosophy

March 1983

TABLE OF CONTENTS

LIST OF TABLES

LIST OF FIGURES

Paper 3



Summary and Discussion

Figure

# I. INTRODUCTION AND STATEMENT OF THE PROBLEM

A major impetus to virological research in this decade has been the appreciation that viruses can serve as convenient probes for exploring the complexity of eukaryotic cells. The papovavirus, SV40, isolated in 1960, has proven particularly useful in this regard and has advanced our understanding of cellular replication, transcription and transformation. With its small circular genome capable of encoding only a limited number of proteins, SV40 is heavily dependent upon the host cell for its metabolic functions, and must fulfill them within the constraints of the normal cellular processes. Viral DNA is therefore packaged within a nucleoprotein structure analogous to cellular chromatin, a similarity first recognized in 1975 (1).

When this thesis project was initiated in the Fall of 1978, the entire DNA sequence of SV40 had just been published and molecular information on the organization and expression of the viral genome was rapidly becoming available. SV40 chromatin appeared to be a valuable model system for studying the relationship between chromatin structure and gene expression. In particular, it was of special interest to map the position of nucleosomes in control regions of the viral genome. All of the early investigations along these lines reported a random distribution of nucleosomes with respect to restriction enzyme sites. However, by the end of the year two reports had been published that described a nuclease-sensitive (and thus, possibly nucleosome-free) region of SV40 chromatin located near the viral origin of replication (2, 3).

In our laboratory it had been demonstrated that psoralen derivatives could be employed as probes of the intracellular structure of SV40 chromatin (4). These DNA-photoaffinity agents were capable of discriminating between "linker" and "nucleosomal" regions of DNA and binding preferentially to the former (4, 5, 6). The in vivo nature of the psoralen photoreaction made it seem feasible to probe for the highly accessible region of SV40 chromatin intracellularly, thereby eliminating possible artifacts resulting from cellular and nuclear disruption.

The objectives of this thesis project were:

1. To determine whether the SV40 origin region is preferentially accessible to psoralen photoaddition in vivo.
2. To examine the chromatin structure of various SV40 subpopulations to determine whether they possess structural features (such as an accessible origin) that could be correlated with their biological functions.
3. To develop a technique for locating psoralen adducts on DNA with high resolution (ideally at the level of individual nucleotides) so as to enhance the sensitivity and precision of this approach and to extend its usefulness to in vivo structural analyses of specific regions of cellular chromatin.

# II. LITERATURE REVIEW

## A. Structure and Expression of the SV40 Genome

### 1. Virus Morphology and Life Cycle

Simian Virus 40 (SV40) belongs to a group of very small DNA tumor viruses known as papovaviruses. Other members of this group include the SV40-like polyoma, JC and BK viruses and the larger papilloma viruses. SV40 was originally isolated in 1960 as a contaminant of the Rhesus monkey cell cultures used to produce human poliomyelitis vaccines (7). Intensive study of this virus was stimulated by the discovery soon afterwards that it could induce tumors in newborn hamsters. In cell culture systems SV40 can result in either a lytic infection or cellular transformation. In the former situation, "permissive" cells (such as African Green Monkey Kidney cells) support full SV40 replication leading to the lytic release of infectious virus. In the latter case, "non-permissive" cells (such as mouse 3T3 cells) become stably transformed at a low frequency. These transformants are characterized by the presence of integrated viral DNA and the expression of the viral early gene region (for general reviews of SV40, see references 8-11). Out of this research has come a molecular understanding of many of the events in the viral life cycle and an appreciation that SV40 can serve as a simple model system for investigating eukaryotic control of replication and transcription.

As deduced from electron microscopic analyses, the SV40 "virion" (virus particle) is a roughly spherical particle of about 45 nm in diameter (12). It contains a single covalently closed double stranded DNA molecule of 5.2 kilobases in a nucleoprotein core (described in

detail in section B) composed of viral DNA and cellular histones, which is surrounded by a protein capsid. The capsid contains the principal viral protein VP1, as well as VP2 and VP3, each representing approximately 10% of the virion protein. The presence of a DNA topoisomerase and an endonuclease within the virion has recently been reported (13), but it is not yet known whether these are essential components of the virion. Mature SV40 virions are extremely stable at neutral pH, both at 4° and 37° C, exhibiting little loss in infectivity even in the 2.7M CsCl gradients with which they are purified (14). The importance of disulfide bonds (between VP1 subunits), divalent cations, and pH dependent bonds in maintaining virion integrity is inferred from capsid disruption in the presence of reducing agents, EGTA, and alkaline solutions above pH 10 (15,16).

In a productive infection, SV40 virions adsorb to the cell surface, and a fraction of them are transported by pinocytotic vesicles to the nucleus where they are uncoated (12). In the nucleus, the viral nucleoprotein core directs transcription of the SV40 early mRNAs which code for large (93,000 daltons) and small (17,000 daltons) viral tumor antigens (T and t-antigen, respectively). The large T-antigen is thought to be responsible for inducing the synthesis of histones and enzymes of DNA metabolism which are cellularly encoded but required in viral replication. Both large and small tumor antigens are thought to play a role in cell transformation. Approximately 18 hrs post-infection, viral DNA synthesis commences and concomitantly, late mRNAs coding for the capsid proteins and the agnoprotein (8,000 daltons) (17) begin to appear in the cytoplasm. The multifunctional large T-antigen is directly involved in initiating SV40 DNA replication and in

promoting the switch from the early to the late transcriptional pattern (described in a later section). From this point until the cell is killed and virus is released approximately three days later, newly synthesized nucleoprotein cores and capsid proteins continue to be assembled in the nucleus of the infected cell (described in section B). Because SV40 replication is not under normal cell cycle control, enormous quantities of virus are produced (approximately $10^5$ particles per cell) resulting in amounts of viral and cellular DNA that are equivalent by the time the cell lyses. The onsets of the viral metabolic processes described above are highly asynchronous in lytic infections of cultured cells. Thus, at most times during an infection, a mixture of transcription, replication, and encapsidation intermediates are present. This poses a major difficulty for the analysis of these events in the viral life cycle.

2. Structure and Replication of the SV40 Genome

The SV40 genome is a circular DNA molecule of 5243 bp (virus strain 776) that has been completely sequenced (18) and of which detailed restriction maps are now available. Numerous genetic studies have utilized temperature-sensitive and deletion mutants to precisely characterize initiation, processing, and termination sites for all viral transcripts, the viral protein coding regions, putative transcriptional control elements, and the single origin for DNA replication (8). As depicted in Figure 1, the minimal SV40 origin (85 bp) is placed at the top of the genetic map, (Bgl I site, 0.66 map units) so that the early transcriptional region extends from it in a counterclockwise direction and the late transcriptional region extends from it in a clockwise direction, with both regions terminating near the Bam HI site. Hence,

Figure 1. Genetic Organization of the SV40 Genome

The major structural features of the SV40 genome are indicated with respect to SV40 map units, which begin at the Eco RI site (0/1). Additional reference points include the six Hind III recognition sites (shaded innermost circle) and single sites for Bgl I, Kpn I, and Bam HI. Indicated on the circular genome map are the 5' and 3' ends of early (small t- and large T- antigens) and late (agnoprotein and capsid proteins VP1, VP2, and VP3) mRNAs, the protein coding regions of these mRNAs (open arrows), and the intervening sequences (dotted lines) which are spliced out of mRNAs. Early and late transcription proceed on different DNA strands in counterclockwise and clockwise directions, respectively. A 420bp region (0.64 to 0.72 map units) around the origin of DNA replication has been expanded to show the limits of the SV40 origin, the early gene TATA box, the 21bp and 72bp repeated sequences, the three T-antigen binding sites (I, II, and III), and the major initiation sites for the 5' ends of early (E) and late (L) mRNA transcripts (adapted from reference 8).

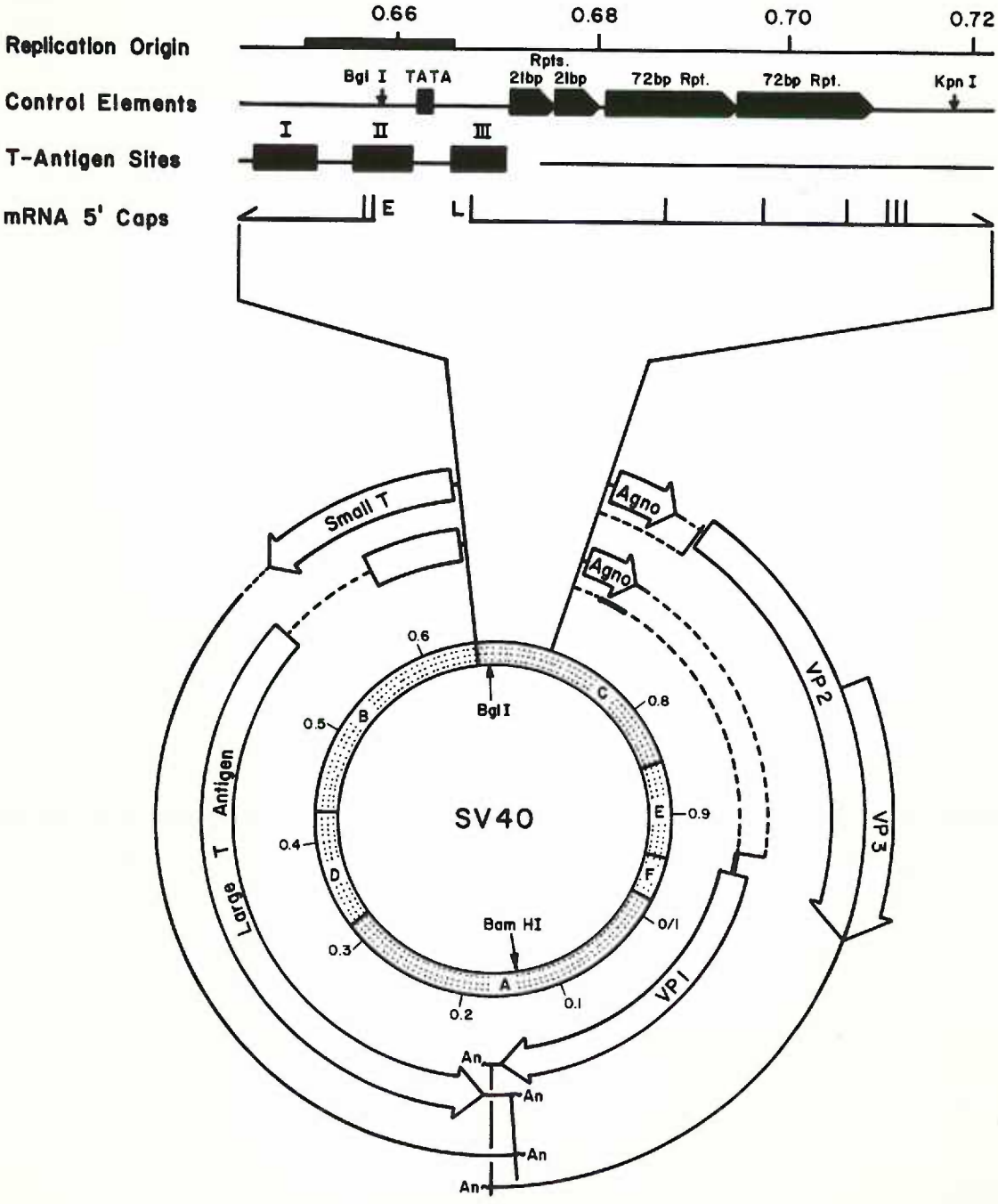
0.66
0.68
0.70
0.72
Replication Origin
Bgl I
TATA
Rpts.
21bp 21bp
72bp Rpt.
72bp Rpt.
Kpn I
Control Elements
I
II
III
T-Antigen Sites
mRNA 5' Caps
E
L
Small T
Agno
Agno
VP2
VP3
VP1
Large T Antigen
SV40
Bgl I
Bam HI
A
B
C
D
E
F
0.1
0.2
0.3
0.4
0.5
0.6
0.8
0.9
0/1
An
An
An
An

different strands of the DNA are used for the transcription of early and late genes. Immediately to the late side of the replication origin lie two tandemly repeated sequence elements of 21bp and 72bp which code for no proteins but appear to be involved in transcriptional control (discussed in the next section).

SV40 DNA replication is carried out in nearly the same fashion as that of cell DNA replication, because SV40 borrows the necessary cellular enzymes (for reviews see 9, 19). However, the initiation of SV40 replication requires the viral large T-antigen in addition to cellular factors, and replication, once initiated at the viral origin, takes longer to complete (15-20 min) than expected on the basis of size. This is presumably due to the topological constraints of replicating a closed circle. Although T-antigen binding to sites within the SV40 origin is essential for the initiation of replication, its presence is not required during the elongation phase of replication (20). Evidence for T-antigen binding is both biochemical and genetic. In vitro, purified T-antigen binds three tandem sequences (I, II, and III, Figure 1) within the SV40 origin of replication in a graded fashion and protects them from DNase I digestion or dimethyl sulfate modification (21). At the non-permissive temperature, SV40 mutants that make temperature-sensitive (ts) T-antigens are defective in DNA replication in vivo (20), and in vitro these mutant T-antigens fail to bind origin DNA at high temperatures (22). Exactly what function T-antigen serves at the origin is unclear. However, T-antigen does possess ATPase activity (23), and may have topoisomerase (24, 25) or proteolytic activity (26), any of which might be involved in "activating" the SV40 origin. DNA synthesis proceeds around the SV40 circle bidirectionally using the

cellular DNA polymerase alpha (27). As in the cell, replication is semiconservative, with the leading DNA strand synthesized continuously (5' to 3' polymerization and growth) while the lagging strand is synthesized discontinuously (5' to 3' polymerization with growth in the 3' to 5' direction) by joining of short RNA-primed Okazaki fragments (19). Replication is terminated when the two replication forks meet, usually about 180° from the origin of replication. Separation of the daughter molecules is a slow, and possibly multistep procedure (28).

3. Viral Transcription and its Regulation

SV40 has been studied extensively with the belief that it provides a simple model of cellular transcription and its control. In spite of its small size, however, a complex picture of viral transcription has gradually unfolded (for reviews see 8, 29). The amounts and types of mRNA vary markedly with time following infection. At early times (up to 18 hours post-infection) only 0.01-0.06% of the cellular RNA is virus specific, whereas by 40 to 96 hours viral RNA has increased 300-1000 fold due at least in part to the enormous increase in the number of SV40 transcriptional templates that result from viral DNA replication. A qualitative difference is also observed at the two times. Early in infection most of the viral mRNA comes from the "early" strand and codes for the two T-antigens, while at late times, 95% of viral mRNA comes from the opposite strand and codes for capsid proteins. This transcriptional switch is thought to occur at the level of initiation and is temporally linked to the onset of DNA replication.

A model for SV40 transcriptional control has been proposed that assigns a central role to large T-antigen (30, 31). Cells infected at restrictive temperature with a ts T-antigen mutant overproduce early

mRNA (relative to permissive temperature), fail to initiate DNA replication, and do not synthesize late mRNA (20, 31, 32). Based on these observations as well as in vitro experiments (33, 34), T-antigen is believed to be a feedback inhibitor, regulating its own synthesis as well as that of viral DNA synthesis. Thus, when levels of functional T-antigen reach a certain intranuclear concentration, early transcription is inhibited, as a result of T-antigen binding at multiple origin sites. This model strongly resembles the situation in bacteriophage λ, in which CI repressor protein regulates its own transcription by binding to three tandem sites within the right operator region (35).

Although in general, recent work with SV40 has supported the above model, two additional transcriptional control mechanisms may be operating. Evidence for selective degradation of nuclear RNA comes from the finding that early in infection a significant amount of nuclear RNA (detected by short pulse-labeling) is synthesized from the late strand but is rapidly degraded and never used as mRNA (36). In contrast to this early situation, at late times of infection selective degradation of RNA does not occur. No satisfactory explanation for this phenomenon is available. Support for a switch in the transcriptional pattern mediated by an alteration of the transcriptional template during replication comes from several studies (32, 37). First there is the timing of the two events; late mRNA starts to appear only after DNA replication has begun. As mentioned earlier this could be explained if bound T-antigen regulates both events. However, in experiments using temperature-sensitive T-antigen the ratio of early/late transcripts did not revert to the early infection pattern following a shift-up in

temperature at late times (32). Thus barring a change in the specificity of the RNA polymerase late in infection (to date none has been reported), there appear to be template changes occurring, probably at the time of replication, which affect the efficiency of transcription of the early and late strands. The nature of possible template changes will be discussed in section B.

The RNA transcripts that encode both the early and the late proteins have been mapped to multiple 5'-initiation sites within a 370bp region near the replication origin (early, 0.66 map units; late, 0.66-0.72 map units) (8). These viral transcripts are also synthesized as large (half or full genome length) RNAs that are subsequently processed (spliced) and polyadenylated. Early transcripts can be spliced to give either small t-antigen or large T-antigen mRNA (38). The splicing pattern for late transcripts is more complex due to the greater number of initiation sites and proteins coded within this region.

The transcriptional promoters of SV40 have been localized to the non-coding regions near the origin of replication and include a Hogness-Goldberg or "TATA" box between T-antigen binding sites II and III. From work with numerous eukaryotic genes a "TATA" box sequence has been shown to fix the site of RNA initiation to approximately 20-30 nucleotides downstream from this sequence (39). Experimentation with SV40 has proven that its "TATA" box serves in this capacity for early mRNAs in vitro and in vivo (40, 41, 42). An analogous "TATA" box for the SV40 late mRNAs was considered absent, but very recent work has identified a "TACCTAA" box 20-30 nucleotides upstream from a major initiation site that appears to fulfill the same function (43). Similar

non-canonical "TATA" boxes may direct transcription from the many other initiation sites observed late in infection.

An additional regulatory sequence 120bp upstream from the early SV40 "TATA" box is indispensable for early transcription in vivo but not in vitro (44, 45). Remarkable experiments with the SV40 "72bp repeat" sequences have demonstrated that they are cis-acting components of the early promoter capable of functioning in an orientation independent manner and acting at distances up to 3000bp away from the "TATA" box (46, 47). A single copy of this repeat is sufficient for the transcriptional "enhancer" function (45) which is not specific for SV40 genes since an effect is observed after linkage of the repeat to many eukaryotic genes (46, 47). Since their discovery in 1981, other genetic elements that functionally replace the "72bp repeats" have been identified and include a 73bp repeat from the long terminal repeat (LTR) of Moloney murine sarcoma virus (48), a 60bp fragment from bovine papilloma virus (49), and a 244bp sequence from polyoma virus (50). Surprisingly, these elements bear little sequence homology to the "72bp repeats" except for a 16bp segment. Sequences more than 100 bases upstream from the initiation sites of sea urchin histone H2a and herpes simplex virus II thymidine kinase are also critical in regulating transcriptional efficiency in vivo and may possess analogous "enhancer" elements (51, 52). Explanations to account for the "72bp repeat" activity are speculative at this point. They include site specific topoisomerases (thereby creating negative supertwists) and binding of RNA polymerase II in a preliminary fashion, followed by migration to the actual promotor. This region may also be involved in dictating a special nucleoprotein structure in vivo. Finally, it may be significant

for SV40 transcriptional control that the T-antigen binding sites lie between the "72bp repeats" and the initiation sites for early transcription (30).

In contrast to the wealth of information available on the early SV40 promoter, very little is known regarding the late promoter. A recent report of work with SV40 deletion mutants has suggested that the "72bp repeats" are unnecessary whereas the immediately adjacent "21bp repeats" are critical for efficient late transcription in vivo (53).

## B. SV40 Minichromatin

### 1. Viral Nucleoprotein Structure

The DNA of all eukaryotes is packaged by association with nuclear proteins into a complex structure known as chromatin (see reviews 54-57). This structure consists of many superimposed levels of nucleoprotein organization, all of which play a role in condensing the DNA in the nucleus. The best understood of these levels is that of the basic 10nm chromatin fiber, within which the length of DNA is condensed 6 or 7 fold. Under the electron microscope this fiber appears as a repeating pattern of "beads" or nucleosomes arrayed on a DNA string (58, 59) (see Figure 2). Each nucleosome is thought to consist of a core particle composed of two molecules each of the histones H2a, H2b, H3 and H4, around which 146 bp of DNA is wound in two superhelical turns. Evidence from micrococcal nuclease digestion indicates that nucleosomes are connected by interbead or "linker" regions of DNA that vary in length depending upon the source of the chromatin but average 30 to 60bp (60). Thus, the repeat length of most 10nm fibers is about 200bp. Histone H1 (H5 in avians) is found at half the molar ratio of the other

Figure 2. The 10nm Fiber of SV40 Chromatin

SV40 chromatin extracted from infected cell nuclei was purified on sucrose gradients, then spread for dark-field electron microscopy. Nucleosomes, a linker region, and a 200bp repeat unit are indicated (taken from reference 96).

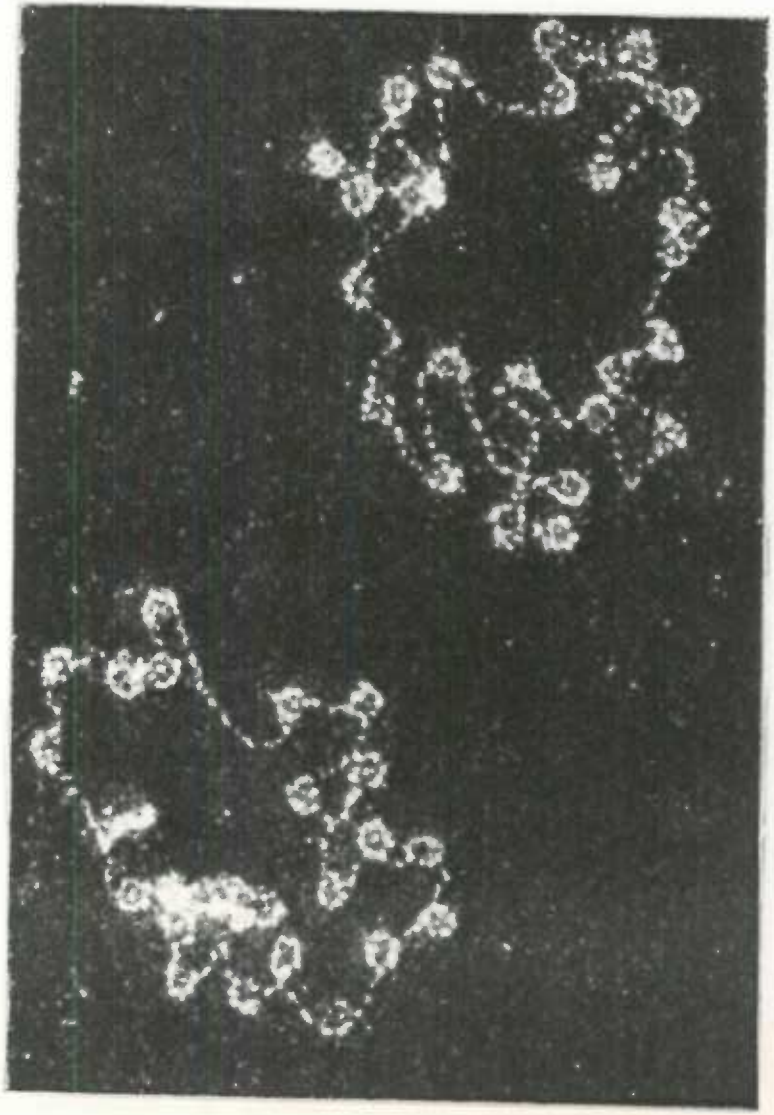

← LINKER DNA

← NUCLEOSOMES

⌐¬ REPEAT UNIT

histones and is thought to play a role in condensing 10nm chromatin fibers into fibers 30nm in diameter (61, 62). The thicker fiber represents the second level of chromatin organization and results in a net DNA compression of approximately 25 fold, close to that found in interphase chromatin (63). Limited digestions with micrococcal nuclease have demonstrated that histone H1 is associated with and protects 20 bp of linker DNA at the sites where the DNA enters and leaves the nucleosome (64-66) (see Figure 3). The binding of H1 to DNA is less stable than that of the core histones since H1 can be displaced from chromatin by extensive nuclease digestion or by 0.6M NaCl (whereas the other histones require at least 1.2M salt before dissociation occurs). In addition to its role in chromatin condensation, H1 also appears to stabilize the nucleosome repeat length of 200bp by preventing the nucleosomes from sliding along the DNA (67). Two models for nucleosome folding in the 30nm fiber have been proposed (57). In the first model, H1 interactions are envisioned to lead to clustering of adjacent nucleosomes into large globular arrays or "superbeads" that are packed in tandem to form the thick fiber. In a second model, similar H1 interactions are proposed to stabilize a regular helical solenoid in which there are six nucleosomes per turn. This model appears to fit the available data better than the superbead model but many of the detailed features of the solenoid model are still undergoing revision. Both superbead and solenoid-type chromatin structures are observed in the electron microscope following gentle lysis of nuclei.

The intracellular nucleoprotein complexes of SV40 strongly resemble cellular chromatin. Under conditions where histone H1 is dissociated, SV40 chromatin or "minichromatin" appears as a ring of viral DNA, with

Figure 3. Helical Solenoid Model of Nucleosome Packaging in the 30nm Chromatin Fiber.

In the absence of histone H1 no ordered structures are formed. Once H1 is bound, nucleosomes assume a zig-zag (lower portion of diagram) arrangement as a result of the DNA entering and leaving at sites close together on the same side of the nucleosome. It is postulated that this zig-zag structure further condenses and eventually forms a helical solenoid with about six nucleosomes per turn. Details of histone H1 interactions are not specified in this model taken from Kornberg, R. D. and Klug, A. (Sci. Am. 244, 52-64, 1982).

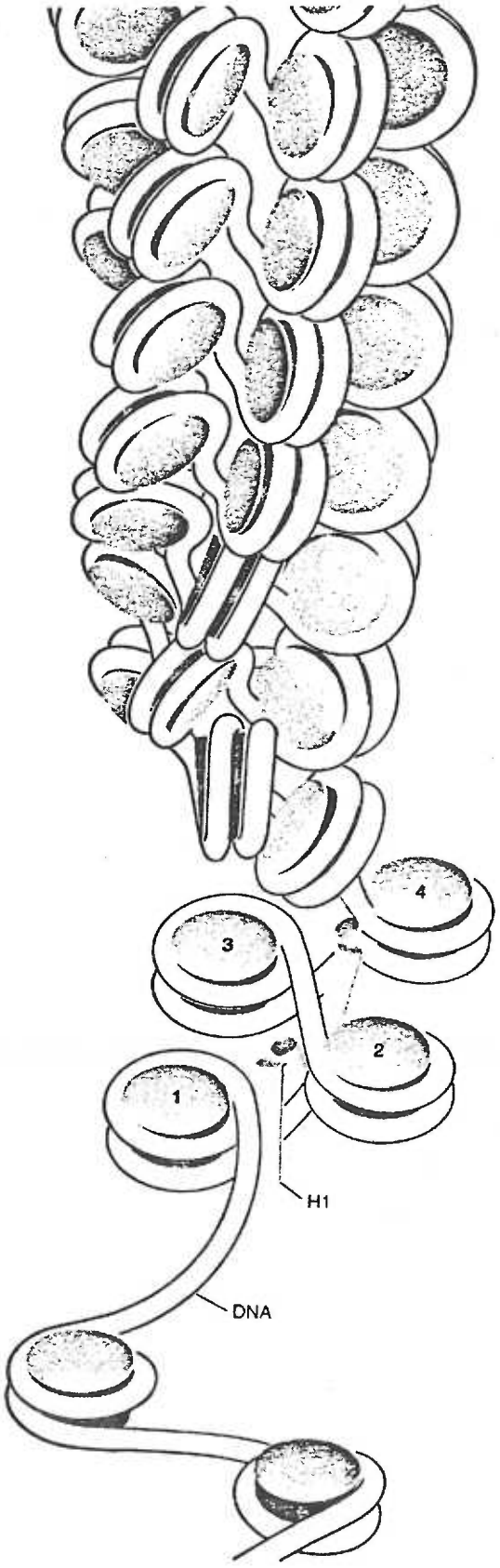
4
3
2
1
H1
DNA

22-26 nucleosomes bound to it (1, 68). These nucleosomes are composed of histones made by the host cell and are thought to be identical to nucleosomes from host chromatin. Similarly viral linker regions average about the same size as host cell linker regions. When minichromatin is extracted under conditions where the complex retains histone H1, its conformation is that of a chromatin superbead (62, 69). A solenoid conformation may not be possible with small circular DNA. Because SV40 chromatin is already completely compact at the superbead stage no higher levels of chromatin condensation are possible. By contrast, in cellular chromatin, the extent of DNA condensation has been estimated to be 5000 fold in metaphase cells (70). Viral chromatin structure is maintained throughout the SV40 life cycle, and free viral DNA has not been detected intracellularly; thus these complexes are thought to function as the templates for early and late transcription, DNA replication and virion assembly.

2. Functional Minichromatin Complexes

Starting at approximately 24hrs post-infection virions are assembled by the gradual deposition of capsid proteins onto minichromatin molecules. Although the exact order of addition of the three capsid proteins is not known, pulse-chase experiments have shown that labeled DNA passes from mature minichromatin (75S) into heterogeneous pre-virion particles (180-240s) and finally into mature virions (250s) (71, 72) (see Figure 4). Several important changes in the viral chromatin take place during this 4-5 hr process. First, along with the addition of VP1 and VP3 (73) there is a gradual increase in acetylation of histones H3 and H4 (74, 75). Then in the transition from immature to mature virus, histone H1 is displaced (or degraded), VP2 is

Figure 4. Schematic Representation of SV40 Chromatin Complexes during the Lytic Cycle.

Viral minichromosomes are represented by a string of beads (nucleosomes). Previrion and virion complexes are represented by icosahedral particles. Typical sedimentation values (s) are given for each type of nucleoprotein complex (adapted from reference 19).

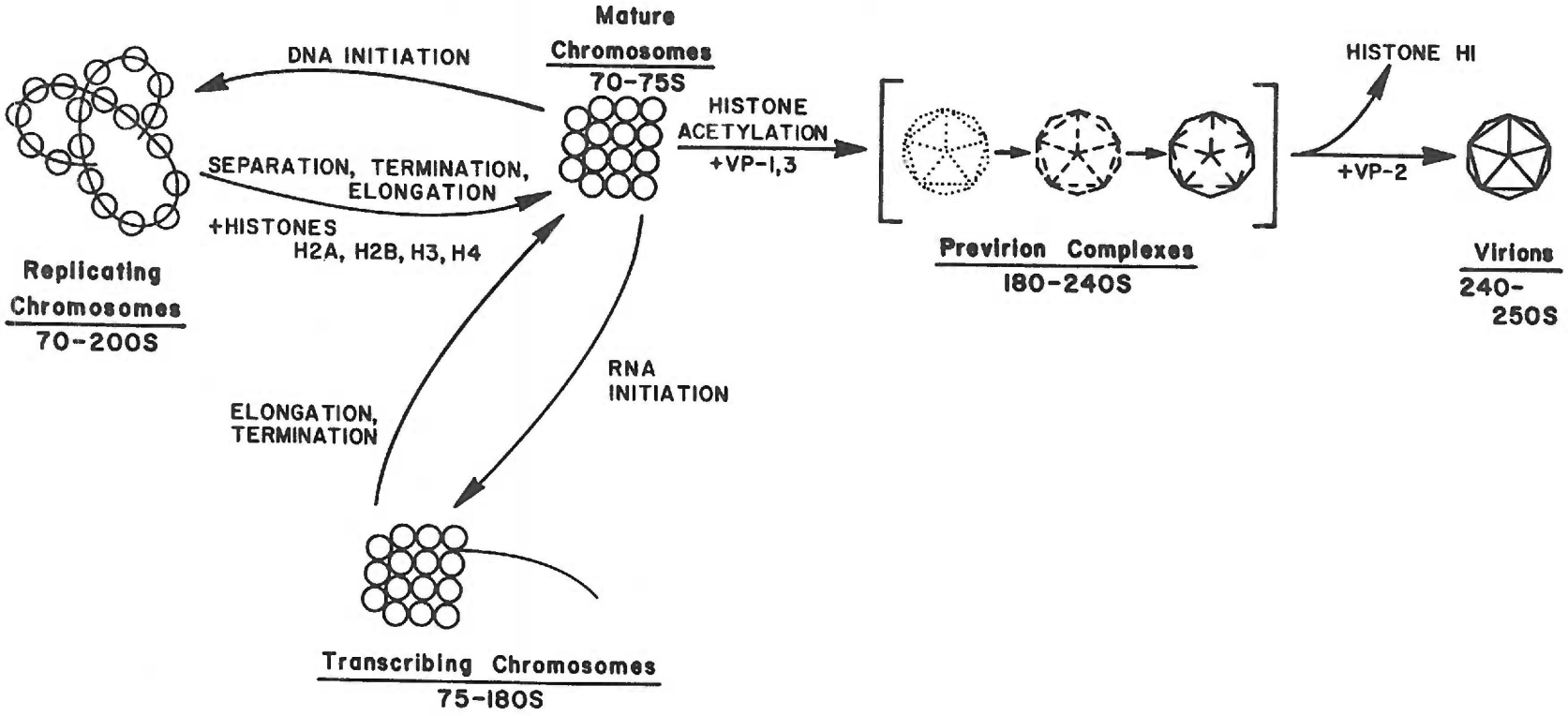
Mature
Chromosomes
70-75S
DNA INITIATION
HISTONE
ACETYLATION
+VP-1,3
HISTONE HI
+VP-2
SEPARATION, TERMINATION,
ELONGATION
+HISTONES
H2A, H2B, H3, H4
Replicating
Chromosomes
70-200S
Previrion Complexes
180-240S
Virions
240-
250S
RNA
INITIATION
ELONGATION,
TERMINATION
Transcribing Chromosomes
75-180S

bound and a final maturation process takes place (71, 75). Neither large nor small T-antigens are packaged inside virions nor are they required for the virion assembly process. At some point during the latter stages of virion maturation, the minichromatin structure of this complex undergoes a poorly understood conformational alteration. This alteration has been probed by treatment of the virion chromatin with various enzymes following gentle dissociation of the virion capsid in vitro. An "open" conformation of this chromatin was inferred from its increased sensitivity to nucleases and its high template efficiency for transcription with exogenous RNA polymerase (E. coli) (15, 76). Experiments that used saturating levels of psoralen photoaddition to measure the chromatin conformation within intact virions (this thesis) substantiated these findings. This special structure of virion chromatin may aid the virus in establishing a new infection.

SV40 transcriptional complexes have been isolated by a number of procedures that rely upon selective extraction of SV40 chromosomes from isolated nuclei. These complexes are heterogeneous, represent about 1% of the total SV40 chromatin, and sediment more rapidly on sucrose gradients than bulk chromatin. They have been found to contain cellular histones, RNA polymerase II and short lengths of nascent RNA which can be extended in vitro (77, 78). Sedimentation velocity experiments and direct electron microscopy have confirmed that these complexes possess a compact minichromatin structure (78). Very few biochemical studies of transcriptional complexes have been carried out due to the rather low purity of these preparations. However, it has been shown that SV40 chromatin structure can strongly influence the specificity of RNA synthesis initiated by E. coli RNA polymerase (79). In the presence of

α-amanitin (which inhibits eukaryotic RNA pol II) the E. coli enzyme preferentially transcribed late SV40 RNA from a late minichromatin template whereas exclusively early RNA was synthesized from a purified SV40 DNA template. Nucleosomes, tightly bound factors or bound T-antigen may have mediated the specificity shift observed with the minichromatin. No analogous experiments to test the specificity of the E. coli enzyme on early minichromatin templates have been reported.

Replicating SV40 chromatin complexes have been isolated by extraction procedures similar to those used for transcriptional complexes. They also represent about 1% of bulk minichromatin late in infection, sediment heterogeneously on sucrose gradients and appear to possess the normal minichromatin structure, as determined by electron microscopy. These complexes are associated with much higher levels of T-antigen than are bulk, non-replicating molecules (80, 81).

Studies of replicating minichromatin in isolated nuclei (reviewed in 19, 55) have demonstrated that DNA replication and nucleosome assembly are closely synchronized, so that nucleosome-free regions of DNA exist only transiently. During SV40 replication parental (old) nucleosomes are segregated semiconservatively to the two daughter DNA strands, so that only the DNA strand replicating in a continuous fashion (5' to 3' growth) receives parental nucleosomes; the other strand receives newly synthesized nucleosomes (82). Because SV40 replication proceeds bidirectionally from its origin, both daughter DNA molecules will receive half new and half old nucleosomes and will be mirror isomers with respect to the placement of new (or old) nucleosomes in the early (or late) transcriptional region. Thus, a transcriptional switch (early to late) could be mediated by DNA replication if new nucleosomes

were different from old ones in some way. Specific nucleosome changes that have been suggested to affect eukaryotic transcription include biochemical alterations such as histone phosphorylation or acetylation (83) and association with HMG proteins 14 and 17 (84), or positional alterations that change the alignment of nucleosomes with respect to transcriptional promoters (described in the next section).

3. Nucleosome Positioning

One of the most intriguing questions in eukaryotic gene expression concerns the relationship between chromatin structure and gene control. In certain well-documented cases it appears that the extent of DNA condensation plays a role in regulating transcription (85). For instance at the electron microscopic level, there appears to be an association between highly condensed chromatin (as in heterochromatin) and transcriptional inactivity. In an opposite situation the highly active ribosomal RNA genes of Xenopus and Drosophila show very low packaging ratios. However, these cases may not be representative of most eukaryotic transcriptional units.

As a first step it would be valuable to know whether the basic nucleosomal packaging of DNA serves simply as a means of DNA condensation, or whether differential function can be expressed through this structure. In systems where this question has been addressed, study has focussed on the possibility of nucleosome "positioning" (see reviews 57, 86). "Positioning," or "phasing" as it is sometimes termed, refers to specific placement of nucleosomes with respect to underlying DNA sequence such that certain sequences are always in either core or linker locations. The importance of such an arrangement within the cell would be that of placing effector sites for regulatory proteins in

"closed" or "open" positions respectively. Until the development of the indirect end-labeling technique (discussed in the next section) it was only feasible to test this hypothesis for 5S or tRNA genes which are present in some cells as long tandem repeats, or for the SV40 genome which is present in many episomal copies.

SV40 chromosomes were an early favorite for these studies because intact minichromatin could be isolated and because the positions of nucleosomes could be determined with respect to a defined DNA sequence. From 1976 to 1978 several investigators tested the hypothesis of random nucleosome placement on SV40 by digesting virion-derived (88, 89) or intracellular (3, 87, 89-92) minichromatin with restriction enzymes known to cut SV40 DNA at one or very few sites. By determining a cutting frequency for each enzyme recognition site, an assessment of the relative accessibility at each site was possible. These experiments showed that no site was 100% accessible (in linker region) on all minichromatin molecules. In fact, many of these studies showed that at all sites the accessibility was at most 20-30%, consistent with a random positioning of linker regions, and hence nucleosomes (87-90, 92).

However, investigators who employed restriction enzymes with recognition sites near the replication origin (0.66 map units) found much higher (2 to 4 fold) cutting frequencies with these enzymes (3, 91). Limited digestions with endonucleases lacking strong site specificity on naked SV40 DNA were then employed to map the accessibility of SV40 chromatin in greater detail. Both micrococcal nuclease (93) and a nuclease endogenous to monkey cells (2, 94) cleaved one third of the minichromatin molecules at a single site. From 30 (93, 2) to 100% (94) of these cleavages were made at the SV40 origin region

(approximately 0.65-0.74; see Figure 5 for exact map coordinates). These findings suggested that precise nucleosome positioning on SV40 DNA might be restricted to a small region of the genome and be present on only a fraction of minichromatin molecules. Electron microscopic studies subsequently detected a "nucleosome-free" region of DNA that was 320bp (95) or 250bp (96) long on 20-25% of the minichromatin molecules extracted at late times of infection. By the combined use of restriction enzymes and electron microscopy this region was determined to extend from the origin of replication into the late transcriptional region, in good agreement with the nuclease digestion studies.

Although the accumulated evidence of electron microscopy and nuclease digestion was strong, serious artifacts were possible with both these techniques. Micrococcal nuclease was shown to have stronger DNA sequence specificity than originally believed resulting in cleavage of some linker regions more frequently than others (97, 98). There was also the possibility of nucleosome sliding or displacement during the minichromatin isolation procedures required for both of these approaches (99). Substantiation of the findings discussed above came from concurrent experimentation with two linker region-specific DNA-binding agents, N-acetoxy-acetylaminofluorene (N-AAAF) (100) and psoralen (this thesis), both of which identified the SV40 origin region as highly accessible within intact cells.

As mentioned earlier, positioning of nucleosomes has also been investigated for tandemly repeated tRNA and 5s RNA genes. This has been done by digesting chromatin with micrococcal nuclease to degrade linker regions, and subsequently digesting the purified DNA with restriction enzymes to map protected regions to specific DNA sequences. The genes

Figure 5. Map Coordinates of the "Open Region" of SV40 Chromatin Determined by Different Methods

The upper half of this figure depicts the SV40 replication origin, the control elements, and the 5'-mRNA cap sites as in Figure 1. The region from 0.64 to 0.74 map units spans 524bp. The lower half of this figure is a composite of results from SV40 chromatin mapping studies in which as "open region" was detected. The position and extent of this region is indicated for the first eight studies with brackets. For the three remaining studies, the approximate positions of major and minor nuclease hypersensitive sites, early (E) or late (L) in infection, are indicated with arrows.

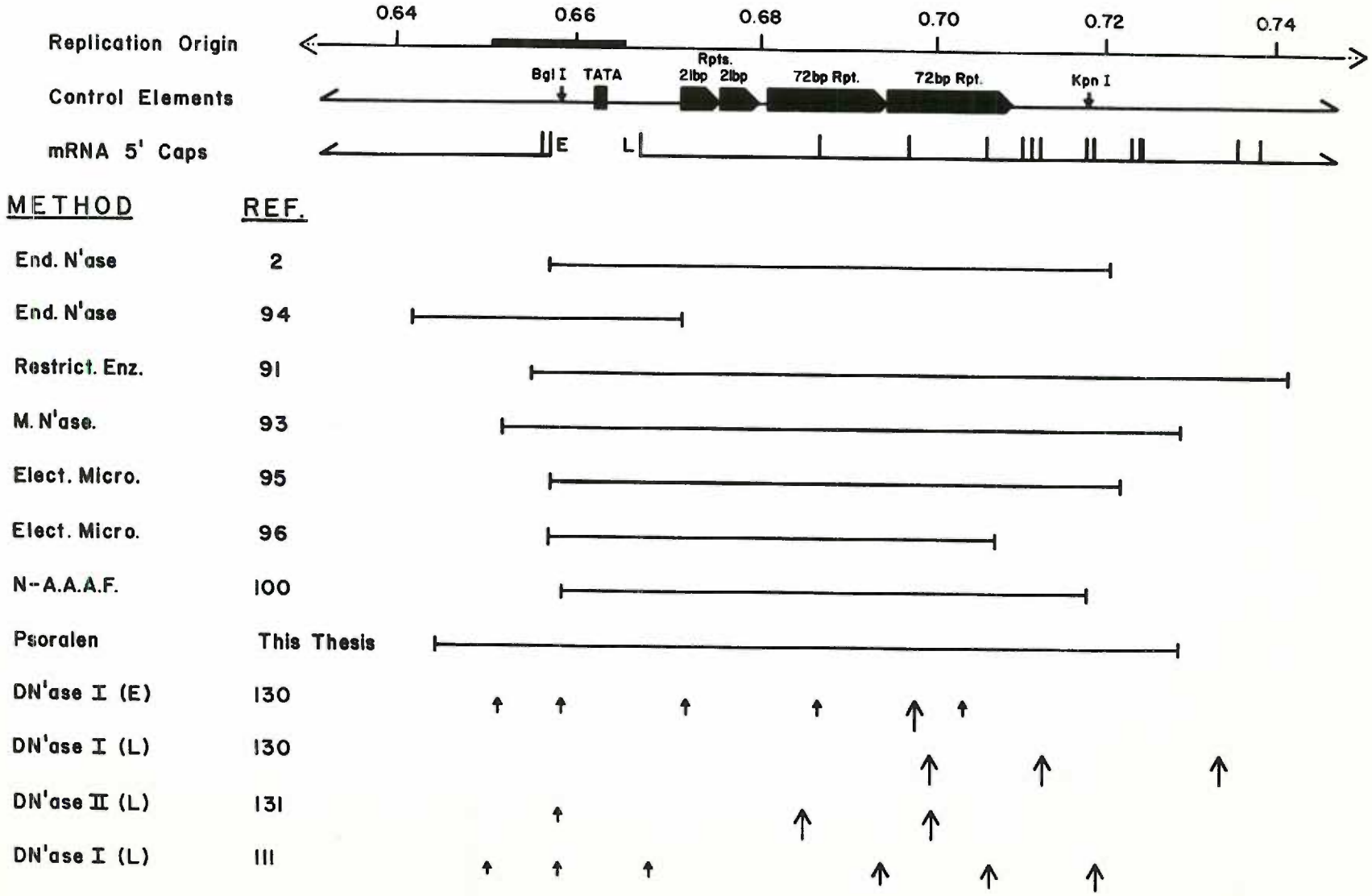
0.64
0.66
0.68
0.70
0.72
0.74
Replication Origin
Bgl I
TATA
Rpts.
21bp
21bp
72bp Rpt.
72bp Rpt.
Kpn I
Control Elements
mRNA 5' Caps
E
L
METHOD
REF.
End. N'ase
2
End. N'ase
94
Restrict. Enz.
91
M. N'ase.
93
Elect. Micro.
95
Elect. Micro.
96
N-A.A.A.F.
100
Psoralen
This Thesis
DN'ase I (E)
130
DN'ase I (L)
130
DN'ase II (L)
131
DN'ase I (L)
111

of interest were located on gels by blotting with labeled probes. No large nucleosome-free regions of these genes were identified. Several studies have suggested that a subset of the total 5s RNA genes have nucleosomes that are precisely positioned so as to expose a potential regulatory sequence (101, 102). However these findings and similar ones with the tRNA genes (103) need to be confirmed by independent methods, given the possibility of strong sequence specificity with micrococcal nuclease digestion (97, 98).

A major question regarding the nucleosome-free region of SV40 concerns the mechanism that dictates it. Experiments with SV40 insertion mutants that contain a duplication of sequences from 0.66 to 0.716 map units have shown that the DNA sequence of this region is partly responsible for this peculiar chromatin structure. These studies used endogenous nuclease or electron microscopy to show that a nucleosome-free region can form at either the original or inserted origin (104, 105). Several theories to explain this finding have been proposed and include: a) features of the DNA sequence itself preclude formation of nucleosomes, or b) proteins associated with this region prevent or shift the location of nucleosome binding. When the first theory was tested by in vitro reconstitution of SV40 chromatin, only slight sequence specificity for nucleosome formation was detected (106-108). Other in vitro work has demonstrated that almost any synthetic or natural double stranded DNA can be packaged into chromatin; exceptions are poly dA:poly dT DNA and left-handed helical DNA (Z-DNA) (109, 110). The second theory appears more attractive both because of the above results and because the nucleosome-free region spans the known T-antigen binding sites, the replication origin and the transcriptional

control sequences of SV40. Experiments employing a ts T-antigen mutant have shown that both before and after raising the temperature the origin region was preferentially nuclease sensitive, thus bound T-antigen is not required to maintain this "open region" (111). Other investigators, in attempts to pinpoint the genesis of the "open region" molecules, studied replicating SV40 chromatin by electron microscopy and restriction enzyme digestion. They reported that newly synthesized minichromatin was not enriched in molecules with a nucleosome-free region (112). It was also possible that "open region" molecules were preferred templates for, or the consequence of, partial encapsidation into virions. For this reason the minichromatin structure of disrupted virions was analyzed by limited nuclease digestion. This analysis showed that the nucleosome-free region was lost or altered during encapsidation or during disruption (113). Experiments involving psoralen photoaddition to intact virions (this thesis) convincingly demonstrated that the "open region" was lost during encapsidation. In summary, the 300-400bp nucleosome-free region on SV40 chromatin appears to be at least indirectly dictated by the DNA sequence of this region but the sequence per se does not preclude histone binding.

4. DNase I Sensitivity

Significant advances in the understanding of active chromatin structure have come about through the use of DNase I, a relatively nonspecific endonuclease that makes double-stranded cuts at accessible regions of DNA (for reviews of this subject see references 57, 63, 114). Unlike micrococcal nuclease which recognizes all chromatin linker regions with approximately equal efficiency, DNase I appears to recognize a hierarchy of different accessible regions (ranked as:

insensitive (bulk), intermediate, sensitive and hypersensitive) with efficiencies ranging over several orders of magnitude.

The special recognition properties of DNase I were first demonstrated by Weintraub and his colleagues who showed in 1976 that the globin gene of chick erythrocyte nuclei was preferentially sensitive (10X over bulk DNA) to digestion with DNase I (115). This effect was tissue-specific since the globin gene was not preferentially digested in the chick oviduct. Much additional work has since demonstrated that DNase I sensitivity is associated with transcribed or potentially transcribed regions and is maintained in part by the tight binding of HMG proteins 14 and 17 (84, 116) to the nucleosomes of these regions. Surrounding these DNase I sensitive regions and sometimes extending many kilobases to either side are tracts of chromatin that are intermediately sensitive (2-5X over bulk) to DNase I (117). Although micrococcal nuclease does not preferentially degrade potentially active genes to acid solubility (115, 118), it does appear to recognize some feature of genes undergoing transcription, since these sequences are more rapidly degraded to mononucleosome-sized fragments (146-185bp) than are bulk DNA sequences (118).

In 1980, a new class of DNase I sensitivity, termed hypersensitivity (100X over bulk), was identified by the use of a powerful mapping technique. The indirect end-labeling technique (119, 120), in contrast to the earlier hybridization analyses, permitted the location of individual DNase I cleavage sites in chromatin to be mapped with great accuracy (± 50bp). DNAse I hypersensitive sites were initially observed when gel-blot hydridization (Southern analysis) was used to examine the bands produced by very light DNase I digestion of

Drosophila nuclei (120, 121). DNA purified from the digested chromatin was redigested with a restriction enzyme. The DNA fragments were then separated on a gel, transferred to nitrocellulose, and hybridized to a short, $^{32}$P-labeled cloned fragment which abuts the restriction site. As a result of this procedure, the size of the visualized fragments define the distance from the recognition site to the site cut by DNase I in nuclei. Surprisingly, even very light digestion with DNase I gave rise to prominent bands which were indicative of very specific cleavage sites in chromatin. These DNase I hypersensitive sites were shown to map predominantly at or near the 5' end of transcription units and to consist of a stretch of 100-200 sensitive nucleotides (121-123). Further experimentation has generalized this finding to many genes from Drosophila, rat, chicken and yeast cells. These sites sometimes appear before the onset of transcription, persist after it is finished and can be transmitted vertically during replication (124-126). Like other biochemical alterations that have been associated with transciptionally active genes, such as hypomethylated CpG sequences in DNA (127, 128) and hyperacetylated histones H3 and H4 (83,129), 5' DNase I hypersensitive sites appear to be necessary but not sufficient for transcription (63,114). Finally, because they are detectable within chromatin but not on purified DNA, hypersensitive sites are thought to reflect chromatin packaging which leaves certain regions of DNA exposed or in highly accessible conformations (e.g. SS-DNA, Z-DNA).

Low resolution mapping of SV40 chromatin with DNase I was carried out in 1978 before the discovery of DNase I hypersensitivity, and was used to confirm the location and size of the accessible region at the SV40 origin (2). In a later study SV40 hypersensitive sites within

nuclei were precisely mapped by indirect end-labeling and changes in the number and location of these sites were correlated with the shift from early to late transcription. Thus, at early times one major site (within the 72bp repeats) and several minor sites (closer to the Bgl I site) were detected, whereas at late times two additional major sites appeared (close to the original one) and the minor sites disappeared (130) (see Figure 5). Another investigation confirmed the three major sites at late times but in addition detected three minor sites (near the Bgl I site) (111). This study further demonstrated that the hypersensitive sites were not dependent upon bound HMG proteins 14 and 17, T-antigen, or viral capsid proteins. A third group has reported that the nuclease DNase II also recognizes unique features of this region and cuts once within each 72bp repeat late in infection (131).

Taken together, these findings suggest that DNase I hypersensitive sites on SV40 chromatin include a major transcriptional control element of the virus, the 72bp repeats. Furthermore, if the SV40 findings can be generalized, some of the 5' DNase I hypersensitive sequences of other eukaryotes may represent similar promoter elements that are maintained in nucleosome-free conformations. As mentioned earlier, work with the herpes simplex virus thymidine kinase gene has demonstrated that a region 100 bp upstream from its "TATA" box is required for efficient transcription in vivo. Very recently it has been shown that this same region becomes hypersensitive to DNase I in thymidine kinase-transformed cells expressing the gene whereas thymidine kinase transformants that fail to express thymidine kinase mRNA lack the hypersensitive site (132). Thus, the thymidine kinase story that is unfolding represents a very close parallel to the SV40 situation.

C. Psoralen Photoaddition and Chromatin Structure

Psoralen derivatives are tricyclic planar compounds than can, like ethidium bromide, intercalate between the stacked bases of double stranded nucleic acids (DNA or RNA) and unwind the helix. In marked contrast to ethidium bromide, an intercalated psoralen molecule can undergo a photochemical reaction upon absorption of a photon of long wavelength ultraviolet light (320 - 380nm) that results in formation of a covalent attachment between the psoralen and nearby pyrimidine of the DNA (133-136). Either the 4',5' (furan) or 3,4 (pyrone) double bond of the psoralen can react with the 5,6 double bond on the pyrimidine to form a cyclobutane adduct (133, 134, 137). If two pyrimidines are located adjacently, but on opposite strands, absorption of a second photon of ultraviolet light can convert a psoralen monoadduct into a diadduct (138-140). Thus as depicted in Figure 6, when both reactive moieties are photoactivated the psoralen molecule covalently crosslinks the two DNA strands.

The sequence specificity of most psoralen derivatives is influenced by constraints of both intercalation and photoreaction although the relative contribution of these factors is difficult to determine. Information about the distribution of stereoisomers for a variety of psoralen derivatives has been provided by analyses of psoralen-modified DNA enzymatically digested to nucleosides, separated by HPLC and examined by mass spectrometry and $^{1}$H-NMR. In every case, thymidine adducts predominate (>90%), while cytosine adducts are much less common (141-143). Experiments using photoaddition to synthetic double-stranded DNA polymers have demonstrated that the most highly preferred sites are those where adenine and thymidine bases alternate in a DNA strand (144).

Figure 6. Schematic Representation of a Psoralen Crosslink.

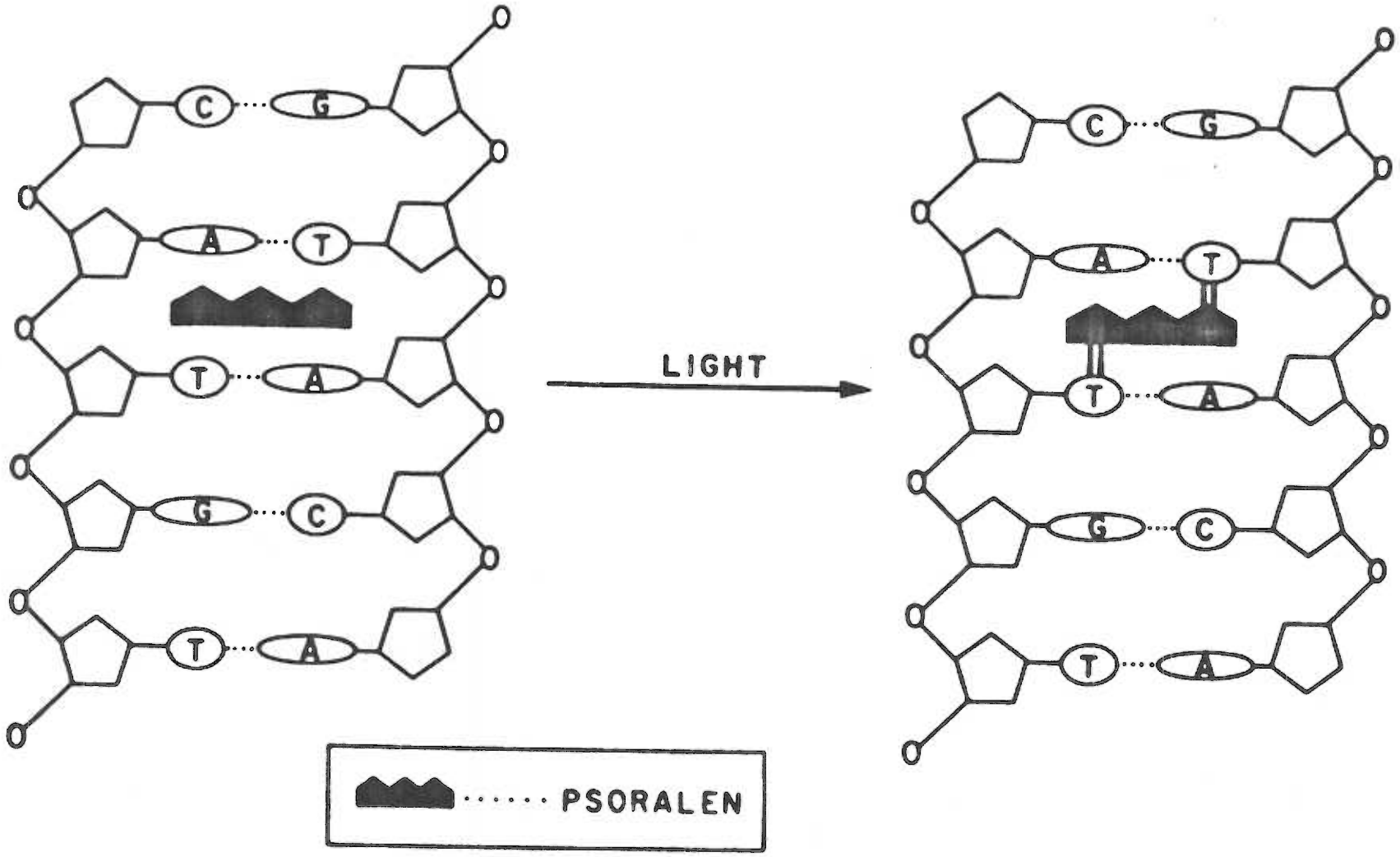
C
G
A
T
T
A
G
C
T
A
LIGHT
C
G
A
T
T
A
G
C
T
A
PSORALEN

Alternating guanine and thymidine sites are also somewhat preferred, whereas sites that contain a series of any one base are unfavorable for adduct formation. Site specificity with more complexity than that of the dinucleotide has not been investigated, primarily because a sequencing methodology for locating psoralen adducts on intact DNA does not exist.

Several clinical programs have utilized psoralen derivatives in conjunction with ultraviolet irradiation for the treatment of pigmentation disorders such as vitiligo and for the control of severe psoriasis (145). Another major application of these reagents has been as probes of nucleic acid structure. In particular the cross-linking capability of psoralen derivatives has been exploited for mapping regions of secondary structure in single-stranded nucleic acids (146), for mapping interactions between mRNA and 18s rRNA in intact ribosomes (147), and for analyzing DNA-protein complexes (4, 5, 6). Psoralen photoaddition has also proven useful for inactivating RNA and DNA viruses (148-150) and for studies of cellular DNA repair mechanisms (151).

Psoralen derivatives readily penetrate intact cells and have therefore been used to probe intracellular nucleoprotein complexes. The specificity of psoralens for internucleosomal (linker) regions of chromatin was originally established with Drosophila (5), mouse L-cell (6) and SV40 (4) chromatin in two types of experiments. In the first experiment the DNA of intracellular chromatin was saturated with photoadducts of 4,5',8-trimethylpsoralen (TMP) by repeated drug addition and irradiation. The plateau level of adducts achieved was one TMP molecule for every 40-50 bp, a level which was only 10-15% of the level

attained when purified DNA was photoreacted with TMP (one TMP for every 4-8 bp). In addition, when the TMP-crosslinked DNA was purified from the cells and spread under totally denaturing conditions for electron microscopy, a series of single-stranded DNA loops were detected. Regions at the base of the loops where the DNA remained double-stranded contained the TMP crosslinks. Histograms compiled from size measurements of the loops suggested that the TMP adducts were located at intervals of 180-200 bp (or multiples thereof, i.e. 380bp, 570bp). In contrast, when DNA control samples cross-linked in vitro were examined, random-sized loops were detected. Together, these results indicated that most of the DNA present in eukaryotic cells was protected from psoralen photoaddition and that susceptible regions were regularly interspersed between larger protected regions.

In the second type of experiment it was shown that micrococcal nuclease preferentially excised [$^{3}$H]TMP-containing regions of DNA from chromatin. This was despite the fact that TMP-containing regions of purified DNA were known to resist cleavage by micrococcal nuclease. Thus these experiments strongly suggested that the TMP-susceptible regions of chromatin were located between nucleosomes. An explanation for why psoralen photoaddition does not occur within nucleosomal DNA is lacking. However, Hearst and his colleagues have proposed that DNA wrapped around a nucleosome may be constrained from unwinding, and thereby inhibit optimal psoralen intercalation or psoralen orientation for the photoreaction (152). Except for nucleosomes, the only type of protein complex reported to protect DNA from psoralen photoaddition is one that binds to five clustered sites at the origin of replication on mitochondrial DNA (mt DNA) (153). Sites on mt DNA (which lacks

nucleosomes) that were protected in vivo were mapped on the purified DNA by the use of electron microscopy as in earlier work. Unfortunately, this system has not been further characterized.

Because the psoralens are reactive in vivo, psoralen photoaddition has been applied to the study of chromatin complexes that only function with fidelity inside intact cells. Separate studies of the chromatin structure of actively transcribed, extrachromosomal ribosomal RNA genes of Tetrahymena (154) and of Physarum (155) were carried out using the same general approach as in the earlier mt-DNA analysis. Following psoralen photoaddition, the positions of crosslinks on the purified DNA were mapped and were found to be several fold more frequent in the transcribed regions than in the non-transcribed spacer regions of the gene. The Tetrahymena work further demonstrated that within the transcribed region, TMP adducts were not located at regular 180-200 bp intervals. This result was consistent with other reports of non-integral nucleosomal repeat lengths detected by micrococcal nuclease digestion and by electron microscopic visualization of the rRNA chromatin and argued for an altered composition or conformation of the nucleosomes present. TMP photoaddition to the rRNA genes during a transcriptionally inactive stage of the life cycle of Physarum demonstrated the loss of preferential cross linking in the transcribed region. These results suggested that the process of transcription or requirements for it may have led to the altered chromatin structure observed.

Given the features of chromatin structure that allow micrococcal nuclease and psoralen to differentiate nucleosomal from linker DNA, it is not surprising that other DNA damaging agents have been found to

possess similar specificities. These include the carcinogens N-acetoxy-acetylaminofluorene, aflatoxin B1, benzo(a)pyrene, and the antibiotic bleomycin, among others (156-159). However the specificity of these agents for linker DNA is either not as high as that of psoralen derivatives or has been less well characterized.

D. Organization of Thesis

The three manuscripts which make up this thesis are presented on the following pages in the order that the experiments were completed. Paper 1 describes the methods that were developed in order to map psoralen adducts at the level of restriction enzyme fragments, and the results obtained when the chromatin structure of intracellular SV40 was examined by psoralen photoaddition. Paper 2 presents an analysis of SV40 chromatin structure in intact virus particles employing the methods of Paper 1. Paper 3 deals with two types of experiments. In the first part methods for the fluorescent quantitation of DNA restriction fragments were compared. These methods are the same ones used in Papers 1 and 2 for estimating DNA distributions, although it was the distribution of radioactivity (psoralens) that provided the specific activity ratios. In the second part these fluorescent methods are employed to determine the inhibitory effect of psoralen photoadducts on Bgl I digestion of pBR322 DNA. Finally, in the Summary and Discussion section, the significance of these findings is discussed and a scheme for the fine-structure mapping of psoralen adducts on DNA is presented.

REFERENCES

1. Griffith, J. D. (1975). Chromatin structure: deduced from a minichromosome. Science 187, 1202-1203.

2. Scott, W. A. and Wigmore, D. J. (1978). Sites in SV40 chromatin which are preferentially cleaved by endonucleases. Cell 15, 1511-1518.

3. Varshavsky, A. J., Sundin, O. H., Bohn, M. J. (1978). SV40 viral minichromosome: preferential exposure of the origin of replication as probed by restriction endonucleases. Nucl. Acids Res. 5, 3469-3477.

4. Hallick, L. M., Yokota, H. A., Bartholomew, J. C. and Hearst, J. E. (1978). Photochemical addition of the cross-linking reagent 4,5',8-trimethylpsoralen (trioxsalen) to intracellular and viral SV40 DNA-histone complexes. J. Virol. 27, 127-135.

5. Wiesehahn, G. P., Hyde, J. E. and Hearst, J. E. (1977). The photoaddition of trimethylpsoralen to Drosophila melanogaster nuclei: A probe for chromatin substructure. Biochem. 16, 925-932.

6. Cech, T. and Pardue, M. L. (1977). Cross-linking of DNA with trimethylpsoralen is a probe for chromatin structure. Cell 11, 631-640.

7. Sweet, B. and Hilleman M. (1960), The vacuolating virus, SV40. Proc. Soc. Exp. Biol. Med. 105, 420-427.

8. Lebowitz, P. and Weissman, S. M. (1979). Organization and transcription of the Simian Virus 40 genome. Cur. Top. Microbiol. and Immunol. 87, 43-172.

9. Levine, A. J., Vliet, P. C. and Sussenback, J. S. (1976). The replication of papovavirus and adenovirus DNA. Cur. Top. Microbiol. and Immunol. 73, 68-124.

10. Fareed, G. and Davoli, D. (1977). Molecular biology of papovaviruses. Ann. Rev. Biochem. 46, 471-552.

11. Kelly, T. and Nathans, D. (1977). The genome of Simian Virus 40. Adv. in Virus Research, 21, 85-173, Academic Press, New York.

12. Griffin, B. E. (1981). Structure and genome organization of SV40 and polyoma virus., pp. 61-124., in J. Tooze (ed.), DNA Tumor Viruses, Cold Spring Harbor Laboratory, Cold Spring Harbor, New York.

13. Bina, M., Beecher, S. and Blasquez, V. (1982). Stability and components of mature SV40. Biochem. 21, 3057-3063.

14. Kondoleon, S. K., personal communication.

15. Brady, J. N. Lavialle, C. and Salzman, N. (1980). Efficient transcription of a compact nucleoprotein complex isolated from purified SV40 virions. J. Virol. 35, 371-381.

16. Christiansen, G. Landers, T. and Griffith, J. and Berg, P. (1977). Characterization of components released by alkali disruption of SV40. J. Virol. 21, 1079-1084.

17. Jay, G., Nomura, S., Anderson, C. W. and Khoury, G. (1981). Identification of the SV40 agnogene product: a DNA binding protein. Nature (London) 291, 346-349.

18. Reddy, V. B., Thimmappaya, B., Dahr, R., Subramanian, K. A., Zain, B. S., Pan, J., Ghosh, P. K., Celma, M. L. and Weismann, S. M. (1978). The genome of SV40. Science 200, 494-502.

19. DePamphilis, M. L. and Wassarman, P. M. (1982). Organization and replication of papovavirus DNA., pp. 37-114., in A. S. Kaplan (ed.)., Organization and Replication of Viral DNA, CRC Press, Bota Raton, Fl.

20. Tegtmeyer, P. (1972). SV40 DNA synthesis: the viral replicon. J. Virol. 10, 591-598.

21. Tjian, R. (1978). The binding site on SV40 DNA for a T-antigen-related protein. Cell 13, 165-179.

22. Wilson, V. G., Tevethia, M. J., Lewton, B. A. and Tegtmeyer, P. (1982). DNA binding properties of SV40 temperature-sensitive A proteins. J. Virol. 44, 458-466.

23. Tjian, R. and Robbins, A. (1979). Enzymatic activites associated with a purified SV40 T-antigen-related protein. Proc. Natl. Acad. Sci. U.S.A. 76, 610-614.

24. Myers, R. M., Kligman, M. and Tjian, R. (1981). Does SV40 T-antigen unwind DNA? J. Biol. Chem. 256, 10156-10160.

25. Giacherio, D. and Hager, L. P. (1980). A specific DNA unwinding activity associated with SV40 large T-antigen. J. Biol. Chem. 255, 8963-8966.

26. Seif, R. (1982). New properties of SV40 large T-antigen. Mol. Cell Biol. 2, 1463-1471.

27. Krokan, H., Schaffer, P. and DePamphilis, M. L. (1979). Involvement of eucaryotic DNA polymerase α and γ in the replication of cellular and viral DNA. Biochem. 18, 4431-4443.

28. Sundin, O. and Varshavsky, A. (1980). Terminal stages of SV40 DNA replication proceed via multiple intertwined catenated dimers. Cell 21, 103-114.

29. Acheson, N. H. (1981). Lytic cycle of SV40 and polyoma virus., pp. 125-204., in J. Tooze. (ed.), DNA Tumor Viruses, Cold Spring Harbor Laboratory, Cold Spring Harbor, N.Y.

30. Tjian, R. (1981). Regulation of viral transcription and DNA replication by the SV40 large T-antigen. Curr. Top. Microbiol. and Immunol. 93, 5-24.

31. Reed, S. I., Stark, G. R. and Alwine, J. C. (1976). Autoregulation of SV40 gene A by T-antigen. Proc. Natl. Acad. Sci. U.S.A. 73, 3083-3087.

32. Khoury, G. and May, E. (1977). Regulation of early and late SV40 transcription: overproduction of early viral RNA in the absence of a functional T-antigen. J. Virol. 23, 167-176.

33. Rio, D., Robbins, A., Myers, R. and Tjian, R. (1980). Regulation of SV40 early transcription in vitro by a purified tumor antigen. Proc. Natl. Acad. Sci. U.S.A. 77, 5706-5710.

34. Myers, R. M. and Tjian, R. (1980). Construction and analysis of SV40 origins defective in T-antigen binding and DNA replication. Proc. Natl. Acad. Sci. U.S.A. 77, 6491-6495.

35. Ptashne, M., Backman, K., Hamayun, M. Z., Jeffrey, A., Maurer, B., Meyer, B. and Sauer, T. (1976). Autoregulation and function of a repressor in bacteriophage lambda. Science 194, 151-161.

36. Birkenmeier, E. H., Chiu, N., Radonovich, M. F., May, E. and Salzman, N. P. (1979). Regulation of SV40 early and late gene transcription without viral DNA replication. J. Virol. 29, 983-989.

37. Green, M. H. and Brooks, T. L. (1978). Recently replicated SV40 DNA is a preferential template for transcription and replication. J. Virol. 26, 325-334.

38. Khoury, G., Gruss, P., Dhar, R. and Lai, C. (1979). Processing and expression of early SV40 mRNA: a role for RNA conformation in splicing. Cell 18, 85-92.

39. Lewin, B. (1980). Sequences of splicing junctions., pp. 815-824., in B. Lewin (ed.), Gene Expression 2: Eucaryotic Chromosomes, 2nd ed., John Wiley and Sons, N.Y.

40. Mathis, D. J. and Chambon, P. (1981). The SV40 early region TATA box is required for accurate in vitro initiation of transcription. Nature (London) 290, 310-315.

41. Gluzman, Y., Sambrock, J. F. and Frisque, R. J. (1980). Expression of early genes of origin-defective mutants of SV40. Proc. Natl. Acad. Sci. U.S.A. 77, 3898-3902.

42. Ghosh, P. K., Lebowitz, P., Frisque, R. J., and Gluzman, Y. (1981). Identification of a promoter component involved in positioning the 5' termini of SV40 early mRNAs. Proc. Natl. Acad. Sci. U.S.A. 78, 100-104.

43. Brady, J., Radonovich, M., Vodkin, M., Natarajan, V., Thoren, M., Das, G., Janik, J., Salzman, N. (1982). Site-specific base substitution and deletion mutations that enhance or suppress transcription of the SV40 major late RNA. Cell 31, 625-633.

44. Benoist, C. and Chambon, P. (1981). In vivo sequence requirements of the SV40 early promoter region. Nature (London) 290, 304-310.

45. Gruss, P., Dhar, R. and Khoury, G. (1981). SV40 tandem repeated sequences as an element of the early promoter. Proc. Natl. Acad. Sci. U.S.A. 78, 943-947.

46. Banerji, J., Rusconi, S. and Schaffner, W. (1981). Expression of a β-globin gene is enhanced by remote SV40 DNA sequences. Cell 27, 299-308.

47. Moreau, P., Hen, R., Wasylyk, B., Everett, R., Gaub, M. P. and Chambon, P. (1981). The SV40 72bp repeat has a striking effect on gene expression both in SV40 and other chimeric recombinants. Nucl. Acids Res. 9, 6047-6067.

48. Levinson, B., Khoury, G., Woude, G. V. and Gruss, P. (1982). Activation of SV40 genome by 72bp tandem repeats of Moloney sarcoma virus. Nature (London) 295, 568-572.

49. Botchan, M., Robbins, P., Lusky, M., Berg, L. and Weiher, H. (1982). Characterization of the SV40 enhancer/activator sequence and other related experiments. 1982 DNA Tumor Virus Meeting Abstract.

50. de Villiers, J. and Schaffner, W. (1981). A small segment of polyoma virus DNA enhances the expression of a cloned β-globin gene over a distance of 1400bp. Nucl. Acids Res. 9, 6251-6264.

51. Grosschedl, R. and Birnstiel, M. L. (1980). Identification of regulatory sequences in the prelude sequences on an H2a histone gene by the study of specific deletion mutants in vivo. Proc. Natl. Acad. Sci. U.S.A. 77, 1432-1436.

52. McKnight, S. L., Gavis, E. R. Kingsbury, R. and Axel, R. (1981). Analysis of transcriptional regulatory signals of the HSV thymidine

kinase gene: identification of an upstream control region. Cell 25, 385-398.

53. Hertz, G. Z., Trimble, L. A., Barkan, A., Somasekhar, M. and Mertz, J. E. (1982). Sequences involved in the promotion and initiation of late strand transcription. 1982 DNA Tumor Virus Meeting Abstract.

54. Kornberg, R. D. (1977). Structure of chromatin. Ann. Rev. Biochem. 46, 931-955.

55. Cremisi, C., (1979). Chromatin replication revealed by studies of animal cells and papovaviruses (SV40 and polyoma). Microbiol. Rev. 43, 297-319.

56. McGhee, J. D. and Felsenfeld, G. (1980). Nucleosome structure. Ann Rev. Biochem. 49, 1115-1156.

57. Cartwright, I., Abmayr, S. M., Fleischmann, G., Lowenhaupt, K., Elgin, S.C.R., Keene, M. A. and Howard, G. C. (1982). Chromatin structure and gene activity: the role of nonhistone chromosomal proteins. CRC Crit. Rev. Biochem. 13, 1-86.

58. Olins, A. L. and Olins. D. E. (1974). Spheroid chromatin units (V bodies). Science 183, 330-332.

59. Oudet, P., Gross-Bellard, M. and Chambon, P. (1975). Electron microscopic and biochemical evidence that chromatin structure is a repeating unit. Cell 4, 281-300.

60. Elgin, S. C. R. and Weintraub, H. (1975). Chromosomal proteins and chromatin structure. Ann Rev. Biochem. 44, 725-774.

61. Finch, J. T. and Klug, A. (1976). Solenoid model for superstructure in chromatin. Proc. Natl. Acad. Sci. U.S.A. 73, 1897-1901.

62. Muller, U., Zentgraf, H., Eicken, I. and Keller, W. (1978). Higher order structure of SV40 chromatin. Science 201, 406-415.

63. Weisbrod, S. (1982). Active chromatin. Nature (London) 297, 289-295.

64. Noll, M. and Kornberg, R. D. (1977). Action of micrococcal nuclease on chromatin and the location of histone H1. J. Mol. Biol. 109, 393-404.

65. Simpson, R. T. (1978). Structure of the chromatosome, a chromatin particle containing 160bp of DNA and all the histones. Biochem. 17, 5524-5531.

66. Allan, J., Hartman, P. G., Crane-Robinson, C. and Aviles, F. X. (1980). The structure of histone H1 and its location in chromatin. Nature (London) 288, 675-679.

67. Steinmetz, M., Streeck, R. E. and Zachau, H. G. (1978). Closely spaced nucleosome cores in reconstituted histone-DNA complexes and histone-H1-depleted chromatin. Eur. J. Biochem. 83, 615-628.

68. Germond, J. E., Hirt, B., Oudet, P. Gross-Bellard, M. and Chambon, P. (1975). Folding of the DNA double-helix in chromatin-like structures from SV40. Proc. Natl. Acad. Sci. U.S.A. 72, 1843-1847.

69. Varshavsky, A. J., Bakayev, U. V., Chumackov, P. M. and Georgiev, G. P. (1976). Minichromosome of SV40: presence of histone H1. Nucl. Acids Res. 3, 2101-2113.

70. Lewin, B. (1980). Coiling of the nucleosome thread, pp. 416-420., in B. Lewin (ed.), Gene Expression 2: Eucaryotic Chromosomes, 2nd ed., John Wiley and Sons, N.Y.

71. Coca-Prados, M. and Hsu, M-T., (1979). Intracellular forms of SV40 nucleoprotein complexes. II. Biochemical and electron microscopic analysis of SV40 virion assembly. J. Virol. 31, 199-208.

72. Fanning, E. and Baumgartner, I. (1980). A role of fast-sedimenting SV40 nucleoprotein complexes in virus assembly. Virol. 102, 1-12.

73. Garber, E. A., Seidman, M. M. and Levine, A. J. (1980). Intracellular SV40 nucleoprotein complexes: synthesis to encapsidation. Virol. 107, 389-401.

74. Coca-Prados, M., Vidali, G. and Hsu, M.-T. (1980). Intracellular forms of SV40 nucleoprotein complexes. III. Study of histone modifications. J. Virol. 36, 353-360.

75. LaBella, F. and Vesco, C. (1980). Late modifications of SV40 chromatin during the lytic cycle occur in an immature form of virion. J. Virol. 33, 1138-1150.

76. Brady, J. N., Radonovich, M., Lavialle, C. and Salzman, N. P. (1981). SV40 maturation: chromatin modifications increase the accessibility of viral DNA to nuclease and RNA polymerase. J. Virol. 39, 603-611.

77. Green, M. H. and Brooks, T. L. (1976). Isolation of two forms of SV40 nucleoprotein containing RNA polymerase from infected monkey cells. Virol. 72, 110-120.

78. Gariglio, P., Llopis, R., Oudet, P. and Chambon, P. (1979). The template of the isolated native SV40 transcriptional complex is a minichromosome. J. Mol. Biol. 131, 75-105.

79. Jacobovits, E. B., Saragosti, S., Yaviv, M. and Aloni, Y. (1980). E. coli RNA polymerase in vitro mimics SV40 in vivo transcription

when the template is viral nucleoprotein. Proc. Natl. Acad. Sci. U.S.A. 77, 6556-6560.

80. Mann, K. and Hunter, T. (1979). Association of Simian Virus 40 T-Ag with SV40 nucleoprotein complexes. J.Virol. 29, 232-241.

81. Reiser, J., Renart, J., Crawford, L. V. and Stark, G. R. (1980). Specific association of SV40 tumor antigen with SV40 chromatin. J. Virol. 33, 78-87.

82. Seidman, M. M., Levine, A. J. and H. Weintraub. (1979). The asymmetric segregation of parental nucleosomes during chromosome replication. Cell 18, 439-449.

83. Davie, J. R. and Candido, E. P. (1978). Acetylated histone H4 is preferentially associated with template-active chromatin. Proc. Natl. Acad. Sci. U.S.A. 75, 3574-3577.

84. Weisbrod, S., Groudine, M. and Weintraub, H. (1980). Interaction of HMG 14 and 17 with actively transcribed genes. Cell 19, 289-301.

85. Lewin, B. (1980). Chromatin under transcription, pp. 404-408., in B. Lewin (ed.), Gene Expression 2: Eucaryotic Chromosomes, 2nd ed., John Wiley and Sons, N. Y.

86. Kornberg, R. (1981). The location of nucleosomes in chromatin: specific or statistical? Nature (London) 292, 579-560.

87. Cremisi, C., Pignatti, P. R. and Yaniv, M. (1976). Random location and absence of movement of the nucleosomes on SV40 nucleoprotein complex isolated from infected cells. B.B.R.C. 73, 548-554.

88. Ponder, B. A. J. and Crawford, L. V. (1977). The arrangement of nucleosomes in nucleoprotein complexes from polyoma virus and SV40. Cell 11, 35-49.

89. Das, G. C., Allison, D. P. and Niyogi, S. K. (1979). Sites including those of origin and termination are not freely available to single-cut restriction endonucleases in the supercompact form of SV40 minichromosome. B.B.R.C. 89, 17-25.

90. Liggins, G. L., English, M. and Goldstein, D. A. (1979). Structural changes in SV40 chromatin as probed by restriction endonucleases. J. Virol. 31, 718-732.

91. Varshavsky, A. J., Sundin, O. and Bohn, M. (1979). A stretch of "late" SV40 viral DNA about 400bp long which includes the origin of replication is specifically exposed in SV40 minichromosomes. Cell 16, 453-466.

92. Shelton, E. R., Wassarman, P. M. and DePamphilis, M. L. (1980). Structure, spacing and phasing of nucleosomes on isolated forms of mature SV40 chromosomes. J. Biol. Chem. 255, 771-781.

93. Sundin, O. and Varshavsky, A. (1979). Staphylococcal nuclease makes a single non-random cut in the SV40 viral minichromosome. J. Mol. Biol. 132 535-546.

94. Waldeck, W., Fohring, B., Chowdhury, K., Gruss, P., and G. Sauer. (1978). Origin of DNA replication in papovavirus chromatin is recognized by endogenous endonuclease. Proc. Natl. Acad. Sci. U.S.A. 75, 5964-5968.

95. Jakobovits, E. B., Bratosin, S. and Aloni, Y. (1980). A nucleosome-free region in SV40 minichromosomes. Nature (London) 285, 263-265.

96. Saragosti, S., Moyne, G. and Yaniv, M. (1980). Absence of nucleosomes in a fraction of SV40 chromatin between the origin of

replication and the region coding for late leader RNA. Cell 20, 65-73.

97. Keene, M. A. and Elgin, S. C. R. (1981). Micrococcal nuclease as a probe of DNA sequence organization and chromatin structure. Cell 27, 57-64.

98. Dingwall, C., Lomonossoff, G. R. and Laskey, R. A. (1981). High sequence specificity of micrococcal nuclease. Nucl. Acids Res. 9, 2659-2673.

99. Beard, P. (1978). Mobility of histones on the chromosome of SV40. Cell 15, 955-967.

100. Beard, P., Kaneko, M. and Cerutti, P. (1981). N-acetoxy-acetylaminofluorene reacts preferentially with a control region of intracellular SV40 chromosome. Nature (London) 291, 84-85.

101. Gottesfeld, J. M. and Bloomer. L. S. (1980). Nonrandom alignment of nucleosomes on 5s RNA genes of X. laevis. Cell 21, 751-760.

102. Louis, C., Schedl, P., Samal, B. and Worcel, A. (1980). Chromatin structure of the 5s genes of D. melanogaster. Cell 22, 387-392.

103. Wittig, B. and Wittig, S. (1979). A phase relationship associates tRNA structural gene sequences with nucleosome cores. Cell 18, 1173-1183.

104. Wigmore, D. J., Eaton, R. W. and Scott, W. A. (1980). Endonuclease-sensitive regions in SV40 chromatin from cells infected with duplicated mutants. Virol. 104, 462-478.

105. Jakobovits, E. B., Bratosin, S. and Aloni, Y. (1982). Formation of a nucleosome-free region in SV40 minichromosomes is dependent upon a restricted segment of DNA. Virol. 120, 340-348.

106. Wasylyk, B., Oudet, P. and Chambon, P. (1979). Preferential in vitro assembly of nucleosome cores on some A-T-rich regions of SV40 DNA. Nucl. Acids Res. 7, 705-713.

107. Simpson, R. T. and Stein, A. (1980). Random protection of single-cut restriction endonuclease sites in SV40 minichromosomes assembled in vitro. FEBS Lett. 111, 337-339.

108. Hiwasa, T., Segawa, M., Yamaguchi, N. and Oda, K. (1981). Phasing of nucleosomes in SV40 chromatin reconstituted in vitro. J. Biochem. 89, 1375-1389.

109. Strauss, F., Gaillard, C. and Prunell, A. (1981). Helical periodicity of DNA. Poly (dA):poly (dT) and poly (dA-dT):poly (dA-dT) in solution. Eur. J. Biochem. 118, 215-222.

110. Nickol, J., Behe, M. and Felsenfeld, G. (1982). Effect of the B-Z transition in poly (dG-$m^5$dC):poly (dG-$m^5$dC) on nucleosome formation. Proc. Natl. Acad. Sci. U.S.A. 79, 1771-1775.

111. Saragosti, S., Cereghini, S. and Yaniv, M. (1982). Fine structure of the regulatory region of SV40 minichromosomes revealed by DNase I digestion. J. Mol. Biol. 160, 133-146.

112. Tack, L. C., Wassarman, P. M. and DePamphilis, M. L. (1981). Chromatin assembly: relationship of chromatin structure to DNA sequence during SV40 replication. J. Biol. Chem. 256, 8821-8828.

113. Hartman, J. P. and Scott, W. A. (1981). Distribution of DNase I-sensitive sites in SV40 nucleoprotein complexes from disrupted virus particles. J. Virol. 37, 908-915.

114. Elgin, S. C. R. (1981). DNAase I-hypersensitive sites of chromatin. Cell 27, 413-415.

115. Weintraub, H. and Groudine, M. (1976). Chromosomal subunits in active genes have an altered conformation. Science 193, 848-856.

116. Weisbrod, S. and Weintraub, H. (1976). Isolation of a subclass of nuclear proteins responsible for conferring a DNase I-sensitive structure on globin chromatin. Proc. Natl. Acad. Sci. U.S.A. 76, 630-634.

117. Lawson, G. M., Knoll, B. J. March, C. J., Woo, S. L. C., Tsai, M.-J. and O'Malley, B. W. (1982). Definition of 5' and 3' structural boundaries of the chromatin domain containing the ovalbumin multigene family. J. Biol Chem. 257, 1501-1507.

118. Bellard, M., Gannon, F. and Chambon, P. (1977). Nucleosome structure. III. The structure and transcriptional activity of the chromatin containing the ovalbumin and globin genes in chick oviduct nuclei. Cold Spring Harbor Symp. Quant Biol. 42, 779-791.

119. Nedospasov, S. A., Georgiev, G. P. (1980). Non-random cleavage of SV40 DNA in the compact minichromosome and free in solution by micrococcal nuclease. BBRC 92, 532-539.

120. Wu, C. (1980). The 5' ends of Drosophila heat shock genes in chromatin are hypersensitive to DNase I. Nature (London), 286, 854-860.

121. Wu, C., Bingham, P. M., Livak, K. J., Holmgren, R. and Elgin, S. C. R. (1979). The chromatin structure of specific genes: 1. Evidence for higher order domains of defined DNA sequence. Cell 16, 797-806.

122. Kolata, G. B. (1981). Genes regulated through chromatin structure. Science 214, 775-776.

123. McGhee, J. D., Wood, W., Dolan, M., Engel, J. D. and Felsenfeld, G. (1981). A 200 bp region at the 5' end of a chicken adult β-globin gene is accessible to nuclease digestion. Cell 27, 45-55.

124. Weintraub, H. (1979). Assembly of active chromatin structure during replication. Nucl. Acids Res. 7, 781-792.

125. Groudine, M. and Weintraub, H. (1981). Activation of globin genes during chicken development. Cell 24, 393-401.

126. Keene, M. A., Croces, V., Lowenhaupt, K. and Elgin, S.C.R. (1981). DNase I hypersensitive sites in Drosophila chromatin occur at the 5' ends of regions of transcription. Proc. Natl. Acad. Sci. U.S.A. 78, 143-146.

127. Doerfler, W. (1981). DNA methylation-a regulatory signal in eukaryotic gene expression. J. Gen. Virol. 57, 1-20.

128. Van der Ploeg, L. H. T. and Flavell, R. A. (1980). DNA methylation in the human γδβ-globin methylation in the human nonerythroid tissues. Cell 19, 947-958.

129. Vidali, G., Boffa, L. C., Bradbury, E. M. and Allfrey, V. G. (1978). Butyrate suppression of histone deacetylation leads to accumulation of multi-acetylated forms of histones H3 and H4 and increased DNase I sensitivity of the associated DNA sequences. Proc. Natl. Acad. Sci. U.S.A. 75, 2239-2243.

130. Cremisi, C. (1981). The appearance of DNase I hypersensitive sites at the 5' end of the late SV40 genes is correlated with the transcriptional switch. Nucl. Acids Res. 9, 5949-5964.

131. Shakhov, A. N., Nedospasov, S. A. and Georgiev, G. P. (1982). Deoxyribonuclease II as a probe to sequence-specific chromatin

organization: preferential cleavage in the 72bp modulator sequence of SV40 minichromosome. Nucl. Acids Res. 10, 3951-3965.

132. Sweet, R. W., Chao, M. V. and Axel, R. (1982). The structure of the thymidine kinase gene promoter: nuclease hypersensitivity correlates with expression. Cell 31, 347-353.

133. Musajo, L., Rodighiero, G., Breccia, R., Dall'Acqua, F. and Malesani, G. (1966). Skin-photosensitizing furocoumarins: photochemical interaction between DNA and $-O^{14}CH_3$ bergapten (5-methoxy-psoralen). Photochem. Photobiol. 5, 739-745.

134. Krauch, C. H., Kramer, D. M. and Wacker, A. (1967). Zum Wirkungsmechanismum photodynamischer furocoumarine. Photoreaktion von psoralen-(4-$^{14}$C) mit DNS, RNS, homopolynucleotiden und nucleosiden. Photochem. Photobiol. 6, 341-354.

135. Pathak, M. A. and Kramer, D. M. (1969). Photosensitization of skin in vivo by furocoumarins (psoralens). Biochim. Biophys. Acta 195, 197-206.

136. Cole, R. S. (1970). Light-induced cross-linking of DNA in the presence of a furocoumarin (psoralen). Biochim. Biophys. Acta 217, 30-39.

137. Musajo, L., Rodighiero, G. and Dall'Acqua, F. (1965). Evidences of a photoreaction of the photosensitizing furocoumarins with DNA and with pyrimidine nucleosides and nucleotides. Experientia 21, 24-26.

138. Dall'Acqua, F., Marciani, S. and Rodighiero, G. (1970). Inter-strand cross-linkages occurring in the photoreaction between psoralen and DNA. FEBS Lett. 9, 121-123.

139. Cole, R. S. (1971). Psoralen monoadducts and interstrand cross-links in DNA. Biochim. Biophys. Acta 251, 30-39.

140. Dall'Acqua, F., Marciani, S., Vedaldi, D. and Rodighiero, G. (1972). Formation of inter-strand cross-linkings on DNA of guinea pig skin after application of psoralen and irradiation at 365nm. FEBS Lett. 27, 192-194.

141. Straub, K., Kanne, D., Hearst, J. E. and Rapoport, H. (1981). Isolation and characterization of pyrimidine-psoralen photoadducts from DNA. J. Am. Chem. Soc. 103, 2347-2355.

142. Kanne, D., Straub, K., Rapoport, H. and Hearst, J. E. (1982). Isolation and characterization of pyrimidine-psoralen diadducts from DNA. J. Am. Chem. Soc. 104, 6754-6764.

143. Kanne, K., Straub, K., Rapoport, H. and Hearst, J. E. (1982). Psoralen-DNA photoreaction. Characterization of the monoaddition products from 8-methoxypsoralen and 4,5',8-trimethylpsoralen. Biochem. 21, 861-871.

144. Dall'Acqua, F., Terbojevich, M., Marciani, S., Vedaldi, D. and Recher, M. (1978). New chemical aspects of the photoreactions between psoralen and DNA. Chem-Biol. Interact. 21, 103-115.

145. Fitzpatrick, T. B., Pathak, M., Harber, L., Seiji, M., Kukita, A. (eds.), Sunlight and Man: Normal and Abnormal Photobiologic Responses, Univ. of Tokyo Press, Tokyo, Japan, 1975.

146. Rabin, D. and Crothers, D. M. (1979). Analysis of RNA secondary structure by photochemical reversal of psoralen crosslinks. Nucl. Acids Res. 7, 689-703.

147. Nakashima, K., Darzynkiewicz, E. and Shatkin, A. J. (1980). Proximity of mRNA 5'-region and 18s rRNA in eukaryotic initiation complexes. Nature (London) 286, 226-230.

148. Swanstrom, R., Hallick, L. M., Jackson, J., Hearst, J. E. and Bishop, J. M. (1981). Interaction of psoralen derivatives with the RNA genome of Rous sarcoma virus. Virol. 113, 613-622.

149. Redfield, D. C., Richman, D. D., Osman, M. N. and Kronenberg, L. H. (1981). Psoralen inactivation of Influenza and Herpes Simplex viruses and of virus-infected cells. Infect. Immun. 32, 1216-1226.

150. Kondoleon, S. K., Walter, M. A. and Hallick, L. M. (1982). Kinetics of SV40 and Lambda inactivation by photoaddition of psoralen derivatives. Photochem. Photobiol. 36, 325-331.

151. Zolan, M. E., Cortopassi, G. A., Smith, C. A. and Hanawalt, P. C. (1982). Deficient repair of chemical adducts in α DNA of monkey cells. Cell 28, 613-619.

152. Hearst, J. E., personal communication.

153. Potter, D. A., Fostel, J. M., Berninger, M., Pardue, M. L. and Cech, T. (1980). DNA-protein interactions in the Drosophila melanogaster mitochondrial genome as deduced from trimethylpsoralen crosslinking patterns. Proc. Natl. Acad. Sci. U.S.A. 77, 4118-4122.

154. Cech, T. R. and Karrer, K. M. (1980). Chromatin structure of the ribosomal RNA genes of Tetrahymena thermophila as analyzed by trimethylpsoralen cross-linking in vivo. J. Mol. Biol. 136, 395-416.

155. Judelson, H. A. and Vogt, V. M. (1982). Accessibility of ribosomal genes to trimethylpsoralen in nuclei of Physarum polycephalum. Mol. Cell. Biol. 2, 211-220.

156. Kaneko, M. and Cerutti, P. A. (1980). Excision of N-acetoxy-2-acetylaminofluorene-induced DNA adducts from chromatin fractions of human fibroblasts. Cancer Res. 40, 4313-4319.

157. Bailey, G. S., Nixon, J. E., Hendricks, J. D., Sinnhuber, R. O. and VanHolde, K. E. (1980). Carcinogen aflatoxin B1 is located preferentially in internucleosomal DNA following exposure in vivo in rainbow trout. Biochem. 19, 5836-5842.

158. Jack, P. L. and Brookes, P. (1981). The distribution of benzo(a)pyrene DNA adducts in mammalian chromatin. Nucl. Acids Res. 9, 5533-5552.

159. Elgin, S. C. R., personal communication.

# III. MANUSCRIPTS

## PAPER 1.

## Mapping the In Vivo Arrangement of Nucleosomes on Simian Virus 40 Chromatin by the Photoaddition of Radioactive Hydroxymethyltrimethylpsoralen

ABSTRACT

Intracellular simian virus 40 (SV40) chromatin was photoreacted with a $^{3}$H-labeled psoralen derivative, hydroxymethyltrimethylpsoralen (HMT), at 48 h postinfection. Psoralen compounds have been shown to readily penetrate intact cells and, in the presence of long wavelength UV light, form covalent adducts to DNA, preferentially at regions unprotected by nucleosomes. The average distribution pattern of [$^{3}$H]HMT on the SV40 genome was determined by specific activity measurements of the DNA fragments generated by Hind III plus Hpa II or Atu I restriction enzyme digestion. At levels of 1 to 10 [$^{3}$H]HMT photoadducts per SV40 molecule, the radiolabel was found to be distributed nonrandomly. Comparison of the labeling pattern in vivo with that of purified SV40 DNA labeled in vitro revealed one major difference. A region of approximately 400 base pairs, located between 0.65 and 0.73 on the physical map, was preferentially labeled under in vivo conditions. This finding strongly suggests that the highly accessible region near the origin of replication, previously observed on isolated SV40 "minichromosomes" exists on SV40 chromatin in vivo during a lytic infection.

## INTRODUCTION

The intracellular and viral nucleoprotein complexes of simian virus 40 (SV40) have a repeating structure of nucleosome beads very similar to that of cellular chromatin (for reviews, see 6, 24, 32). Both cellular and viral nucleosomes contain a core particle that consists of 146 base pairs (bp) of DNA (29, 50) wound around an octamer of proteins, two molecules each of the histones H2A, H2B, H3, and H4 (see reviews cited above). Histone H1 is thought to be associated with the internucleosomal or linker regions both of cellular chromatin (55, 58, 60, 64) and of the intracellular viral complex (50, 59). The small size of SV40 and the availability of molecular information on the sequence and expression of the viral genome make it an attractive model for cellular chromatin structure and replication. A number of early studies utilizing SV40 chromatin supported the idea that nucleosomes are positioned randomly with respect to the DNA sequence (7, 9, 28, 37, 38). However several recent investigations have indicated that a nonrandom arrangement exists on at least a subpopulation of SV40 chromatin molecules. A nucleosome-free region of approximately 300 to 400 bp has been detected at map positions 0.66 to 0.75 on isolated SV40 nucleoprotein complexes by electron microscopy (22, 45) and by endonuclease digestion (47, 53, 61-63). The function of this "open region" is unknown; however, these sequences contain the origin of replication (15, 35, 52), the region encoding the 5' ends of early and late SV40 mRNA (13, 40, 56), as well as the preferred binding sites for T antigen (23, 42, 51, 57).

We have developed a system to analyze the positioning of nucleosomes on SV40 DNA in vivo, using the photoreaction of furocoumarin (psoralen) derivatives with intracellular DNA. These compounds that have the ability to penetrate intact cells, intercalate into DNA and under the influence of long-wavelength UV light, covalently bind to pyrimidines of the DNA (4, 25, 33, 36). Because nucleosomal core DNA is preferentially protected from psoralen photoaddition (2, 65, 66), these derivatives are useful probes for studying the structure of both cellular (2, 3, 17, 66) and viral (16) chromatin.

In the experiments described below, a radioactive psoralen derivative was used as a reagent for labeling accessible regions of DNA in intracellular SV40 chromatin. SV40 DNA was isolated and restriction fragments were examined to determine the distribution of radioactive drug on the SV40 genome. This approach eliminates the extraction or fixation of SV40 chromatin required by previous in vitro nucleosome analyses. A region around the SV40 replication origin preferentially accessible to photoaddition was identified, demonstrating that there is a nonrandom distribution of nucleosomes on SV40 chromatin in vivo.

## MATERIALS AND METHODS

Cells and virus stocks. All infections and virus preparations were carried out in CV-1 cells, an African green monkey kidney line obtained from P. Berg. SV40 strain 776 was obtained from K. Danna. Cells were grown in Dulbecco modified Eagle medium (GIBCO Laboratores, Grand Island, N.Y.) supplemented with 5% fetal calf serum (Sterile Systems, Ogden, Utah). Virus stocks were prepared by low-multiplicity infection

(0.01 PFU/cell) from plaque-purified stocks and were titered on CV-IP cells, a derivative of CV-1 cells obtained from P. Berg. Infections used for in vivo labeling experiments were carried out at a multiplicity of 1 to 10 by adsorbing virus at 37°C for 1 h in Tris-buffered salt solution (0.14 M NaCl, 5 mM KCl, 0.7 mM $Na_2HPO_4$, 5.5 mM glucose, 100 U of penicillin per ml, 100 μg/ml of streptomycin, and 25 mM Trizma base [Sigma Chemical Co., St. Louis, Mo.], pH 7.4), with occasional rocking. Medium was then added, and the infection was allowed to proceed at 37°C for 46 to 48 h, a time when SV40 DNA replication is maximal under these conditions (16; S. Kondoleon, personal communication).

HMT. Tritiated 4'-hydroxymethyl-4,5',8-trimethylpsoralen (HMT) was generously provided by S. Isaacs and J. Hearst. Stock solutions of approximately 80 μg/ml were made in ethanol. Radioactivity measurements were determined by counting equal portions in a mixture of 1 ml of water and 10 ml of Omnifluor-Triton scintillation fluid (2 liters of toluene, 1 liter of Triton X-100 [Research Products International Corp., Elk Grove Village, Ill.], and 12 g of Omnifluor [New England Nuclear Corp., Boston, Mass.]) in a Beckman LS-345 scintillation counter. The absorbance at 249 nm of an aqueous dilution of HMT was measured in a Beckman Acta III spectrophotometer, and specific activities were calculated by using an extinction coefficient in 100% water at this wavelength of 25,000 $M^{-1}$ $cm^{-1}$ (21). The HMT stock solutions in the reported experiments had a specific activity of 4 X $10^7$ cpm/μg of HMT.

[$^3$H]HMT labeling of infected cells. The medium was removed from cells at 46 h postinfection and replaced with "albino" medium lacking UV absorbents as described by Hallick et al. (16). Cells were then labeled with [$^3$H]HMT by one of two methods. In the first method, a large tissue

culture plate (500 $cm^2$; Vanguard International, Inc., Neptune, N.J.) of infected cells was preincubated for 30 min with the fresh medium, after which time all but 10 ml of it was aspirated. Tritiated HMT was added at a concentration of 1.2 to 12.0 $\mu g/10^8$ cells, and the plate was irradiated directly on a bank of six General Electric F15T8 BLB fluorescent tubes at an incident light intensity of 2.2 $mW/cm^2$ for 30 min. The tissue culture dish was rocked and rotated frequently to ensure uniform drug distribution and irradiation. Irradiations were performed in a cold room to counteract the heat from the light source; the temperature of the medium equilibrated to 22°C after 5 min and remained constant throughout the course of the irradiation.

In the second method, cells from five tissue culture dishes were scraped with a rubber policeman and pelleted by centrifugation for 5 min at 600 X g. Cells were suspended in 2.0 ml of albino medium and transferred to a 100-mm bacterial culture dish (Falcon Plastics, Oxnard, Calif.) to prevent reattachment of the cells. Drug addition and cell irradiation took place exactly as described in the first method.

Isolation of SV40 DNA. SV40 DNA was isolated from infected cells by a modification of the Hirt procedure (19) as described by Hallick et al.(16). [$^3$H]HMT-labeled cell suspensions were washed with Tris-saline and pelleted by centrifugation for 5 min at 600 X g. After the Hirt extraction, SV40 DNA in the supernatant was deproteinized with self-digested pronase (Sigma) and banded by density equilibrium centrifugation in ethidium bromide-CsCl (4.10 gm of CsCl [Merck & Co., Inc., Rahway, N.J.], 4.15 ml of DNA solution, and 50 µl of 20mg/ml ethidium bromide for 16 to 19 h at 53,000 rpm and 20°C in the Beckman VTi 65 rotor) to separate supercoiled SV40 DNA from nicked circular and

linear DNA. The supercoiled DNA was extracted five times with butanol and dialyzed against TE buffer (10 mM Tris-hydrochloride-1 mM EDTA, pH 8.1).

[$^3$H]HMT labeling of purified SV40 DNA. Unlabeled SV40 DNA purified as described above and twice banded on ethidium bromide-CsCl gradients (>90% supercoiled molecules) was used for preparing in vitro psoralen-labeled DNA samples. SV40 DNA was diluted into 1.0 ml of TE buffer or, where indicated, TE buffer plus 0.15 M NaCl. Tritiated HMT was added at a concentration of 140 to 4300 pg of drug per μg of DNA, and the mixture was irradiated for 30 min in a 35 mm tissue culture dish (Falcon) on the bank of fluorescent lights previously described. After irradiation, the [$^3$H]HMT-labeled DNA solution was made 1.0 M in NaCl and extracted three times with chloroform-isoamyl alcohol (24:1) to remove noncovalently bound [$^3$H]HMT and dialyzed against TE buffer.

Restriction enzyme digestions. Supercoiled SV40 DNA, [$^3$H]HMT-labeled either in vitro or in vivo, was concentrated by ethanol precipitation at -20°C. Precipitates were collected after centrifugation at 12,000 rpm for 30 min in a Sorvall HB-4 rotor and suspended in TE buffer at a concentration of 1 μg of DNA/μl.

Restriction endonucleases Hind III, Hpa II, and Atu I were obtained from Bethesda Research Laboratories (Bethesda, Md). Figure 1 shows the restriction map of SV40 for these three enzymes. SV40 DNA digestions with Atu I were performed at 37°C for 4 h in 20 mM Tris-hydrochloride, pH 7.4, 7mM $MgSO_4$, 60 mM NaCl, 10 mM dithiothreitol, and 500 μg of gelatin per ml. The Hind III concentration was 5U/μg of DNA, and the Hpa II concentration was 3 U/μg of DNA.

Figure 1. Physical Map of SV40 DNA.

The sites of cleavage by the various restriction enzymes are shown relative to the single cleavage site for Eco RI. There are six cleavage sites for Hind III, one site for Hpa II and 17 sites for Atu I, an isoschizomer of Eco RII. The location of the replication origin is also indicated.

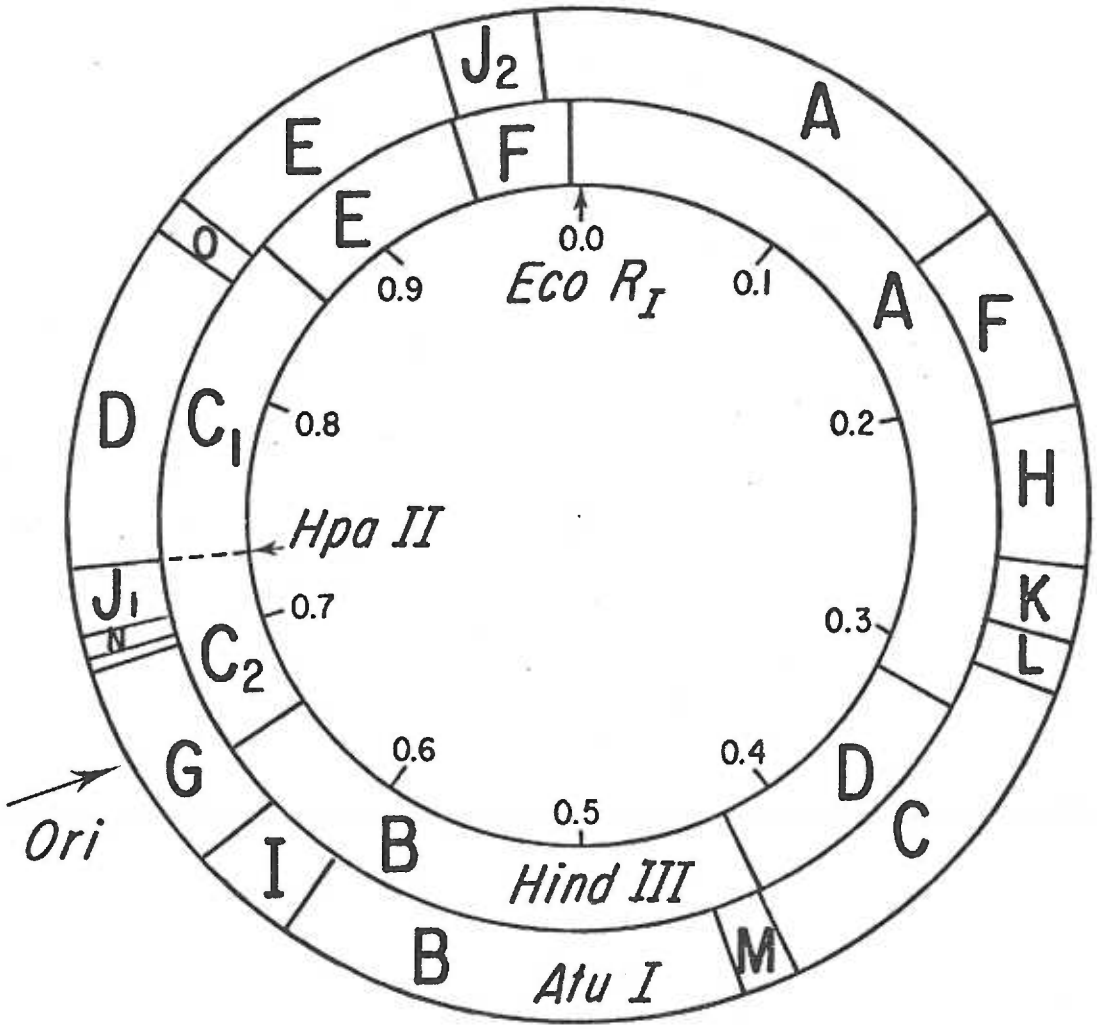
J2
A
E
F
E
0.0
0.9
Eco RI
0.1
A
F
O
D
C1
0.8
0.2
H
Hpa II
J1
N
0.7
0.3
K
L
C2
G
0.6
0.4
D
Ori
0.5
I
B
Hind III
C
B
Atu I
M

Gel electrophoresis. The DNA fragments, containing 150 μg of bromphenol blue per ml, 5% (wt/vol) Ficoll, 0.3% sodium dodecyl sulfate, and 10mM Tris-hydrochloride, pH 8.0, were separated in vertical 4.5% polyacrylamide slab gels (20:1, acrylamide/bisacrylamide; 15 by 14 by 0.15 cm) in E buffer (40 mM Tris, pH 7.1, 20mM sodium acetate, and 2mM EDTA). The restriction digests were electrophoresed at 60 V for 17 h (Hind III-Hpa II digests) or at 42 V for 18 h (Atu I digests). Buffer was continuously recirculated between the top and bottom chambers during electrophoresis.

Assessment of DNA distribution in gels. Polyacrylamide gels were stained for 30 min in E buffer which contained ethidium bromide (2.5 μg/ml) and DNA framents were visualized on a Chromatovue transilluminator (Ultra-Violet Products, Inc., San Gabriel, Calif.). DNA distributions in individual gel lanes were estimated from ethidium bromide fluorescence by a modification of the method of Pulleyblank et al. (39). Photographic negatives of the stained gel were produced by using Kodak Tri-X film (4 by 5 inch [ca. 10 by 12.5 cm]) and a Linhoff-Technikoff camera equipped with a Wratten 23A filter. Negatives were scanned with a densitometer (Transidyne, Ann Arbor, Mich.).

Determination of radioactivity in restriction enzyme digest fragments. Individual gel lanes were sliced into 1.3 mm fractions and solubilized in scintillation vials by the method of Mahin and Lofberg (30) (0.2 ml of 60% perchloric acid and 0.4 ml of 30% hydrogen peroxide, incubated with shaking for 4.5 h at 60°C). Fractions were counted after adding 0.5 ml of water and 10 ml of Omnifluor-Triton scintillation fluid and allowing 24 h for dark adaptation. The channel ratio method was employed to monitor tritium quenching. The amount of tritium

radioactivity present in DNA bands was determined by pooling appropriate fractions after aligning the peaks from parallel gel lanes of in vivo- and in vitro-labeled samples. Thus, the same number of fractions was included for a given fragment in both samples.

## RESULTS

Photoaddition of [$^3$H]HMT to SV40 DNA. To determine the in vivo distribution of nucleosomes on the SV40 genome, SV40 DNA was labeled intracellularly with the psoralen derivative [$^3$H]HMT by irradiation with UV light 48 h after infection (Table 1). A low level of HMT photoaddition (1 to 10 drug molecules/SV40 genome) was chosen to minimize alterations in chromatin structure and interference with subsequent restriction enzyme digestion which might occur with the intercalation of high levels of psoralen derivatives. The first two samples were prepared by irradiating a suspension of cells, whereas the third sample was irradiated as a monolayer of infected cells attached to a single large tissue culture dish. The higher specific activity and labeling density achieved with a cell monolayer probably reflects the greater efficiency of irradiation under these conditions.

Control samples of purified DNA were labeled over approximately the same 10-fold range as the in vivo-labeled samples (Table 1). This in vitro-labeled DNA serves as a model for labeled chromatin in the case where nucleosomes are positioned randomly with respect to the SV40 map. In both situations, all sites on the genome should be equally accessible to photoaddition. In vitro DNA also provides a control for any sequence-specific binding of psoralens to particular regions of the SV40

TABLE 1.

[$^3$H]HMT-Labeled SV40 DNA Preparations[a]

| Expt | Irradiation condition | μg of HMT/ $10^8$ cells | pg of HMT/ μg of SV40 DNA | HMT adducts/ SV40 genome | Spc act ($^3$H cpm/ μg of DNA) |
|---|---|---|---|---|---|
| Prepn | | | | | |
| In vivo labeled | | | | | |
| 1 | Suspension | 1.2 | | 1.3 | 3,800 |
| 2 | Suspension | 12.0 | | 6.3 | 18,600 |
| 3 | Monolayer | 8.7 | | 11.0 | 31,300 |
| In vitro labeled | | | | | |
| 1 | TE buffer | | 135 | 1.6 | 4,700 |
| 2 | TE buffer | | 935 | 8.2 | 24,500 |
| 3 | TE buffer | | 1,190 | 10.1 | 30,000 |
| 4 | TE buffer | | 1,350 | 13.6 | 38,000 |
| 5 | TE buffer + 0.15 M NaCl | | 4,270 | 19.1 | 56,800 |

[a] Samples were irradiated, purified, and analyzed for specific activity as described in the text.

genome which might occur over that range of drug additions.

In all of the in vitro-labeled samples but the last one (number 5), the photoaddition of HMT to purified SV40 DNA was carried out in TE buffer. In those samples, the labeling density achieved was roughly proportional to the amount of drug added. In the last sample, the DNA was irradiated in TE buffer plus physiological saline. As expected, from the results of Hyde and Hearst (20), the efficiency of photoaddition was twofold lower at this elevated ionic strength.

Quantitation of [$^3$H]HMT photoaddition. SV40 DNA labeled with [3H]HMT intracellularly or under in vitro conditions was examined for the distribution of drug on the viral genome. Samples were digested simultaneously with the restriction enzymes Hind III and Hpa II (see Fig. 1), and the resulting DNA fragments were separated by electrophoresis on 4.5% polyacrylamide slab gels (Fig. 2). In all cases, digests of in vivo- and in vitro-labeled samples were electrophoresed in parallel on the same gel to control for any losses of smaller fragments during gel staining. Data obtained by the use of a photographic method of DNA quantitation indicated that such losses did occur to a limited extent, but that the overall distributions of DNA in parallel gel lanes were equivalent (unpublished data).

The gels containing the digested fragments were sliced, and the DNA was analyzed for radioactivity (Fig. 2 and Table 2). The amount of radioactive HMT bound to each restriction fragment is expressed in two ways. In the first method, the amount of radioactivity in each fragment is given as a percentage of the total radioactivity for all restriction fragments recovered (Table 2). The only significant difference in

Figure 2. Hind III-Hpa II Cleavage Pattern of SV40 DNA.

The DNA was labeled with [$^{3}$H]HMT under in vitro (A) or in vivo (B) conditions as described in the text. SV40 form I DNA was purified and digested with Hind III and Hpa II restriction endonucleases. The resulting fragments were separated by gel electrophoresis and analyzed for radioactivity as described in the text. Inserts show photographs of ethidium bromide stained gels.

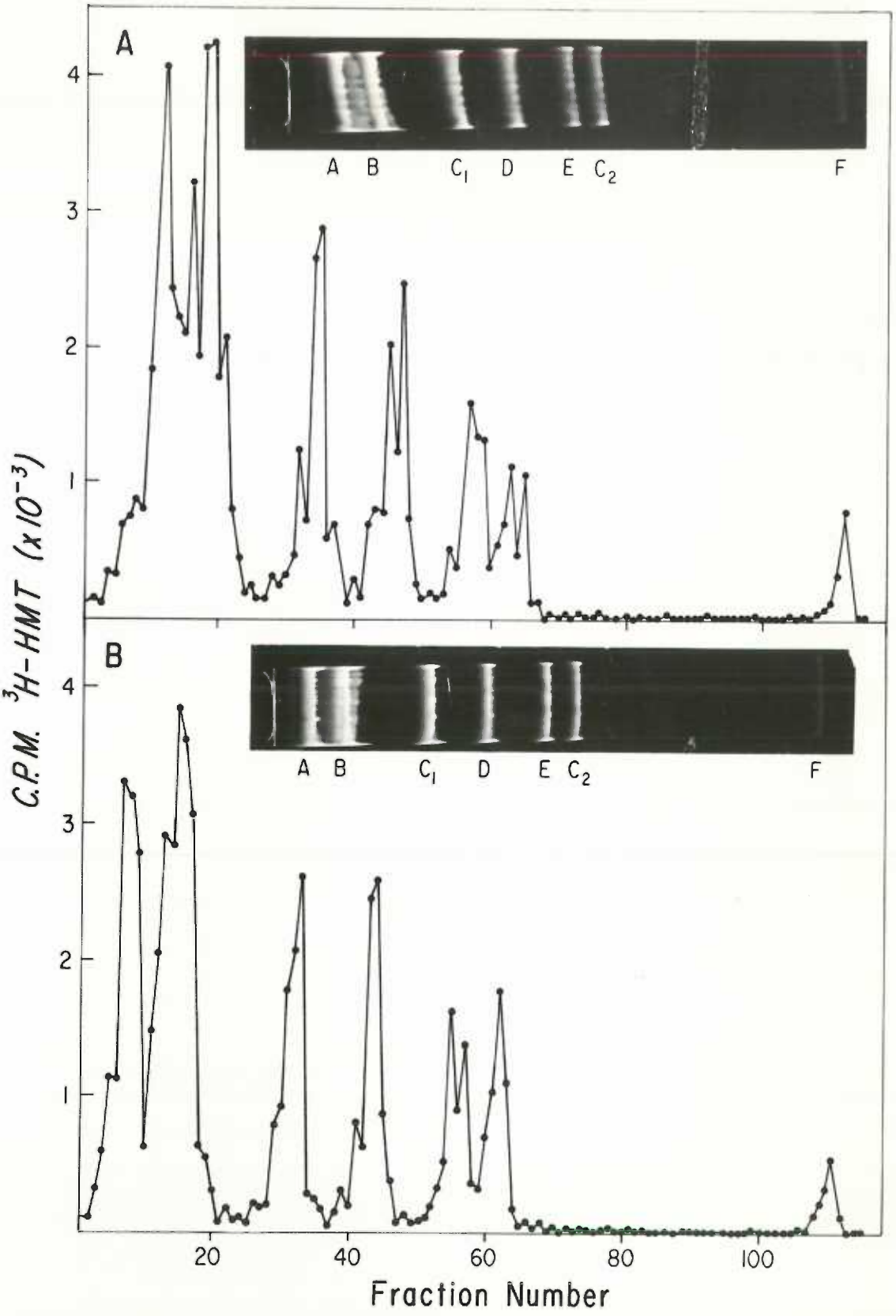
A
A B C1 D E C2 F
B
A B C1 D E C2 F
C.P.M. ³H-HMT (x 10⁻³)
1
2
3
4
20
40
60
80
100
Fraction Number

TABLE 2 LEGEND

[a] The percentage of total radioactivity recovered was calculated for each of four experiments, and the values were averaged. The data are presented as this average ± the standard error of the mean.

[b] Specific activities were calculated by dividing the counts per minute by the molecular weight of the fragment, normalizing to fragment $C_1$ as 1.0, and averaging four experiments as described in footnote a.

[c] Fragments A and B were combined for analysis due to incomplete separation of these bands on the gels.

[d] N.S., Not significant at $P < 0.05$ by Student's t-test.

TABLE 2.

Hind III-Hpa II Restriction Enzyme Analysis

| Fragment | % Total [$^3$H]HMT[a] | | | |
|---|---|---|---|---|
| | In vivo (N=4) | In vitro (N=4) | Ratio | Significance |
| A[c] B | 53.36 ± 0.82 | 54.07 ± 1.39 | 0.99 | N.S.[d] |
| $C_1$ | 14.93 ± 0.43 | 14.93 ± 0.95 | 1.00 | N.S. |
| D | 12.60 ± 0.50 | 13.53 ± 0.36 | 0.88 | N.S. |
| E | 8.65 ± 0.34 | 9.63 ± 0.31 | 0.90 | N.S. |
| $C_2$ | 8.45 ± 0.27 | 5.51 ± 0.18 | 1.53 | p<0.001 |
| F | 2.03 ± 0.20 | 2.34 ± 0.18 | 0.87 | N.S. |
| | Normalized sp act[b] | | | |
| A[c] B | 0.85 ± 0.02 | 0.88 ± 0.08 | 0.97 | N.S. |
| $C_1$ | 1.00 ± 0.00 | 1.00 ± 0.00 | 1.00 | |
| D | 1.13 ± 0.08 | 1.22 ± 0.08 | 0.93 | N.S. |
| E | 0.91 ± 0.05 | 1.02 ± 0.07 | 0.89 | N.S. |
| $C_2$ | 1.00 ± 0.05 | 0.65 ± 0.04 | 1.54 | p<0.005 |
| F | 0.45 ± 0.05 | 0.52 ± 0.07 | 0.87 | N.S. |

labeling density between the in vivo and in vitro samples was found with the C2 fragments. As can be seen from the ratio of the in vivo to the in vitro samples (Fig 3), the fragment labeled intracellularly contained 53% more radioactive label than the control.

Fragment radioactivities expressed as percentage of total [$^3$H]HMT can bias the data slightly because all fragment values are pooled for the calculation and thus become dependent on one another. For this reason, a second method of analysis was used in which specific activities were calculated for each fragment by dividing $^3$H counts per minute recovered by the molecular weight for that fragment predicted by the sequence (41). Specific activities of all fragments were then normalized to the specific activity of fragment $C_1$ which was arbitrarily assigned a value of 1.00. The ratio of in vivo to in vitro values was then calculated as before. The results obtained by this method of analysis indicated that the in vivo-prepared sample contained 54% more HMT on the $C_2$ fragment than the in vitro-prepared sample (Table 2), in complete agreement with the calculation of percentage of total radioactivity described previously.

To further map the [$^3$H]HMT-labeled regions of the SV40 genome, a second restriction enzyme was used. Atu I was used because it allows regions within the $C_2$ fragment and the unseparated A + B fragment in the Hind III-Hpa II digest to be examined (see Fig. 1). When the [$^3$H]HMT-labeled DNA samples were digested with Atu I and the distribution of radioactivity on polyacrylamide gels was determined (Fig. 4), significant differences between the in vivo and in vitro samples were found on three restriction fragments (Table 3 and Fig. 3). By using the methods of analysis previously described (percentage of

Figure 3. Accessibility of the SV40 Genome to [$^3$H]HMT Photoaddition.

The ratio of in vivo to in vitro percentage of total $^3$H counts is indicated. Cross-hatched bars indicate fragments for which ratios of in vivo/in vitro values were statistically different than 1.0.

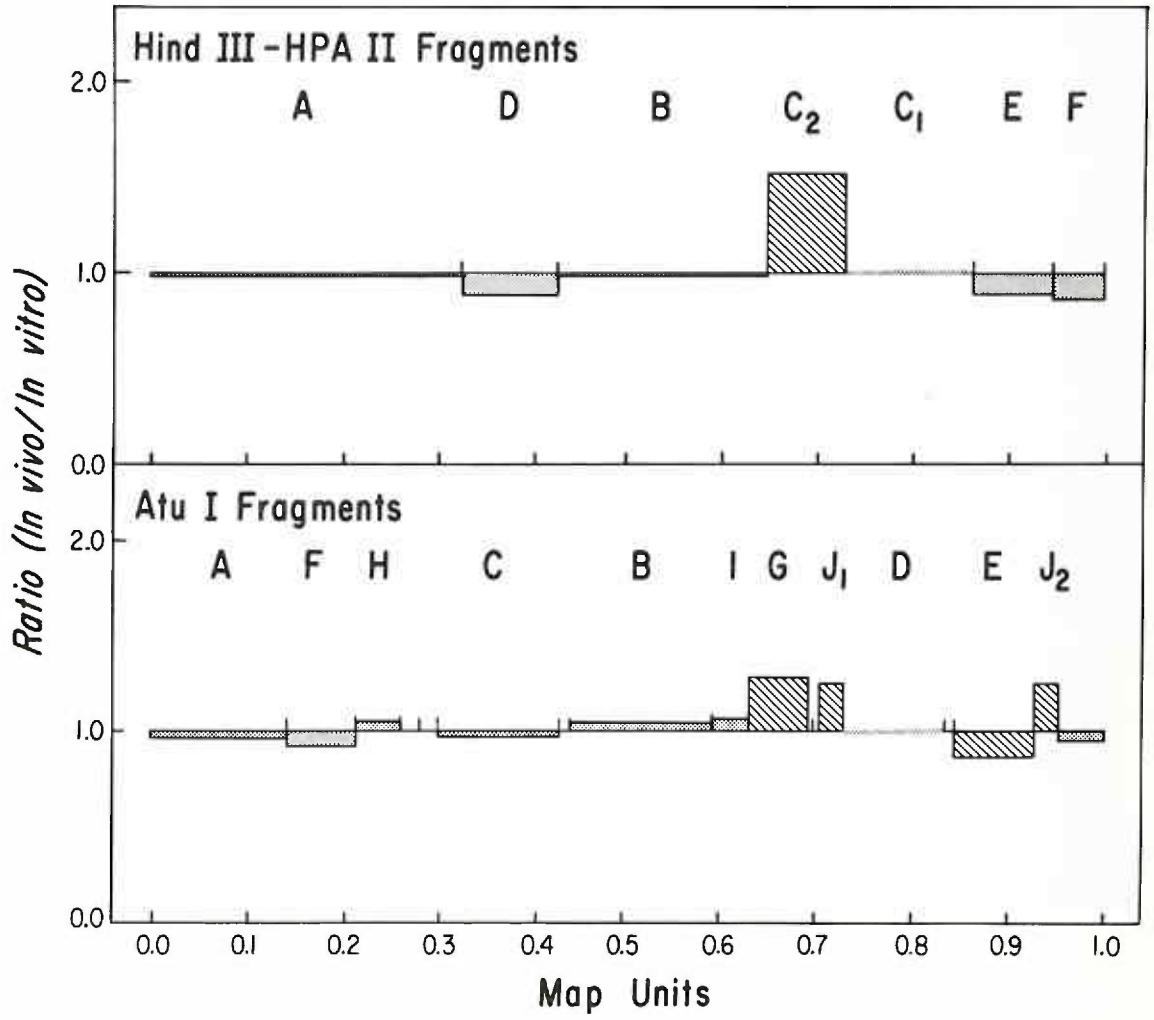
Hind III - HPA II Fragments
A
D
B
C2
C1
E
F
2.0
1.0
0.0
Atu I Fragments
A
F
H
C
B
I
G
J1
D
E
J2
2.0
1.0
0.0
0.0
0.1
0.2
0.3
0.4
0.5
0.6
0.7
0.8
0.9
1.0
Map Units
Ratio (In vivo/In vitro)

Figure 4. Atu I Cleavage Pattern of SV40 DNA.

The DNA was labeled with [$^{3}$H]HMT under in vitro (A) or in vivo (B) conditions as described in the text. Labeled SV40 form I DNA was purified and digested with Atu I, and the resulting fragments were separated by gel electrophoresis and analyzed for radioactivity as described in the text. Inserts show photographs of ethidium bromide-stained gels.

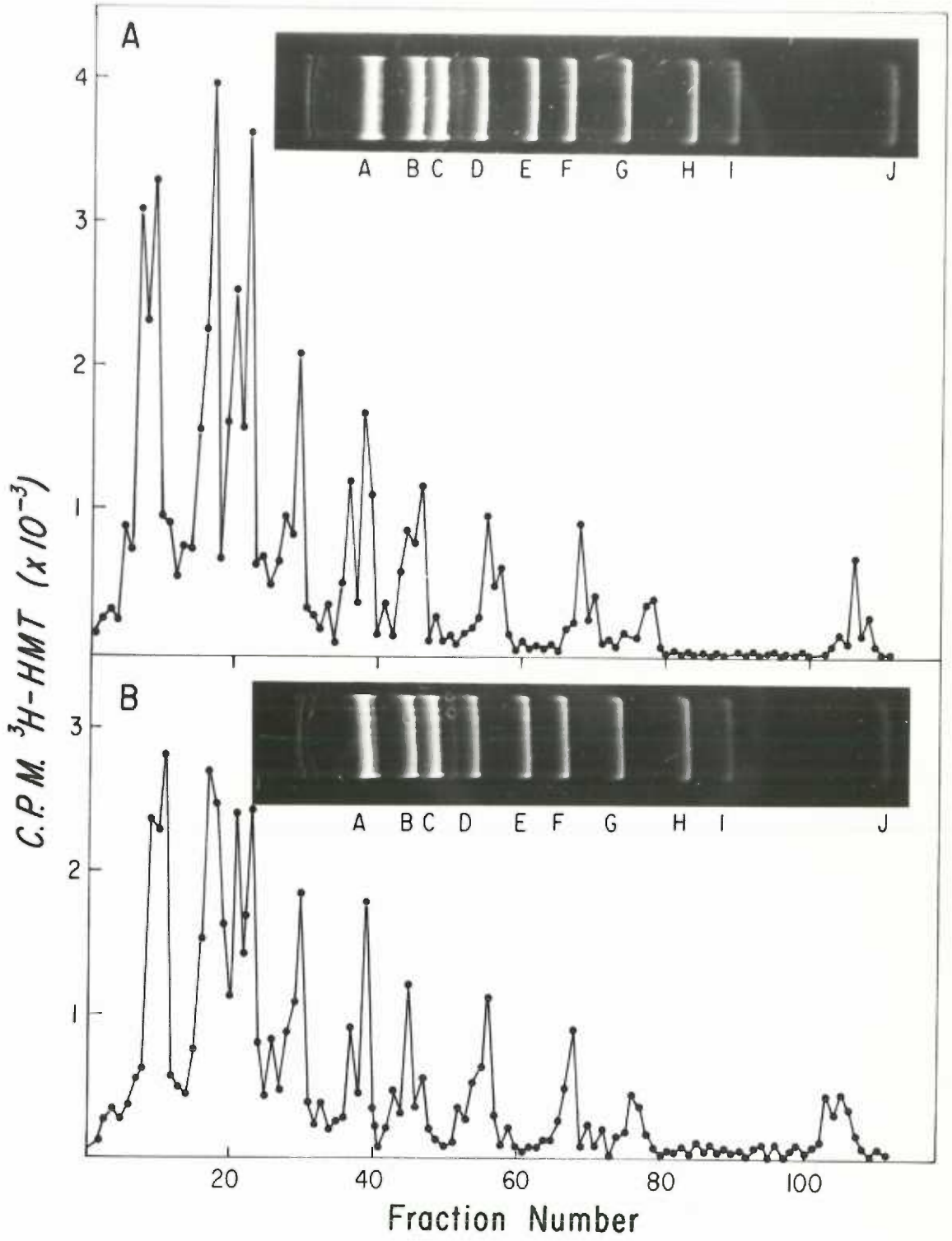
A
B
A B C D E F G H I J
A B C D E F G H I J
C.P.M. $^3$H-HMT (x10$^{-3}$)
1
2
3
4
20
40
60
80
100
Fraction Number

TABLE 3 LEGEND

[a] Percentage of total radioactivity recovered and specific activities were calculated as described in Table 2. Normalization was to fragment D.

[b] N.S., Not significant at $p<0.05$ by Student's t-test.

[c] Fragments K through P represent 5% of the total genome and were run off the gel during electrophoresis; fragment J is composed of $J_1$ (127 bp) and $J_2$ (126 bp).

TABLE 3.

Atu I Restriction Enzyme Analysis[a]

| Fragment | % Total [$^3$H]HMT | | | |
|---|---|---|---|---|
| | In vivo (N=8) | In vitro (N=6) | Ratio | Significance |
| A | 20.79 ± 0.81 | 21.66 ± 0.56 | 0.96 | N.S.[b] |
| B | 20.87 ± 1.21 | 20.13 ± 0.98 | 1.04 | N.S. |
| C | 16.24 ± 0.79 | 16.69 ± 0.98 | 0.97 | N.S. |
| D | 10.56 ± 0.25 | 10.59 ± 0.37 | 1.00 | N.S. |
| E | 8.29 ± 0.07 | 9.49 ± 0.20 | 0.87 | p<0.001 |
| F | 6.73 ± 0.31 | 7.35 ± 0.09 | 0.92 | N.S. |
| G | 6.66 ± 0.24 | 5.22 ± 0.08 | 1.28 | p<0.001 |
| H | 4.22 ± 0.21 | 4.06 ± 0.14 | 1.04 | N.S. |
| I | 2.23 ± 0.08 | 2.19 ± 0.04 | 1.06 | N.S. |
| J[c] | 3.31 ± 0.17 | 2.64 ± 0.08 | 1.25 | p<0.01 |
| | Normalized sp act | | | |
| A | 1.10 ± 0.05 | 1.15 ± 0.06 | 0.96 | N.S. |
| B | 1.33 ± 0.08 | 1.28 ± 0.06 | 1.04 | N.S. |
| C | 1.27 ± 0.07 | 1.31 ± 0.11 | 0.97 | N.S. |
| D | 1.00 ± 0.00 | 1.00 ± 0.00 | 1.00 | |
| E | 0.98 ± 0.03 | 1.12 ± 0.04 | 0.88 | p<0.001 |
| F | 0.96 ± 0.05 | 1.05 ± 0.04 | 0.91 | N.S. |
| G | 1.13 ± 0.06 | 0.88 ± 0.02 | 1.28 | p<0.005 |
| H | 0.89 ± 0.06 | 0.86 ± 0.04 | 1.03 | N.S. |
| I | 0.61 ± 0.02 | 0.58 ± 0.03 | 1.05 | N.S. |
| J[c] | 0.69 ± 0.05 | 0.54 ± 0.02 | 1.28 | p<0.025 |

total [$^3$H]HMT and normalized specific activity), Atu I fragments G and J of the in vivo-labeled samples were found to contain 28% more [$^3$H]HMT than the in vitro-labeled samples. In contrast, fragment E contained 13% less HMT in the in vivo samples than in the in vitro samples.

In all of the experiments described above, in vivo- and in vitro-prepared samples were labeled with HMT to the same molar ratio and electrophoresed in the same gel to reduce the effect of systematic experimental errors. No significant differences by the chi-square test of homogeneity were ever noted between different in vitro samples labeled over the indicated range of HMT densities or labeled in the presence or absence of 0.15 M NaCl. Similarly, no differences were noted among in vivo samples labeled over the range of HMT densities or among samples irradiated as cell suspensions or monolayers. The data from all appropriate experiments were therefore pooled, and averages are presented in Tables 2 and 3.

From the restriction map of the SV40 genome (Fig. 1), it can be seen that the Hind III-Hpa II fragment $C_2$ and the Atu I fragments G and J all mapped between 0.646 and 0.726 map units. The results from Tables 2 and 3 indicate that this region was preferentially photolabeled with HMT under in vivo labeling conditions relative to in vitro labeling conditions.

## DISCUSSION

The sites of intracellular SV40 chromatin most accessible to psoralens are not randomly distributed over the genome. The results from the analysis of psoralen distribution patterns using two sets of

restriction enzymes show that the region encompassing the origin of SV40 DNA replication, the T-antigen-binding sites, and the promoters of early and late transcription is preferentially labeled. The coordinates of this region agree remarkably well with those previously determined for the location of a nucleosome-free region on extracted minichromatin. The open region detected by either endonuclease digestion or electron microscopy generally extends from 0.66 to 0.75 map units.

In the Atu I digestion (Table 3), two additional fragments have specific activities that are significantly different ($P<0.05$) for in vivo DNA and in vitro control DNA. Fragment E (0.84 to 0.93 map units) was protected from photoaddition in vivo, whereas fragment $J_2$ (0.93 to 0.95 map units) exhibited an enhanced specific activity. A comparison with the Hind III-Hpa II results (Table 2) suggests that the protected region may in fact be real even though its biological importance is not known. A similar comparison suggests that the enhanced $J_2$ region is probably an artifact that results from unseparated $J_1$ and $J_2$ fragments. Thus, the actual increase in specific activity of the $J_1$ fragment may be as high as 50%, equivalent to the increase observed in the Hind III-Hpa II digests.

The size of the accessible region of in vivo chromatin can be estimated if two assumptions are made. The first assumption is that the ease of psoralen photoadditon to this open region is comparable to that seen for other non-nucleosomal regions of chromatin. The second assumption, frequently made in nuclease digestion studies is that DNA treated in vitro serves as a model for chromatin with randomly positioned nucleosomes. SV40 minichromosomes contain approximately 24 nucleosomes (45). Thus, each nucleosome is separated by an average of

72 bp of internucleosomal (accessible) DNA and protects 146 bp of core DNA. Table 4 shows the portion of each restriction fragment in a Hind III-Hpa II digest that would be accessible to [$^3$H]HMT photoaddition if the nucleosomes were positioned randomly. It can be seen that 138 of 417 bp would be accessible to drug on the $C_2$ fragment. When the comparison was made between in vivo and in vitro (random chromatin) HMT-labeling patterns, approximately 50% more label was found on this fragment in vivo (Fig. 2 and Table 2). Therefore, an average of 207 of 417 bp on the $C_2$ fragment from intracellular SV40 chromatin should be accessible to drug. This value is based on labeling analyses of total SV40 chromatin; thus, it is a valid estimate only if all chromatin molecules have this nucleosome configuration. Our results do not distinguish between this possibility and an alternative situation, in which a fraction of the molecules contain a larger open region. Recent electron microscope studies have reported that approximately 20 to 25% of total SV40 minichromosomes possess a nucleosome-free region (22, 45). If we take 25% of the molecules as an average figure, we can then estimate that 414 of 417 bp should be exposed to psoralen derivatives on this fraction of total chromatin molecules. This size estimate is consistent with the reported electron micrograph measurements (250 to 320 bp) of the accessible region (22, 45) and also with the estimates reported in nuclease digestion experiments (315 to 400 bp) (47, 62).

The theory of the photoaddition technique for determining accessible regions of DNA in chromatin is based upon the same rationale as that of endonuclease digestion. Both the nucleases and the psoralens permanently "mark" accessible (primarily linker) regions of DNA in chromatin, the nucleases by cutting and the psoralens by binding to DNA

TABLE 4.

Accessibility of Hind III-Hpa II Restriction Fragments with Randomly Positioned Nucleosomes[a]

| Fragment | Molecular length (bp) | Protected DNA (bp) | Accessible DNA (bp) |
|---|---|---|---|
| A<br>B | 2,937 | 1,968 | 969 |
| $C_1$ | 701 | 470 | 231 |
| D | 526 | 352 | 174 |
| E | 447 | 299 | 148 |
| $C_2$ | 417 | 279 | 138 |
| F | 215 | 144 | 71 |
| Total | 5,243 | 3,512 | 1,731 |

[a] This model is based on SV40 minichromosomes that possess 5,243 bp of DNA and 24 nucleosomes randomly distributed around the genome. Each nucleosome protects 146 bp of DNA and is separated from the adjacent nucleosomes by an average of 72 bp. It is assumed that 72/218 = 0.33 of each fragment is available for psoralen photoaddition.

at these sites. Thus, highly accessible regions within chromatin should be marked with a high frequency with either method (66). A potential problem with the use of both these methods is that of DNA sequence specificity in the marking reagent. For example, psoralen derivatives are thought to react primarily with thymidine residues. Thus, two linker regions of identical size could be marked with different frequencies if one of the linkers contained highly A-T-rich sequences. This could lead to the erroneous conclusion that the two linker regions were of different size. We have corrected for the sequence specificity of psoralens by comparing marker patterns produced with purified DNA as a substrate against the patterns observed with chromatin as a substrate. A separate study of potential sequence effects on psoralen photoaddition will be reported elsewhere.

Psoralen photoaddition appears to be a powerful technique for examining the accessibility of DNA in chromatin structures. The major advantage of this approach over conventional approaches which use isolated minichromatin for analysis is that chromatin structure can be probed within intact cells with little if any disruption of nuclear organization. The covalent nature of psoralen photoadducts ensures that a stable record of nucleosome position remains on the DNA, and thereby makes it unnecessary to maintain chromatin structure once the actual labeling is completed. Therefore, the labeled DNA can be quantitatively extracted and rigorously purified before the determination of drug distribution. Thus, DNA samples used in the experiments reported here accurately represent the total population of intracellular SV40 supercoiled molecules.

When type II restriction enzymes are used for analyses of SV40 chromatin structure, they yield information that is relevant to DNA accessibility at enzyme recognition sites, or at best small regions around the sites. A poor or limited choice of enzymes would lead to conclusions that are not based on accessibility over the entire genome. Like the enzyme micrococcal nuclease, the psoralen derivatives lack strong DNA site specificity. Thus, determinations with the latter two reagents should give information that pertains to the most accessible region on the whole minichromatin molecule.

At present, there is uncertainty over the role played by the psoralen and nuclease-accessible region of SV40 chromatin. Late during infection (40 to 60 h), various subpopulations of chromatin can be isolated that are undergoing replication (31, 43, 48), transcription (12, 14), or encapsidation into virions (11, 49). Any or all of these processes may require a chromatin substrate that has a nucleosome-free region. The finding of an SV40 chromatin subfraction enriched in molecules with an open region would suggest a functional role of this structure. Using electron microscopy and site-specific endonucleases, L. Tack, P. Wassarman, and M. DePamphilis (J. Biol. Chem., in press) have analyzed pulse-labeled replicating chromatin and report that this population is not enriched for open-origin molecules. Virion and intracellular previrion chromatin complexes have been examined by DNase I digestion, and it has been found that preferential cleavage in the open region is lost or altered during encapsidation (18). A correlation between transcription and this open region has not, as yet, been reported.

The intriguing question as to whether T-antigen interacts with this nucleosome-free region has also not been addressed. T-antigen is required for initiation of DNA replication and for regulation of transcription (5, 26, 44, 46, 54). On the basis of in vitro studies, this protein is presumed to function in vivo only after it has become bound to SV40 origin sequences (31, 34, 43, 48). We are currently using temperature-sensitive T-antigen mutants and deletions of small t-antigen in psoralen-labeling experiments to define the relationship between T-antigen binding and chromatin molecules that possess an open region.

While this manuscipt was in preparation, we learned of results obtained by P. Beard and his colleagues (1) on the binding of acetylaminofluorene to intracellular SV40 nucleoprotein complexes. Unlike psoralen derivatives, this compound reacts primarily with guanine residues, and yet the levels bound to a DNA fragment near the origin of replication (0.663 to 0.715 map units) were 1.5 to 2.0-fold higher than the levels bound at other genomic locations. The results of acetylaminofluorene binding are thus in fundamental agreement with our analysis of psoralen binding.

REFERENCES

1. Beard, P., M. Kaneko and P. Cerutti. (1981). N-acetoxy-acetylaminofluorene reacts preferentially with a control region of intracellular SV40 chromosome. Nature (London) 291, 84-85.

2. Cech, T. and M. L. Pardue (1977). Cross-linking of DNA with trimethylpsoralen is a probe for chromatin structure. Cell 11, 631-640.

3. Cech, T. R., D. Porter and M. L. Pardue. (1978). Chromatin structure in living cells. Cold Spring Harbor Symp. Quant. Biol. 42, 191-198.

4. Cole. R. S. (1970). Light-induced cross-linking of DNA in the presence of a furocoumarin (psoralen). Biochem. Biophys. Acta 217, 30-39.

5. Cowan, K., P. Tegtmeyer and D. D. Anthony. (1973). Relationship of replication and transcription of simian virus 40 DNA. Proc. Natl. Acad. Sci. U.S.A. 70, 1927-1930.

6. Cremisi, C. (1979). Chromatin replication revealed by studies of animal cells and papovaviruses (SV40 and polyoma). Microbiol. Rev. 43, 297-319.

7. Cremisi, C., P. F. Pignatti and M. Yaniv. (1976). Random location and absence of movement of the nucleosomes on SV40 nucleoprotein complex isolated from infected cells. Biochem. Biophys. Res. Commun. 73, 548-554.

8. Danna, K. J., G. H. Sack, Jr. and D. Nathans. (1973). Studies of simian virus 40 DNA. VII. A cleavage map of the SV40 genome. J. Mol. Biol. 78, 363-376.

9. Das, G. C., D. P. Allison and S. K. Niyoki. (1979). Sites including those of origin and termination of replication are not available to single cut restriction endonucleases in the supercompact form of SV40 minichromosome. Biochem. Biophy. Res. Commun. 89, 17-25.

10. Felsenfeld, G. 1978. Chromatin. Nature (London) 271, 115-121.

11. Garber, E. A., M. M. Seidman and A. J. Levine. (1978). The detection and characterization of multiple forms of SV40 nucleoprotein complexes. Virology 90, 305-316.

12. Gariglio, P., R. Llopis, P. Oudet and P. Chambon. (1979). The template of the isolated native simian virus 40 transcriptional complex is a minichromosome. J. Mol. Biol. 131, 75-105.

13. Ghosh, P., V. Reddy, J. Swinscoe, P. Lebowitz and J. Weissman. (1978). Heterogeneity and 5'-terminal structures of the late RNA's of simian virus 40. J. Mol. Biol. 126, 813-846.

14. Green, M.H. and T. L. Brooks (1976). Isolation of two forms of SV40 nucleoprotein containing RNA polymerase from infected monkey cells. Virology 72, 110-120.

15. Gutai, M. and D. Nathans. (1978). Evolutionary variants of simian virus 40: nucleotide sequence of a conserved SV40 DNA segment containing the origin of viral DNA replication as an inverted repetition. J. Mol. Biol. 126, 259-274.

16. Hallick, L. M., H. A. Yokota, J. C. Bartholomew and J. E. Hearst. (1978). Photochemical addition of the cross-linking reagent 4,5',8-trimethylpsoralen to intracellular and viral simian virus 40 DNA-histone complexes. J. Virol. 27, 127-135.

17. Hanson, C. V., C. J. Shen and J. E. Hearst, (1976). Cross-linking of DNA in situ as a probe for chromatin structure. Science 193, 62-64.

18. Hartmann, J. P. and W. A. Scott. (1981). Distribution of DNAse I-sensitive sites in simian virus 40 nucleoprotein complexes from disrupted virus particles. J. Virol. 37, 908-915.

19. Hirt, B. (1967). Selective extraction of polyoma DNA from infected mouse cell culture. J. Mol. Biol. 26, 365-369.

20. Hyde, J. E. and J. E. Hearst. (1976). Binding of psoralen derivatives to DNA and chromatin: influence of the ionic environment on dark binding and photoreactivity. Biochemistry. 17, 1251-1257.

21. Isaacs, S. T., J. C. Shen, J. E. Hearst and H. Rapoport. (1977). Synthesis and characterization of new psoralen derivatives with superior photoreactivity with DNA and RNA. Biochemistry 16, 1058-1064.

22. Jakobovits, E. B., S. Bratosin and Y. Aloni. (1980). A nucleosome-free region in SV40 minichromosomes. Nature (London) 285, 263-265.

23. Jessel, D., T. Landau, J. Hudson, T. Lalor, D. Tenen and D. M. Livingston. (1976). Identification of regions of the SV40 genome which contain preferred SV40 T-Antigen binding sites. Cell 8, 535-545.

24. Kornberg, R. D. (1977). Structure of chromatin. Annu. Rev. Biochem. 46, 931-955.

25. Krauch, C. H., D. M. Kramer and A. W. Wacker. 1967. Zum Wirkungsmechanismum photodynamischer furocumarine. Photoreaktion

von psoralen-(4-$^{14}$4C) mit DNS, RNS, homopolynucleotiden und nucleosiden. Photochem. Photobiol. 6, 341-354.

26. Lai, C. and D. Nathans. (1975). A map of temperature-sensitive mutants of simian virus 40. Virology 66, 70-81.

27. LeBon, J., C. Kado, L. Rosenthal and J. Chrikjian. (1978). DNA modifying enzymes of agrobacterium tumefaciens: effect of DNA topoisomerase, restriction endonuclease, and unique DNA endonuclease on plasmid and plant DNA. Proc. Natl. Acad. Sci. U.S.A. 75, 4097-4101.

28. Liggins, G. L., M. English and D. A. Goldstein. (1979). Structural changes in simian virus 40 chromatin as probed by restriction endonucleases. J. Virol. 31, 718-732.

29. Lutter, L. C. (1979). Precise location of DNase I cutting sites in the nucleosome core determined by high resolution gel electrophoresis. Nucleic Acids Res. 6, 41-56.

30. Mahin, D. T. and R. T. Lofberg, (1966), A simplified method of sample preparation for determination of $^{3}$H, $^{14}$C, or $^{35}$S in blood or tissue by liquid scintillation counting. Anal. Biochem. 16, 500-509.

31. Mann, K. and T. Hunter. (1979). Association of simian virus 40 T-antigen with simian virus 40 nucleoprotein complexes. J. Virol. 29, 232-241.

32. McGhee, J. D. and G. Felsenfeld. (1980), Nucleosome structure. Annu. Rev. Biochem. 49, 1115-1156.

33. Musajo, L., G. Rodighiero, A. Breccia, F. Dall'Acqua and G. Malesani. (1966). Skin-photosensitizing furocoumarins:

photochemical interaction between DNA and -o$^{14}CH_3$bergapten (5-methoxypsoralen). Photochem. Photobiol. 5, 739-745.

34. Meyers, R. M. and R. Tijan. (1980). Construction and analysis of simian virus 40 origins defective in tumor antigen binding and DNA replication. Proc. Natl. Acad. Sci. U.S.A. 77, 6491-6495.

35. Nathans, D. and K. J. Danna. (1972). Specific origin in SV40 DNA replication. Nature (London) New Biol. 236, 200-202.

36. Pathak, M. A. and D. M. Kramer. (1969). Photosensitization of skin in vivo by furocoumarins (psoralens). Biochim. Biophys. Acta 195, 197-206.

37. Polisky, B. and B. McCarthy. (1975). Location of histones on SV40 DNA. Proc. Natl. Acad. Sci. U.S.A. 72, 2895-2899.

38. Ponder, B. A., Jr. and L. V. Crawford. 1977. The arrangement of nucleosomes in nucleoprotein complexes from polyoma virus and SV40 Cell 11, 35-49.

39. Pulleyblank, D. E., M. Shure and J. Vinograd. (1977). The quantitation of fluorescence by photography. Nucleic Acids Res. 4, 1409-1418.

40. Reddy, V., P. Ghost, P. Lebowitz, M. Piatak and S. Weissman. (1979). Simian virus 40 early mRNA's. I. Genomic localization of 3' and 5' termini and two major splices in mRNA from transformed and lytically infected cells. J. Virol. 30, 279-296.

41. Reddy, V. B., B. Thimmappaya, R. Dahr, K. N. Subramanian, B. S. Zain, J. Pan, P. K. Ghosh, M. L. Celma and S. M. Weissman. (1978). The genome of SV40. Science 200, 494-502.

42. Reed, S., J. Ferguson R. W. Davis, and G. R. Stark. (1975). T-antigen binds to simian virus 40 DNA at the origin of replication. Proc. Natl. Acad. Sci U.S.A. 72, 1605-1609.

43. Reiser, J., J. Renart, L. V. Crawford and G. R. Stark. (1980). Specific association of simian virus 40 tumor antigen with simian virus 40 chromatin. J. Virol. 33, 78-87.

44. Rio, D., A. Robbins, R. Myers and R. Tijan. (1980). Regulation of simian virus 40 early transcription in vitro by a purified tumor antigen. Proc. Natl. Acad. Sci. U.S.A. 77, 5706-5719.

45. Saragosti, S., G. Moyne and M. Yaniv. (1980). Absence of nucleosomes in a fraction of SV40 chromatin between the origin of replication and the region coding for the late leader RNA. Cell 20, 65-73.

46. Scott, W. A., W. M. Brockman and D. Nathans. (1976). Biological activities of deletion mutants of simian virus 40. Virology 75, 319-334.

47. Scott, W. A. and D. J. Wigmore. (1978). Sites in simian virus 40 chromatin which are preferentially cleaved by endonuclease. Cell 15, 1511-1518.

48. Segawa, M., S. Sugano and N. Yamaguchi. (1980). Association of simian virus 40 T-antigen with replicating nucleoprotein complexes of simian virus 40. J. Virol. 35, 320-330.

49. Seidman, M., E. Garber and A. J. Levine. (1979). Parameters affecting the stability of SV40 virions during the extraction of nucleoprotein complexes. Virology 95, 256-259.

50. Shelton, E. R., P. M. Wassarman and M. L. DePamphilis. (1980). Structure, spacing and phasing of nucleosomes on isolated froms of mature SV40 chromosomes. J. Biol. Chem. 255, 771-782.

51. Shortel, D. R., R. F. Margolskee and D. Nathans. (1979). Mutational analysis of the simian virus 40 replicon: pseudorevertants of mutants with a defective replication origin. Proc. Natl. Acad. Sci. U.S.A. 76, 6128-6131.

52. Subramanian, K. and T. Shenk. (1978). Definition of the boundaries of the origin of replication of simian virus 40. Nucleic Acids Res. 5, 3635-3642.

53. Sundin, O. and A. Varshavsky. (1979). Staphylococcal nuclease makes a single non-random cut in the simian virus 40 minichromosome. J. Mol. Biol. 132, 535-546.

54. Tegtmeyer, P. (1972). Simian virus 40 DNA synthesis: the viral replicon. J. Virol. 10, 591-598.

55. Thoma, R., T. Koller and A. Klug. (1979). Involvement of histone H1 in the organization of the nucleosome and the salt-dependent super-structures of chromatin. J. Cell. Biol. 83, 403-427.

56. Thompson, J. A., M. F. Radonovich and N. P. Salzman. (1979). Characterization of the 5'-terminal structure of simian virus 40 early mRNA's. J. Virol. 31, 437-446.

57. Tijan, R. (1978). The binding site on SV40 DNA for a T-Antigen related protein. Cell 13, 165-179.

58. VanHolde, K. E., C. G. Sahasrubuddhe and B. R. Shaw. (1974). A model for particulate structure in chromatin. Nucl. Acids Res. 1, 1579-1586.

59. Varshavsky, A. J., V. V. Bakayev, P. M. Chumackov and G. P. Georgiev. (1976). Minichromosome of simian virus 40: presence of histone H1. Nucleic Acids Res. 3, 2101-2113.

60. Varshavsky, A. J., V. V. Bakayev, P. M. Chumackov and G. P. Georgiev. (1976). Heterogeneity of chromatin subunits in vitro and location of hisone H1. Nucleic Acids Res. 3, 476-492.

61. Varshavsky, A. J., O. H. Sundin and M. J. Bohn. (1978), SV40 viral minichromosome: preferential exposure of the origin of replication as probed by restriction endonucleases. Nucleic Acids Res. 16, 3469-3477.

62. Varshavsky, A. J., O. Sundin and M. Bohn. (1979). A stretch of late SV40 viral DNA about 400bp long which includes the origin of replication is specifically exposed in SV40 minichromosomes. Cell 16, 453-466.

63. Waldeck, W., B. Fohring, K. Chowdhury, P. Gruss and G. Sauer. (1978). Origin of DNA replication of papovavirus chromatin is recognized by endogenous endonuclease. Proc. Natl. Acad. Sci. U.S.A. 75, 5964-5968.

64. Whitlock, J. P. and R. T. Simpson. (1976). Removal of histone H1 exposes a fifty base pair DNA segment between nucleosomes. Biochemistry. 15, 3307-3314.

65. Wiesehahn, G. P. and J. E. Hearst. (1976). The site of trimethylpsoralen cross-linking in chromatin, p. 27-32. In D.P. Nierlich, W. J. Rutter, and C. F. Fox (ed.). Molecular mechansims in the control of gene expression, ICN-UCLA Symposium, vol. 5, Academic Press, Inc., New York.

66. Wiesehahn, G. P., J. E. Hyde and J. E. Hearst. (1977). The photoaddition of trimethylpsoralen to Drosophila melanogaster nuclei: a probe for chromatin substructure. Biochemistry 16, 925-932.

PAPER 2.

# SV40 Virus Particles Lack a Psoralen-Accessible Origin and Contain an Altered Nucleoprotein Structure

ABSTRACT

The nucleoprotein structure of SV40 virions was examined by photolabeling purified virus with the radioactive psoralen derivative hydroxymethyltrimethylpsoralen (HMT). Unlike SV40 chromatin *in situ*, the viral origin region is not preferentially accessible to drug addition. The ratio of the distribution of radioactivity in the DNA restriction fragments of virion DNA to that of purified SV40 DNA demonstrates that the photoadducts are positioned similarly on the circular molecule in both samples. Virion purified from infected cells was also analyzed for the presence of an open region and found to exhibit the same pattern of [$^3$H]HMT addition as mature extracellular virion. The nucleosome-free region detected at the SV40 replication origin in intracellular minichromosomes is not present in either population of intact virus particles. We also examined the level of drug addition obtained when purified virion or SV40-infected cells were treated with saturating doses of [$^3$H]HMT. Marked differences in the plateau levels of bound drug indicate that an altered nucleoprotein structure exists in SV40 virions that does not protect the DNA from photoaddition to the same extent as do the nucleosomes of intracellular SV40 DNA.

## INTRODUCTION

The SV40 minichromosome isolated from infected cells is organized in a nucleosome structure very similar to that of cellular chromatin (for reviews, see 10, 22, 26,) Each circular viral DNA molecule contains 21 ± 2 nucleosome core particles, and a highly variable linker region of 58 ± 40 base pairs of DNA (13, 38). The spacing of the nucleosomes along the chromatin molecule was shown to be nonrandom in a subpopulation of minichromosomes with a nucleosome-free region approximately 300 base pairs long at map positions 0.66-0.75 (20, 36, 37, 41, 45, 46,). Its existence is particularly intriguing since located within these sequences are the origin of replication (14, 30, 40) the region encoding the 5' ends of early and late SV40 mRNA (12, 32, 42) as well as the preferred binding sites for T antigen (21, 34, 39, 43)

Recently we demonstrated that the technique of psoralen photoaddition to DNA is a powerful tool to analyze viral nucleoprotein structures in infected cells. These compounds have the ability to penetrate intact cells, intercalate into DNA, and under the influence of long-wavelength UV light covalently bind to pyrimidines of the DNA (9, 23, 29, 31). Since nucleosomal core DNA is preferentially protected from psoralen photoaddition (5, 47, 48). psoralen derivatives are valuable probes for examining the structure of both cellular (5, 6, 16,48) and viral (15) chromatin. By photolabeling SV40-infected cells with a radioactive psoralen derivative, hydroxymethyltrimethylpsoralen (HMT), we found that a 400 base pair region around the origin of replication was preferentially labeled indicating that the

nucleosome-free region detected by others in isolated viral chromatin also exists *in vivo* (35).

There is accumulating evidence that the SV40 genome in virus particles is structurally and biochemically different from SV40 minichromosomes in infected cells. Virion chromatin complexes probed with nucleases were unusually sensitive to digestion and the interpretation was that the distinction between nucleosomal DNA and linker DNA was absent (4). Recently Moyne (28) examined nucleoprotein complexes obtained by mild dissociation at neutral pH from virions. Their results indicate that the four core histones, although present in virions, are not arranged in typical nucleosomes in the released complexes. They concluded that the virion proteins were involved in partially unfolding the nucleosomes. The progressive maturation of the intracellular minichromosome to released virus particle is likely a complex process with multiple discrete intermediates characterized by altered structures and unique biochemical activity. It has been demonstrated that SV40 virion prepared from nuclei is distinguishable from released virus by stability, histone content and *in vitro* transcriptional activity (4,24).

We have examined the accessibility of SV40 DNA in virions to psoralen photoaddition in order to determine whether the origin region is preferentially available to labeling as found in intracellular viral complexes. We find that the origin region on the virion genome is not preferentially labeled. When intracellular virus particles were purified from cells late in infection and examined in a similar manner, it was found that the psoralen labeling pattern was identical to that found with mature, extracellular virus. In both cases, no region of the

genome was preferentially labeled with the drug. Finally, experiments with [$^3$H]HMT at saturating drug doses indicate that the level of protection from photoaddition provided by nucleosomes is considerably reduced in virion DNA relative to intracellular SV40.

## MATERIALS AND METHODS

Cells and virus stocks. SV40 strain 776, provided by K. Danna, was grown in the African green monkey kidney cell lines CV-1, obtained from P. Berg, and MA-134, purchased from Microbiological Associates (Bethesda, Md.). The maintenance of cell cultures, the preparation of SV40 stocks and the infection of CV-1 cells for the psoralen labeling of intracellular SV40 DNA have all been described recently (35). High multiplicity infection (moi approximately 10) of MA-134 cells was the source of SV40 for virus purification. The seed stocks, however, are routinely produced by low multiplicity infections. Infections were harvested at 3.5 days to recover cellular virion and released extracellular virion. For total SV40 virion, infections were allowed to proceed to completion, when >90% of the monolayer was destroyed.

Virus Purification. Virion was recovered from infected MA-134 cells and medium (Ann Roman, personal communication). Briefly, cells were removed from the medium by low speed centrifugation and the medium was adjusted to 50 mM Tris, pH 7.4. This medium was the source of released, extracellular virion. Pelleted cells were resuspended in 5 volumes TBS (150 mM NaCl, 5mM KCl, 0.7mM $Na_2HPO_4$, 0.9mM $CaCl_2$, 1mM $MgCl_2$, 20mM Tris, pH 7.4) followed by 3 freeze-thaw cycles. Cell debris was removed by low speed centrifugation. Additional cellular virion was

recovered when the cell debris was resuspended in 1-2 volumes TBS and extracted with one-fifth volume $CHCl_3$. The aqueous phase of the $CHCl_3$ extraction and the preceding cell supernatant were combined for the purification of cellular virion. Cellular fractions and medium were combined for the recovery of total virion. Virus was concentrated by centrifugation onto 5ml of a 1.5 $g/cm^3$ CsCl shelf in a Beckman SW27 rotor centrifuged for 3 hr at 25,000 rpm (4°C). The translucent band immediately below the CsCl shelf was collected and dialyzed into TBS. Virus was further purified by banding to equilibrium in 1.33 $g/cm^3$ CsCl in a Beckman VTi65 rotor at 55,000 rpm for 16 hr (4°C). The virus band at 1.34 $g/cm^3$ was dialyzed into TBS. Purified SV40 was adjusted to 0.5% fetal calf serum and stored at -20°C.

HMT . 4'-hydroxymethyl-4,5',8-trimethylpsoralen (HMT) was generously provided by S. Isaacs and J. Hearst. Ethanol stock solutions of approximately 100 µg/ml were used in most experiments. For psoralen saturation trials, stock HMT solutions were concentrated to 2.9 mg/ml. The specific activity of [$^3$H]HMT was determined as previously described (35) and ranged from approximately $5x10^5$ cpm/µg (saturation of purified SV40 DNA) to $5x10^7$ cpm/µg (photoaddition to purified virion). In all experiments, the conditions for photoirradiation were chosen to produce a level of 5-20 HMT molecules per viral genome.

[$^3$H]HMT labeling of SV40-infected cells and purified virion. SV40-infected CV-1 cells were labeled with [$^3$H]HMT as described (35). Purified virion in either TBS with 5% fetal calf serum or "albino medium" (15) was irradiated in tissue culture dishes with an incident lamp intensity of 2.5-3.0 $mW/cm^2$. Total virion was photoreacted to a level 59,000 cpm [$^3$H]HMT/µg DNA; intracellular and extracellular virion

specific activities were both 25,000 cpm [$^3$H]HMT/μg DNA. Immediately following irradiation, virus was rebanded in CsCl equilibrium density gradients to ensure that only intact virion was used for subsequent analysis. CsCl-banded [$^3$H]HMT-virus was dialyzed into TBS before further treatment.

[$^3$H]HMT labeling of purified SV40 DNA. SV40 FI DNA was [$^3$H]HMT-labeled and served as a control for both intracellular SV40 and purified virion. The control DNA was irradiated in "albino medium" with 5% FCS to a specific activity of 40,000 cpm [$^3$H]HMT/μg DNA. The control DNA in the intracellular-extracellular virion experiment was irradiated in TE plus 0.1M NaCl, to a specific activity of 15,000 cpm [$^3$H]HMT/μg DNA. The incident lamp intensity for irradiation of purified DNA was 2.4 mW/cm$^2$.

[$^3$H]HMT saturation experiments. For the HMT saturation of intracellular SV40 chromatin (48 hr post infection) and of total virion, multiple additions of 15-20 μg/ml [$^3$H]HMT diluted in "albino medium" were made every 30 minutes during irradiation. Drug additions were alternated with complete media changes for the cells or dialysis for the virus such that the ethanol concentration was never greater than 1% or 2% respectively. [$^3$H]HMT-virus was rebanded to equilibrium in CsCl as described above. The virus band was collected and dialyzed into TBS before further treatment. The procedure for the saturation of SV40 FI DNA was identical to that followed for virion saturation except DNA samples were in TE plus 0.12M NaCl. Following irradiation, the [$^3$H]HMT-DNA was ethanol precipitated, collected by centrifugation and resuspended in TE. DNA samples were equilibrium banded in CsCl-ethidium bromide gradients as described below and finally dialyzed into TE.

Isolation of SV40 DNA. SV40 DNA was isolated from infected cells by a modification of the Hirt procedure (18) as described by Hallick et al. (15). Following the Hirt extraction, SV40 DNA in the supernatant was deproteinized with self-digested pronase (Calbiochem) and purified by density equilibrium centrifugation in ethidium bromide-CsCl (4.15g CsCl, 4.15 ml DNA solution, 50µl of 20 mg/ml ethidium bromide) for 20hr at 45,000 rpm at 20°C in a Beckman VTi65 rotor. Pooled DNA fractions were extracted 5 times with n-butanol and dialyzed into TE.

SV40 virions were adjusted to 25mM EDTA, pH 8.0, 1% sarkosyl, 2mg/ml pronase and were digested at 50°C for 3 hr. Viral DNA was banded to equilibrium, butanol extracted and dialyzed as above.

Restriction enzyme digestions. [$^3$H]HMT-labeled SV40 FI DNA was precipitated by ethanol at -20°C. DNA was pelleted by centrifugation at 12,000 rpm for 30 min in a Sorvall HB-4 rotor and resuspended in TE at a concentration of 1µg/µl.

Restriction endonucleases Hind III, Kpn I, Hinf I, Taq I were obtained from Bethesda Research Laboratories (Bethesda, Md.). Figure 1 depicts the restriction map of the SV40 genome for the two double digests Hind III-Kpn I and Hinf I- Taq I. SV40 DNA digestion with Hinf I was performed at 37°C for 3 hr in 10mM Tris, pH 8.0, 10mM $MgSO_4$, 100 mM NaCl, 10mM dithiothreitol (Bio-Rad, Richmond, Ca.), 100 µg/ml gelatin. Hinf I concentration was 5U/µg DNA. This sample was diluted by one-third and incubated with Taq I at 7U/µg DNA at 65°C for 3hr. SV40 DNA digestion with Kpn I was conducted at 37° for 3 hr in 10mM Tris, pH 7.5, 10mM $MgSO_4$, 10mM NaCl, 10mM dithiothreitol, 100 µg/ml gelatin. Kpn I concentration was 6U/µg DNA. Following Kpn I digestion this sample was diluted by one-third volume and the Tris and NaCl

Figure 1. Physical Map of SV40 DNA.

The sites of cleavage by the various restriction enzymes are shown relative to the single cleavage site for Eco RI. There are six cleavage sites for Hind III and one site for Kpn I. There are ten cleavage sites for Hinf I and one site for Taq I. The location of the replication origin is also indicated.

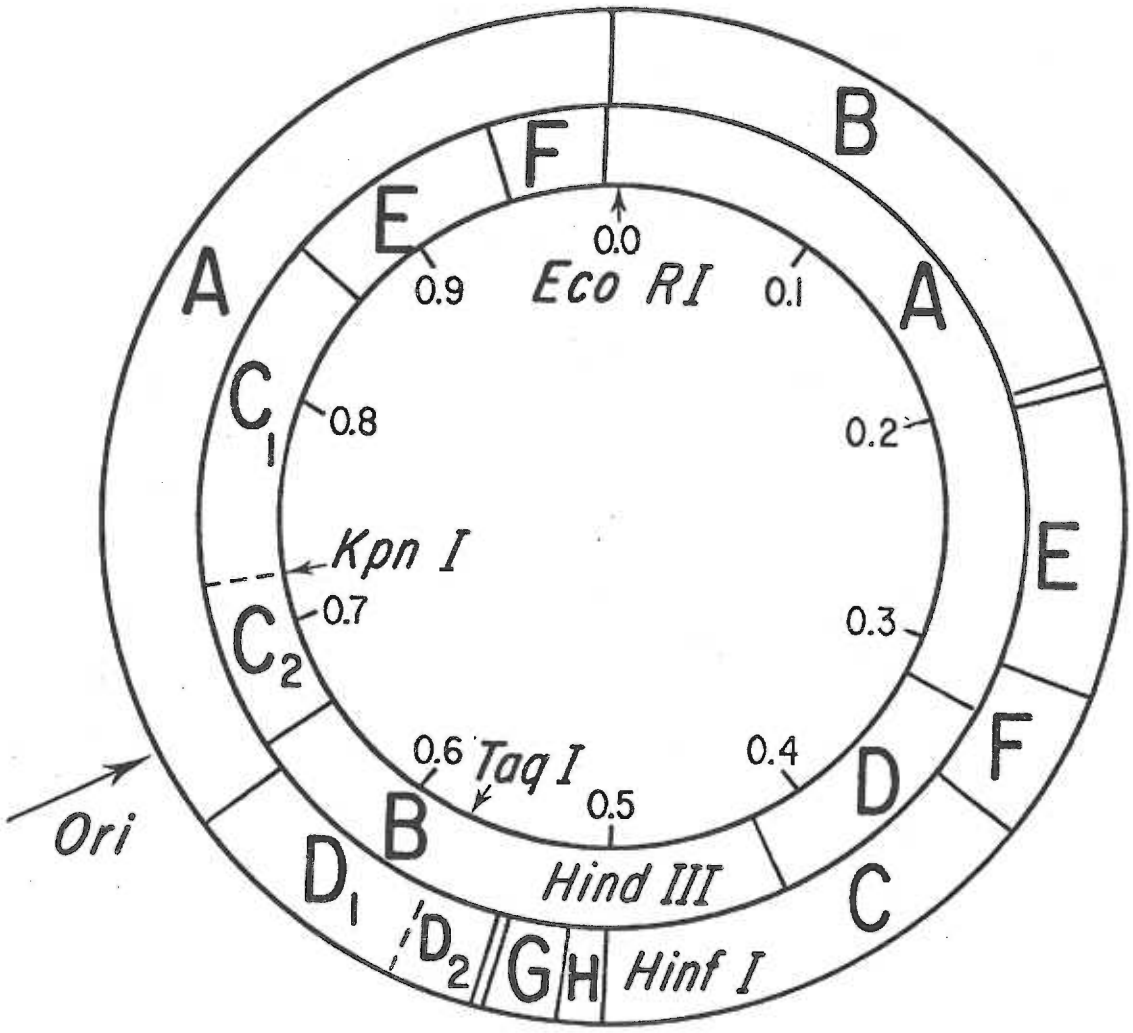
0.0
Eco RI
0.1
0.2
0.3
0.4
0.5
Hind III
0.6
Taq I
0.7
Kpn I
0.8
0.9
Hinf I
Ori
A
B
A
E
F
E
C1
C2
B
D
F
D1
D2
G
H
C

concentrations were both increased to 50mM. Hind III was added at 6U/μg DNA and incubation continued at 37C° for 3hr. Reactions were terminated by adding aliquots of electrophoresis tracking dye to make the final concentration 150μg/ml bromphenol blue, 8% sucrose and 15 mM EDTA, pH 8.1.

Gel electrophoresis. The DNA fragments were separated in vertical 4.5% polyacrylamide slab gels as described previously (35). The restriction digests were electrophoresed at 50V for 18 hr. Digested [$^3$H]HMT-labeled DNA from SV40-infected cells or virion was always electrophoresed in parallel on the same gel with control DNA labeled *in vitro*.

Assessment of DNA distribution in gels. Polyacrylamide gels were stained for 15 min in electrophoresis buffer (40 mM Tris, pH 7.1, 20mM sodium acetate, 2mM EDTA) which contained 2μg/ml ethidium bromide and the DNA fragments visualized on a chromatovue transilluminator (Ultra-violet Products, Inc., San Gabriel, Calif.). The DNA distribution in individual gel lanes was determined by monitoring ethidium fluorescence with a Quick Scan R and D scanning densitometer (Helena Laboratories, Beaumont, Tx.).

Determination of radioactivity in restriction enzyme digest fragments. Individual gel lanes were sliced, solubilized and analyzed for the distribution of radioactivity as already detailed (35).

## RESULTS

Photoaddition of [$^3$H]HMT to SV40 Infected Cells and To Purified Virion. When SV40-infected cells were labeled with psoralen 48 hr.

post-infection it was shown that a 400 base pair (bp) restriction fragment located between 0.65 and 0.73 map units was preferentially labeled (35). It was of interest to determine whether this same region of the SV40 genome was still preferentially accessible to psoralen photoadditon in purified virions. Two virion samples were HMT-labeled independently to levels of 15-20 drug molecules per SV40 genome, and the purified DNA analyzed after digestion with two different sets of restriction enzymes. A low level of HMT photoaddition was chosen to minimize alterations in chromatin structure and interference with subsequent restriction enzyme digestion which might occur with the intercalation of high levels of psoralen derivatives.

Control samples of purified DNA were labeled over approximately the same range of drug addition as the treated viral samples. This [$^3$H]HMT-labeled SV40 DNA served as the model for labeled chromatin where nucleosomes are positioned randomly along the SV40 genome. With both purified DNA and with chromatin possessing randomly spaced nucleosomes, all DNA sites are equally available for psoralen photoaddition. [$^3$H]-HMT-DNA also provides a control for any sequence-specific binding of psoralens to particular regions of the SV40 genome that may occur over this range of photoaddition.

[$^3$H]HMT-labeled SV40 DNA from intact virions was examined for the distribution of psoralen on the viral genome. DNA samples were digested with the restriction enzymes Hind III and Kpn I (see Fig. 1) and the resulting DNA fragments were separated by electrophoresis on 4.5% polyacrylamide slab gels. The gels containing the separated restriction fragments were sliced and the gel slices were processed for radioactivity (Fig. 2). The amount of radioactive HMT bound to each

restriction fragment was expressed as the percentage of the total radioactivity for all restriction fragments recovered (Table 1). When SV40 virion DNA was probed with psoralens, the labeling pattern of restriction fragments was comparable to that seen in the irradiated control DNA. As can be seen in Fig. 3, the ratio of the virion-labeled DNA fragments to those labeled as purified DNA is very close to 1.0 for all seven restriction fragments and no significant differences were observed.

In contrast, when in vivo chromatin was reacted with [$^3$H]HMT, the distribution of drug is nonrandom. For a direct comparison between intracellularly labeled SV40 DNA and virion labeled DNA, SV40-infected CV-1 cells were reacted with [$^3$H]HMT 48 hr post-infection and the purified DNA digested with Hind III and Kpn I. The radioactivity profile of the electrophoretically separated restriction fragments is shown in Fig. 2 and the analysis of the [$^3$H] HMT distribution in Table 2. Although most of the SV40 genome labeled in vivo appears randomly labeled, there is one striking exception. There was significant difference in the labeling density of the $C_2$ fragment. As can be seen from the ratio of the in vivo chromatin and purified DNA samples (Fig. 3), the intracellularly labeled $C_2$ fragment contained 63% more radioactive HMT than the control $C_2$ fragment.

The radioactivity of the restriction fragments expressed as percentage of total [$^3$H]HMT may bias the data slightly because all fragment values are pooled for the calculation and so become dependent on one another. To avoid that possibility, a second method of analysis was used in which specific activities were calculated for each fragment by dividing $^3$H counts per minute recovered by the molecular weight of

Figure 2. Hind III-Kpn I Cleavage Pattern of SV40 DNA.

Intact virion, purified SV40 DNA or *in vivo* chromatin was labeled with [$^3$H]HMT as described in the text. SV40 Form I DNA was purified and digested with Hind III and Kpn I restriction endonucleases. The resulting fragments were separated by gel electrophoresis and analyzed for radioactivity.

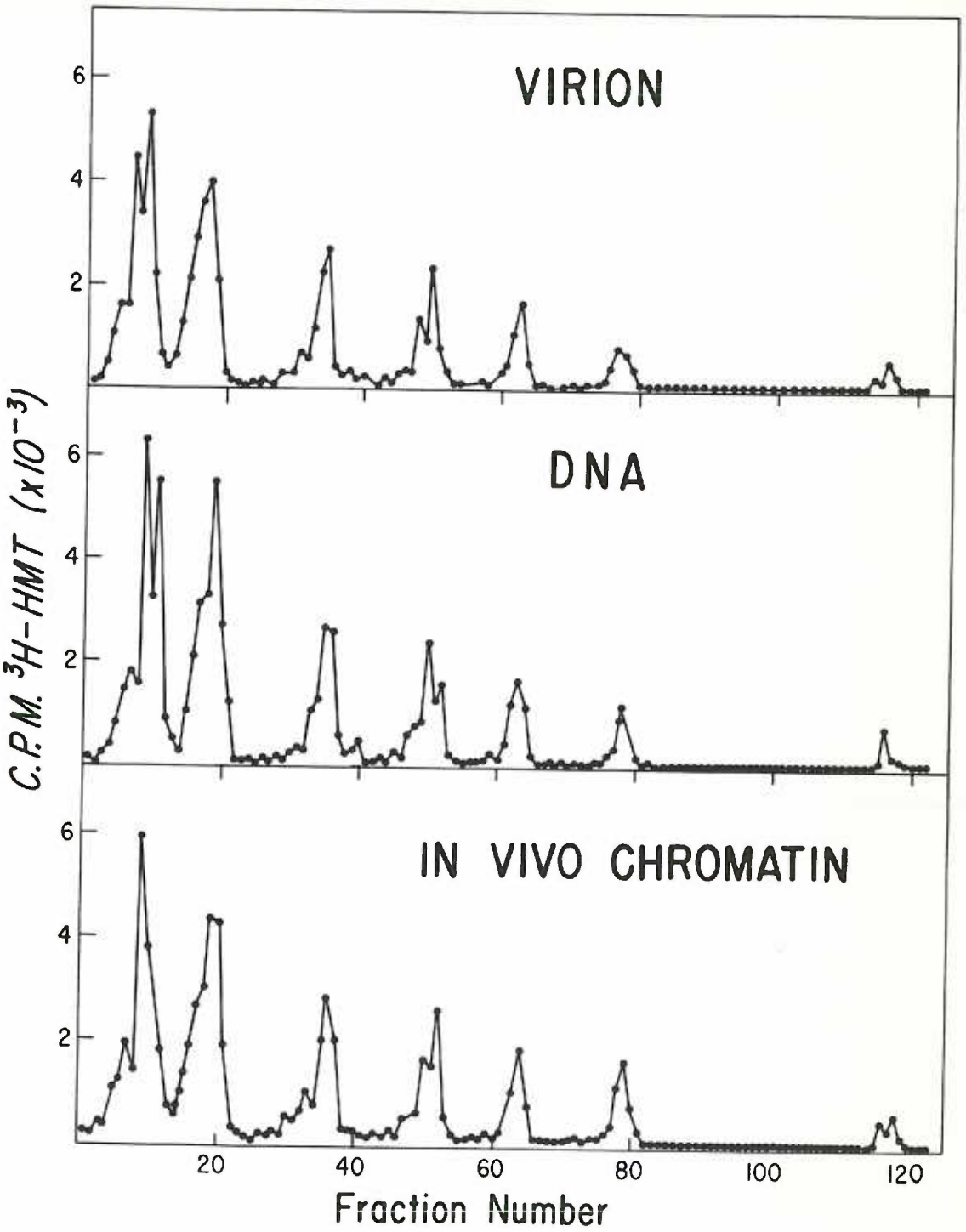
VIRION
DNA
IN VIVO CHROMATIN
C.P.M. ³H-HMT (x10⁻³)
6
4
2
20
40
60
80
100
120
Fraction Number

TABLE 1

Hind III - Kpn I Restriction Enzyme Analysis of Virion Chromatin

| | % TOTAL [$^3$H]HMT[a] | | | |
|---|---|---|---|---|
| FRAGMENT | VIRION (N = 3) | DNA (N = 3) | RATIO | SIGNIFICANCE |
| A | 33.92 ± 0.19 | 33.77 ± 0.05 | 1.00 | N.S.[b] |
| B | 26.98 ± 0.25 | 27.37 ± 0.33 | 0.99 | N.S. |
| $C_1$ | 14.80 ± 0.11 | 14.50 ± 0.40 | 1.02 | N.S. |
| D | 11.10 ± 0.30 | 11.51 ± 0.05 | 0.96 | N.S. |
| E | 7.22 ± 0.20 | 7.26 ± 0.12 | 0.99 | N.S. |
| $C_2$ | 4.28 ± 0.19 | 3.80 ± 0.13 | 1.13 | N.S. |
| F | 1.71 ± 0.05 | 1.79 ± 0.05 | 0.96 | N.S. |

[a] The percentage of total radioactivity recovered was calculated for each of three experiments, and the values averaged. The data are presented as this average ± the standard error of the mean.

[b] N.S., Not significant at $p < 0.05$ by Student's *t*-test.

Figure 3. Accessibility of the SV40 Genome to [$^{3}$H]HMT Photoaddition within Virion or *In Vivo* Chromatin.

For each restriction fragment the ratio of the percentage of total $^{3}$H counts for the sample to the percentage of total radioactivity for purified DNA is indicated. Cross-hatched bars indicate the only fragment for which the ratio was statistically different from 1.0. Upper panel: total virion; low panel: *in vivo* chromatin. The preparation of both samples is described in Materials and Methods.

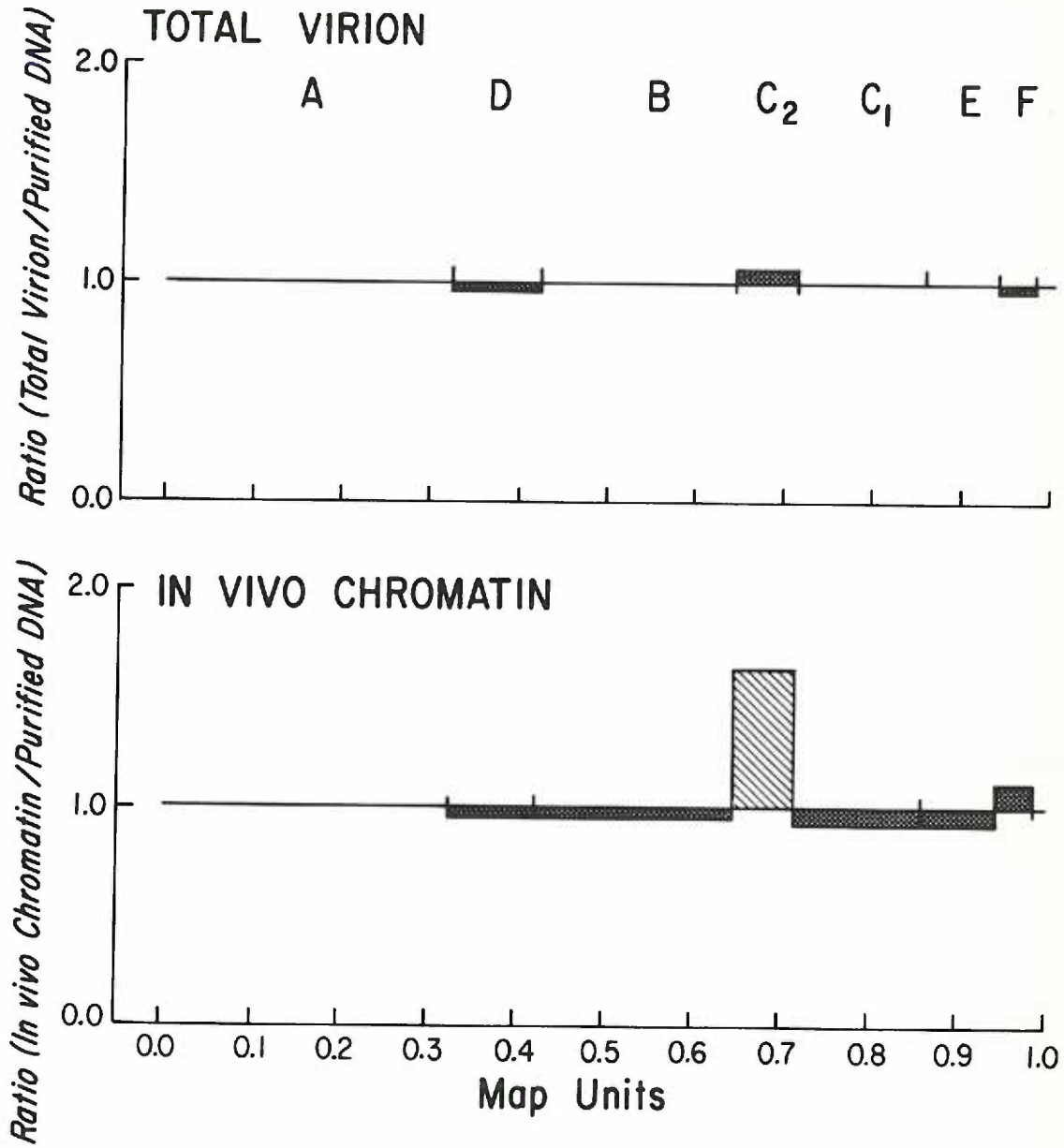
TOTAL VIRION
A
D
B
$C_2$
$C_1$
E
F
2.0
1.0
0.0
Ratio (Total Virion/Purified DNA)
IN VIVO CHROMATIN
2.0
1.0
0.0
Ratio (In vivo Chromatin/Purified DNA)
0.0
0.1
0.2
0.3
0.4
0.5
0.6
0.7
0.8
0.9
1.0
Map Units

TABLE 2

Hind III - Kpn I Restriction Enzyme Analysis
of In Vivo Chromatin

| FRAGMENT | % TOTAL [$^3$H]HMT[a] CHROMATIN (N = 3) | DNA (N = 3) | RATIO | SIGNIFICANCE |
|---|---|---|---|---|
| A | 34.44 ± 0.38 | 33.77 ± 0.05 | 1.02 | N.S.[b] |
| B | 26.09 ± 0.32 | 27.37 ± 0.33 | 0.95 | N.S. |
| $C_1$ | 13.42 ± 0.33 | 14.50 ± 0.40 | 0.93 | N.S. |
| D | 11.10 ± 0.18 | 11.51 ± 0.05 | 0.96 | N.S. |
| E | 6.74 ± 0.18 | 7.26 ± 0.12 | 0.93 | N.S. |
| $C_2$ | 6.20 ± 0.21 | 3.80 ± 0.13 | 1.63 | P<0.001 |
| F | 2.00 ± 0.06 | 1.79 ± 0.05 | 1.12 | N.S. |

[a] The percentage of total radioactivity recovered was calculated for each of three experiments and the values were averaged. The data are presented as this average ± the standard error of the mean.

[b] N.S., Not significant at $p < 0.05$ by Student's *t*-test.

that fragment predicted by the DNA sequence (33). Specific activities of all fragments were than normalized to the specific activity of fragment D, which was arbitrarily assigned a value of 1.00. The ratio of labeled in vivo chromatin to labeled purified DNA was then calculated as before (Data not shown). The results obtained by this method of analysis indicated that the $C_2$ fragment is significantly different and when labeled intracellularly contained 70% more HMT than when photoreacted as purified DNA, in complete agreement with the calculation of percentage of total radioactivity described previously.

In the experiment described above, treated viral DNA was cleaved with Hind III and Kpn I to generate a series of seven restriction fragments well-separated on polyacrylamide gels. If a region preferentially accessible to HMT labeling were still present in virions but "shifted" to an alternate site on the chromosome, our analysis might not detect it if it were located within a sufficiently large restriction fragment. For this reason, a second viral DNA sample and parallel control DNA were digested with an alternate set of restriction enzymes, Hinf I and Taq I (Fig. 1). Four of the five recovered DNA fragments encompass most of the early region of the SV40 genome and subdivide it further than was possible with Hind III and Kpn I digestion. The analysis of the distribution of HMT radioactivity when DNA samples were digested with Hinf I and Taq I is shown in Table 3. There is no significant difference in labeling density between virion-labeled DNA and control DNA in any of the restriction fragments examined, in agreement with the initial results described above. It cannot be ruled out that an open region exists but is not fixed with respect to DNA sequence so that different molecules have alternate regions which are

TABLE 3

Hinf I - Taq I Restriction Enzyme Analysis

of Virion Chromatin

% TOTAL [$^3$H]HMT[a]

| FRAGMENT | VIRION (N = 3) | DNA (N = 3) | RATIO | SIGNIFICANCE |
|---|---|---|---|---|
| A[b] + B | 56.19 ± 0.53 | 54.40 ± 1.11 | 1.03 | N.S.[c] |
| C | 23.36 ± 0.45 | 24.79 ± 0.39 | 0.94 | N.S. |
| E | 9.96 ± 0.25 | 9.95 ± 0.44 | 1.00 | N.S. |
| $D_1$ | 6.71 ± 0.19 | 6.75 ± 0.40 | 0.99 | N.S. |
| F[d] | 3.78 ± 0.22 | 4.10 ± 0.11 | 0.92 | N.S. |

[a] The percentage of total radioactivity recovered was calculated for each of three experiments and the values were averaged. The data are presented as this average ± the standard error of the mean.

[b] Fragments A and B were combined for analysis due to incomplete separation of these bands on the gels.

[c] N.S., Not significant at $p < 0.05$ by Student's *t*-test.

[d] Fragments $D_2$, G, H, $I_1$ and $I_2$ represent 7% of the total genome and were run off the gel during electrophoresis.

more accessible to psoralen photoaddition. Examination of the HMT-crosslinked viral minichromosome by electron microscopy is currently underway to address this question.

Comparison of Intracellular and Extracellular SV40 Virion. During permissive infection, the SV40 minichromosome undergoes progressive alterations and modifications thought to be closely linked to viral gene expression and maturation and packaging of the viral genome. These changes include an increased level of acetylation of histones H3 and H4 (8, 24, 25), the specific association of viral nonhistone proteins with SV40 chromosomes (1, 8, 11) and the removal of histone H1 prior to release of mature virion (8, 25). Presumably, the nucleoprotein complex finally packaged is the active transcription template or at least a precursor to it for the subsequent round of infection. This raised the possibility that the absence of the nucleosome-free region observed in virions may be related to or a result of virion maturation and release from infected cells. Indeed there is considerable evidence that at least two populations of virion exist late in infection. Differences in stability, infectivity, histone content and chromatin structure have been reported (4, 24, 28). To examine this possibility, virion was purified separately from washed cells (intracellular virion) and from culture fluids (extracellular virion) 3.5 days post-infection, a time when the cell monolayer is still largely intact. Each virus sample was photolabeled with approximately 10 HMT molecules per genome and virion DNA was analyzed along with a parallel HMT-labeled DNA control sample. For both intracellular and extracellular virion preparations, none of the ratios of the labeled Hind III-Kpn I DNA fragments to the control

DNA fragments were significantly different from 1.0 (Tables 4,5; Fig 4). Thus, there is no preferential psoralen photoaddition to the origin region (or to any other DNA fragments) even on intracellular virions. It is concluded that the transition from a nucleosome-free origin to a "closed" origin must take place prior to release of mature virus particles. It should be noted that these intracellular particles are stable to CsCl and have been prepared under conditions that allow the recovery of at least 50% of the viability relative to the crude cellular lysate.

Comparison of the Saturation Levels of HMT Photoaddition to in vivo SV40 Chromatin. There is considerable evidence that cellular DNA is protected from the photoaddition of 4,5'-8-trimethylpsoralen (trioxsalen) relative to native DNA (16, 48) by nucleosomes. Hallick et al., (15) found that treating SV40-infected cells with saturating doses of [$^3$H]trioxsalen resulted in a plateau level of approximately 1 drug molecule bound per 40-50 base pairs. When purified SV40 DNA was treated similarly, the saturation level obtained was 1 trioxsalen molecule per 4 base pairs. Linker DNA was approximately 10 times more accessible to psoralen photoaddition than micrococcal nuclease resistant DNA.

It was of interest to examine the level of photoaddition obtained with in vivo SV40 chromatin utilizing the hydroxymethyl psoralen derivative employed throughout these studies and to compare that drug saturation level to results with SV40 virion. SV40-infected cell cultures at 48 hr. post-infection were treated with [$^3$H]HMT at 15-20 µg/ml. Fresh drug additions were made every 30 min. throughout the irradiation to replenish the available HMT. After irradiation the viral

TABLE 4

Hind III - Kpn I Restriction Enzyme Analysis

of Extracellular Virion Chromatin

| FRAGMENT | % TOTAL [$^3$H]HMT[a] EXTRACELLULAR VIRION (N = 3) | DNA (N = 2) | RATIO | SIGNIFICANCE |
|---|---|---|---|---|
| A | 31.76 ± 1.10 | 30.69 ± 0.69 | 1.03 | N.S.[b] |
| B | 26.72 ± 0.42 | 27.56 ± 0.15 | 0.97 | N.S. |
| $C_1$ | 14.77 ± 0.22 | 15.26 ± 0.19 | 0.97 | N.S. |
| D | 12.42 ± 0.20 | 12.14 ± 0.44 | 1.02 | N.S. |
| E | 8.24 ± 0.20 | 8.09 ± 0.20 | 1.02 | N.S. |
| $C_2$ | 4.07 ± 0.13 | 4.08 ± 0.01 | 1.00 | N.S. |
| F | 2.04 ± 0.07 | 2.18 ± 0.01 | 0.94 | N.S. |

[a] The percentage of total radioactivity recovered was calculated for each of three (extracellular virion) or two (DNA) experiments, and the values were averaged. The data are presented as this average ± the standard error of the mean.

[b] N.S., Not significant at $p < 0.05$ by Student's *t*-test.

TABLE 5

Hind III - Kpn I Restriction Enzyme Analysis

of Intracellular Virion Chromatin

| FRAGMENT | % TOTAL [$^3$H]HMT[a] INTRACELLULAR VIRION (N = 3) | DNA (N = 2) | RATIO | SIGNIFICANCE |
|---|---|---|---|---|
| A | 31.80 ± 1.01 | 30.69 ± 0.69 | 1.04 | N.S.[b] |
| B | 26.81 ± 0.42 | 27.56 ± 0.15 | 0.97 | N.S. |
| $C_1$ | 14.82 ± 0.28 | 15.26 ± 0.19 | 0.97 | N.S. |
| D | 12.57 ± 0.44 | 12.14 ± 0.44 | 1.04 | N.S. |
| E | 8.09 ± 0.46 | 8.09 ± 0.20 | 1.00 | N.S. |
| $C_2$ | 4.07 ± 0.16 | 4.08 ± 0.01 | 1.00 | N.S. |
| F | 1.95 ± 0.17 | 2.18 ± 0.01 | 0.90 | N.S. |

[a] The percentage of total radioactivity recovered was calculated for each of three (intracellular virion) or two (DNA) experiments, and the values were averaged. The data are presented as this average ± the standard error of the mean.

[b] N.S., Not significant at $p < 0.05$ by Student's *t*-test.

Figure 4. Accessibility of the SV40 Genome to [$^{3}$H]HMT Photoaddition within Extracellular or Intracellular Virion Chromatin.

The ratio of the percentage of total $^{3}$H counts in extracellular or in intracellular virion to purified DNA is calculated as described in the legend to Fig. 3. Sample preparation is detailed in Materials and Methods. No values were statistically different from 1.0.

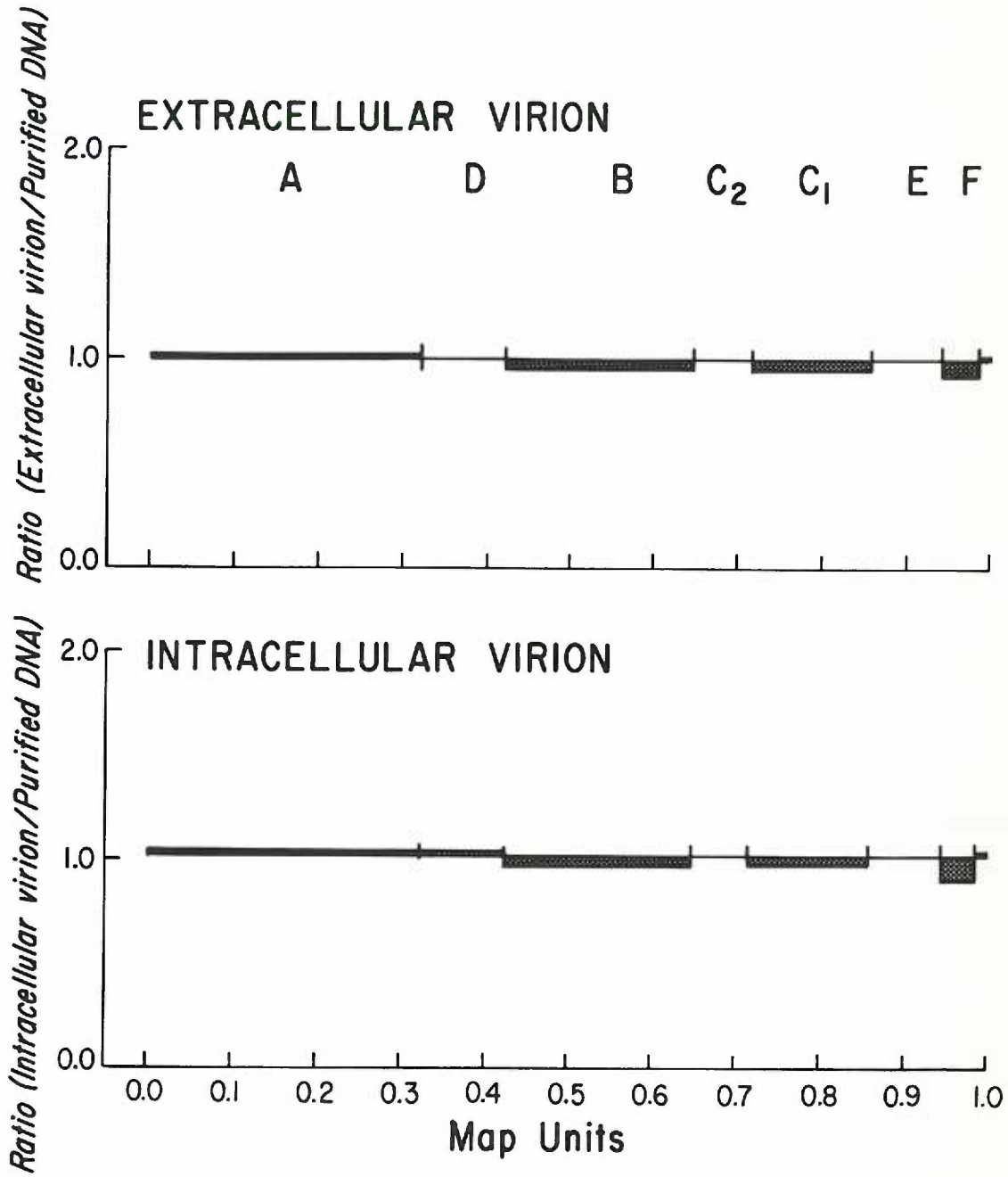
EXTRACELLULAR VIRION
A
D
B
$C_2$
$C_1$
E
F
2.0
1.0
0.0
Ratio (Extracellular virion/Purified DNA)
INTRACELLULAR VIRION
2.0
1.0
0.0
Ratio (Intracellular virion/Purified DNA)
0.0
0.1
0.2
0.3
0.4
0.5
0.6
0.7
0.8
0.9
1.0
Map Units

DNA was extracted by the Hirt procedure (18) purified and the amount of covalently bound HMT was determined. Figure 5 shows that the reactions with intracellular SV40 DNA reaches a plateau at approximately 1 HMT molecule per 50 base pairs of DNA. This saturation level of protection from psoralen addition is very similar to that seen for DNA in cellular chromatin (48) and in SV40 chromatin saturated with trioxsalen (15). In contrast, purified DNA binds 1 HMT molecule per 7 base pairs. SV40 virion, under comparable drug and irradiation conditions, reached a plateau level of 1 HMT adduct per 25-30 bp of DNA (Fig. 5). This marked difference in the level of psoralen protection is perhaps more obvious when the photoaddition level is calculated as total number of HMT molecules bound per genome. SV40 DNA irradiated in vivo had approximately 105 drug molecules bound per genome at saturation, while the treated virion DNA had 175-210 HMT molecules bound per genome, a 67% increase over the intracellularly labeled sample. These results are especially intriguing in light of recent reports indicating that the four core histones, although present in SV40 virions, may not be assembled into canonical nucleosomes (28).

## DISCUSSION

The small size of SV40 and the availability of molecular information on the sequence and organization of the viral genome make it an attractive model for cellular chromatin structure and for regulation of gene expression. The arrangement of nucleosomes on the SV40 genome is not entirely random in at least a subpopulation of minichromosomes. A short segment on the late side of the origin of replication remains free

Figure 5. Kinetics of HMT Photoaddition to *In Vivo* Chromatin DNA, Virion DNA, and Purified DNA.

The conditions for the three samples are described in the text. Each curve represents two experiments.

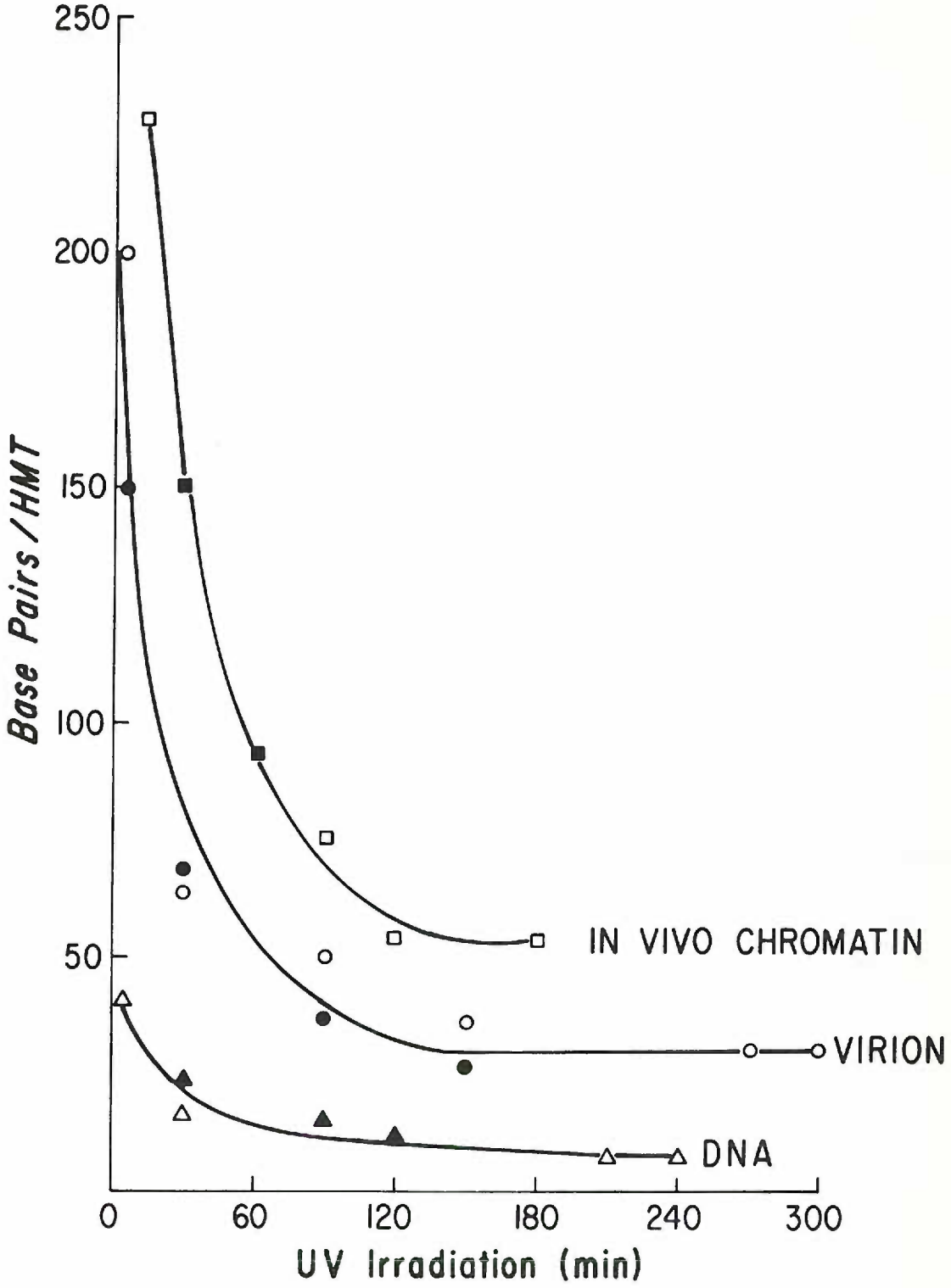
250
200
150
100
50
Base Pairs / HMT
IN VIVO CHROMATIN
VIRION
DNA
0
60
120
180
240
300
UV Irradiation (min)

of nucleosomes in minichromosomes extracted from infected cells (20) and in infected cells *in situ* (2, 35). The significance of a nucleosome-free region on a subpopulation of viral nucleoprotein complexes remains unexplained.

We describe here additional findings with *in vivo* SV40 chromatin. The purified DNA was digested with a second set of restriction enzymes, Hind III and Kpn I, to produce an origin fragment reduced in size to further define the limits of preferential psoralen addition. The $C_2$ fragment which is located at .646-.716 map units (see Fig. 1) is 13% smaller than the origin fragment examined by psoralen photoaddition previously, because the cleavage site is closer to the 72 base pair repeats. Reducing the fragment size did not diminish the level of preferential labeling and, in fact, increased it slightly. This *in vivo* chromatin was the positive control for the new findings reported here.

We examined total SV40 virion for the presence of the open region. The [$^3$H]HMT-labeled DNA, analyzed after digestion with two different sets of restriction enzymes exhibited a random pattern of drug photoaddition. The $C_2$ restriction fragment containing the replication origin and other key regulatory sequences was not preferentially available to psoralen. All seven restriction fragments showed no significant differences in the amount of radioactivity bound when compared to SV40 DNA photolabeled *in vitro*. The loss of the open region in SV40 virion nucleoprotein complexes has been reported by others. Hartmann and Scott (17) found that chromatin, prepared by EGTA-dithiothreitol disruption of virion, unlike the minichromosome recovered from infected cells, lost its DNase I sensitivity at the replication origin and displayed an essentially random cleavage pattern.

Using similar virus disruption techniques, Brady et al. (4) also found modifications in the virus chromatin structure making the nucleoprotein complex more accessible to nucleases and to RNA polymerase.

It was reported that the nucleoprotein complex isolated from an immature form of virus is structurally different from mature, released virion and exhibits nuclease sensitivity properties comparable to minichromosomes (4). The possibility that intracellular virion is structurally unique from extracellular virion led us to examine virus purified from cells at 3.5 days post-infection. We found essentially identical results with this population of intact virus as shown for total virion and for extracellular virion. There was no region of the genome which was preferentially labeled with [$^3$H]HMT. Apparently that population of minichromosomes found to have an open region late in infection either does not undergo virus maturation or the nucleosome arrangement is altered prior to virus encapsidation. The properties described here for intracellular virion and its similarity to extracellular virion are at odds with observations reported by Brady et al. (4). As the methods used for intracellular virus preparation are quite different, it is possible that each procedure selects for a different subpopulation of immature virus, with Brady's nucleoprotein complex sharing many of the properties of the SV40 minichromosome.

Finally, evidence was presented which indicated that the level of protection of psoralen photoaddition afforded by nucleosomes on in vivo SV40 chromatin was comparable to levels obtained for cellular chromatin (16, 48). Surprisingly, virion DNA reached a plateau of drug addition at a level intermediate to in vivo SV40 chromatin and control DNA. Since the histone content of SV40 is thought to be comparable to that

found in minichromosomes (3, 27), the ability to saturate the viral chromatin with psoralens to a greater extent is not due to a decrease in the number of nucleosomes within an intact virus particle. However, mature virus particles are devoid of histone H1 (8, 25). Hyde and Hearst (19) have shown that H1-depleted chromatin in 0.6 M NaCl binds more psoralen than chromatin under physiological conditions when both are compared to the levels of drug bound to purified DNA under the same ionic conditions. The absence of H1 in SV40 virion may account, in part, for the increased level of photoaddition we observe in virus particles. Our results are especially interesting in light of a recent report which describes an altered SV40 chromatin complex obtained when virions are gently disrupted at neutral pH. The resulting nucleoprotein structure is an extended, circular molecule with a full complement of histone proteins but typical nucleosomes are absent (28). It is possible that the numerous small beads they reported upon disruption of the virion reflect the "nonnucleosomal" chromatin structure we observe by psoralen saturation of the intact virus particle. An examination of the HMT-saturated virion DNA by electron microscopy is in progress, and the pattern of cross-links will reveal direct information of the organization of the viral chromatin complex.

REFERENCES

1. Baumgartner, I., C. Kuhn and E. Fanning. (1979). Identification and characterization of fast-sedimenting SV40 nucleoprotein complexes. Virology 96, 54-63.

2. Beard, P., M. Kaneko and P. Cerutti. (1981). N-acetoxy-acetylamino-fluorene reacts preferentially with a control region of intracellular SV40 chromosome. Nature (London) 291, 84-85.

3. Bellard, M., P. Oudet, J.E. Germond and P. Chambon. (1976). Subunit structure of simian virus 40 minichromosomes. Eur. J. Biochem. 70, 543-553.

4. Brady, J., Radonovich, M., Lavialle, C. and Salzman, N.P. (1981). Simian virus 40 maturation: chromatin modifications increase the accessibility of viral DNA to nuclease and RNA polymerase. J. Virol. 39, 603-611.

5. Cech, T. and M. L. Pardue. (1977). Cross-linking of DNA with trimethyl-psoralen is a probe for chromatin structure. Cell 11, 631-640.

6. Cech, T.R., D. Porter and M.L. Pardue. (1978). Chromatin structure in living cells. Cold Spring Harbor Symp. Quant. Biol. 42,191-198.

7. Coca-Prados, M. and M.-T. Hsu. (1979). Intracellular forms of simian virus 40 nucleoprotein complexes. II. Biochemical and electron microscope analysis of simian virus 40 virion assembly. J. Virol. 1, 199-208.

8. Coca-Prados, M., G. Vidali and M.-T. Hsu. (1980). Intracellular forms of simian virus 40 nucleoprotein complexes. III. Study of histone modifications. J. Virol. 36, 353-360.

9. Cole, R.S. (1970). Light-induced cross-linking of DNA in the presence of a fucocoumarin (psoralen). Biochem. Biophys Acta 217, 30-39.

10. Cremisi, C. (1979). Chromatin replication revealed by studies of animal cells and papovaviruses (SV40 and polyoma). Microbiol Rev. 43, 297-319.

11. Garber, E. A., M. M. Seidman and A.J. Levine. (1978). The detection and characterization of multiple forms of SV40 nucleoprotein complexes. Virology 90, 305-316.

12. Ghosh, P., V. Reddy, J. Swinscoe, P. Lebowitz and J. Weissman. (1978). Heterogeneity and 5'-terminal structures of the late RNA's of simian virus 40. J.Mol.Biol. 126, 813-846.

13. Griffith, J. (1975). Chromatin structure: deduced from a minichromosome. Science 187, 1202-1203.

14. Gutai, M. and D. Nathans. (1978). Evolutionary variants of simian virus 40: nucleotide sequence of a conserved SV40 DNA segment containing the origin of viral DNA replication as an inverted repetition. J. Mol. Biol. 126, 259-274.

15. Hallick, L.M., H.A. Yokota, J.C. Bartholomew and J. E. Hearst. (1978). Photochemical addition of the cross-linking reagent 4,5'8-trimethyl-psoralen to intracellular and viral simian virus 40 DNA-histone complexes. J. Virol. 27, 127-135.

16. Hanson, C.V., C.J. Shen and J.E. Hearst. (1976). Cross-linking of DNA in situ as a probe for chromatin structure. Science. 193, 62-64.

17. Hartmann, J. P. and W.A. Scott. (1981). Distribution of DNase I-sensitive sites in simian virus 40 nucleoprotein complexes from disrupted virus particles. J. Virol. 37, 908-915.

18. Hirt, B. (1967). Selective extraction of polyoma DNA from infected mouse cell culture. J. Mol. Biol. 26, 365-369.

19. Hyde, J. E. and Hearst, J. E. (1978) Binding of psoralen derivatives to DNA and chromatin: Influence of the ionic environment on dark binding and photoreactivity. Biochemistry 17, 1251-1257.

20. Jakobovits, E.B., S. Bratosin and Y. Aloni. (1980). A nucleosome-free region in SV40 minichromosomes. Nature (London) 285, 263-265.

21. Jessel, D., T. Landau, J. Hudson, T. Lalor, D. Tenen and D.M. Livingston. (1976). Identification of regions of the SV40 genome which contain preferred SV40 T-Ag binding sites. Cell 8, 535-545.

22. Kornberg, R.D. (1977). Structure of chromatin. Annu. Rev. Biochem. 46, 931-955.

23. Krauch, C.H., D.M.Dramer and A.Wacker. (1967). Zum Wirkungsmechanismum photodynamischer furocumarine. Photoreaktion von psoralen-(4-$^{14}$C) mit DNS, RNS, homopolynucleotiden und nucleosiden. Photochem. Photobiol. 6, 341-354.

24. La Bella, F. and C. Vesco. (1980). Late modifications of simian virus 40 chromatin during the lytic cycle occur in an immature form of virion. J. Virol. 33, 1138-1150.

25. La Bella, F, G. Vidali and C. Vesco. (1979). Histone acetylation in CV-1 cells infected with simian virus 40. Virology 96, 564-575.

26 McGhee, J.D. and G. Felsenfeld. (1980) Nucleosome structure. Annu. Rev. Biochem. 49, 1115-1156.

27. Meinke, W., Hall, M.R. and Goldstein, D.A. (1975). Proteins in intracellular simian virus 40 nucleoprotein complexes: comparison with simian virus 40 core proteins. J. Virol. 15, 439-448.

28. Moyne, G., Harper, F. Saragosti, S. and Yaniv, M. (1982). Absence of nucleosomes in a histone-containing nucleoprotein complex obtained by dissociation of purified SV40 virions. Cell 30, 123-130.

29. Musajo, L., G. Rodighiero, A. Breccia, F. Dall'Acqua and G. Malesani. (1966). Skin-photosensitizing furocoumarins: photochemical interaction between DNA and -O$^{14}$CH$_3$bergapten (5-methoxypsoralen). Photochem Photobiol 5, 739-745.

30. Nathans, D. and K.J. Danna. (1972). Specific origin in SV40 DNA replication. Nature (London) New Biol. 236, 200-202.

31. Pathak, M.A. and D.M. Kramer. (1969). Photosensitization of skin in vivo by furocoumarins (psoralens). Biochim. Biophys. Acta. 195, 197-206.

32. Reddy, V., P. Ghosh, P. Lebowitz, M. Piatak and S. Weissman. (1979). Simian virus 40 early mRNA's. I. Genomic localization of 3' and 5' termini and two major splices in mRNA from transformed and lytically infected cells. J. Virol. 30, 279-296.

33. Reddy, V.B., B. Thimmappaya, R. Dahr, K.N. Subramanian, B.S. Zain, J. Pan, P.K. Ghosh, M.L. Celma and S.M. Weissman. (1978). The genome of simian virus 40. Science 200, 494-502.

34. Reed, S., J. Ferguson, R.W. Davis and G. R. Stark. (1975). T-antigen binds to simian virus 40 DNA at the origin of replication. Proc. Natl. Acad. Sci. U.S.A. 72, 1605-1609.

35. Robinson, G.W. and Hallick, L.M. (1982). Mapping the in vivo arrangement of nucleosomes on simian virus 40 chromatin by the photoaddition of radioactive hydroxymethyltrimethylpsoralen. J. Virol. 41, 78-87.

36. Saragosti, S., Moyne, G. and Yaniv, M. (1980). Absence of nucleosomes in a fraction of SV40 chromatin between the origin of replication and the region coding for the late leader RNA. Cell 20, 65-73.

37. Scott, W.A. and D.J. Wigmore. (1978). Sites in simian virus 40 chromatin which are preferentially cleaved by endonucleases. Cell 15, 1511-1518.

38. Shelton, E.R., P.M. Wassarman and M.L. DePamphilis. (1980). Structure, spacing and phasing of nucleosomes on isolated forms of mature SV40 chromosomes. J. Biol. Chem 255, 771-782.

39. Shortel, D.R., R.F. Margolskee and D. Nathans. (1979). Mutational analysis of the simian virus 40 replicon: pseudorevertants of mutants with a defective replication origin. Proc. Natl. Acad. Sci. U.S.A. 76, 6128-6131.

40. Subramanian, K. and T. Shenk. (1978). Definition of the boundaries of the origin of DNA replication of simian virus 40. Nucleic Acids Res. 5,3635-3642.

41. Sundin, O. and A. Varshavsky. (1979). Staphylococcal nuclease makes a single non-random cut in the simian virus 40 minichromosome. J. Mol. Biol. 132, 535-546.

42. Thompson, J.A., M.F. Radonovich and N.P. Salzman. (1979). Characterizations of the 5'-terminal structure of simian virus 40 early mRNA's. J. Virol. 31, 437-446.

43. Tjian, R. (1978). The binding site on SV40 DNA for a T-Ag-Related protein. Cell 13, 165-179.

44. Varshavsky, A.J., O.H. Sundin and M.J. Bohn. (1978). SV40 viral mini-chromosome: preferential exposure of the origin of replication as probed by restriction endonucleases. Nucleic Acids Res. 5, 3469-3477.

45. Varshavsky, A.J., O. Sundin and M. Bohn. (1979). A stretch of late SV40 viral DNA about 400 bp long which includes the origin of replication is specifically exposed in SV40 minichromosomes. Cell 16, 453-466.

46. Waldeck, W., B. Fohring, K. Chowdhury, P. Gruss and G. Sauer. (1978). Origin of DNA replication of papovavirus chromatin is recognized by endogenous endonuclease. Proc. Natl. Acad. Sci. U.S.A. 75, 5964-5968.

47. Wiesehahn, G.P. and J.E. Hearst. (1976). The site of trimethylpsoralen cross-linking in chromatin, p. 27-32. In D.P. Nierlich, W.J. Rutter and C.F. Fox (ed.), Molecular mechanisms in the control of gene expression, ICN-UCLA Symposium, vol. 5. Academic Press, Inc., New York.

48. Wiesehahn, G.P., J.E. Hyde and J.E. Hearst. 1977. The photoaddition of trimethylpsoralen to Drosophila melanogaster nuclei: a probe for chromatin substructure. Biochemistry. 16, 925-932.

PAPER 3.

# Quantitation of DNA Fragments in Gels: A Comparison of Photographic and Densitometric Methods and Their Application to Site-Specific Psoralen Blockage of the Restriction Endonuclease Bgl I

ABSTRACT

Two methods for determining the relative amounts of DNA in bands on analytical gels were compared. The photographic and direct densitometric methods for measuring fluorescence from DNA-ethidium bromide complexes were found to give nearly identical results in terms of their sensitivity of detection, linearity of response, and overall reproducibility. We have applied the direct fluorescent method to an analysis of the blockage by psoralen photoaddition of pBR322 cleavage by the restriction enzyme Bgl I. All three cutting sites of this enzyme were inhibited in a dose-dependent manner, but one of them was observed to be markedly more sensitive to HMT adducts on the DNA. Inspection of the variable nucleotide sequences within the Bgl I recognition sites suggested that the preferential inhibition was due to the presence of a high frequency target for HMT photoaddition within one of the three sites.

## INTRODUCTION

Gel electrophoresis is a valuable and widely employed method for the separation of DNA fragments resulting from restriction endonuclease digestion. A sensitive way of visualizing the DNA bands entails staining the gel with ethidium bromide so that highly fluorescent DNA-ethidium bromide complexes can form. Under conditions of nearly random DNA base composition, there is a direct relationship between the amount of DNA present and the fluorescence intensity produced by UV illumination:

$$(\text{DNA}) \alpha F.$$

Unfortunately, when photography is used for DNA quantitation, the process distorts this linear relationship (11, 12). Unlike the human eye, which correctly perceives relative light intensity over a wide range, photographic film records the intensity of light in a logarithmic fashion:

$$\text{O.D. (film)} \alpha \log (\text{exposure}).$$

This can be easily demonstrated if a graded fluorescence intensity scale (in which the light intensity is doubled every two steps) is photographed and the images of the graded scale are measured for absolute darkness and plotted. An example of such a characteristic film response curve shows that an exponential relationship holds for the straight portion of this curve (Fig. 1). A portion of the curve where it does not hold, called the subthreshold region, is also apparent.

From this figure it can be estimated that fluorescent bands on a gel differing in intensity by two-fold will differ in darkness on the negative by approximately 30% ($\log 2 = 0.3$). The exact darkness

Figure 1. The Characteristic Response Curve of Kodak Tri-X Film.

The absolute density of the steps on a photographic image of a fluorescence density scale, constructed and photographed as described in Materials and Methods, was measured with a spot densitometer. Measurements of the steps from 30 second (O) and 60 second (●) exposures have been plotted and are out of phase by two steps (e.g. doubling of exposure). An image of the density scale is shown in Figure 3.

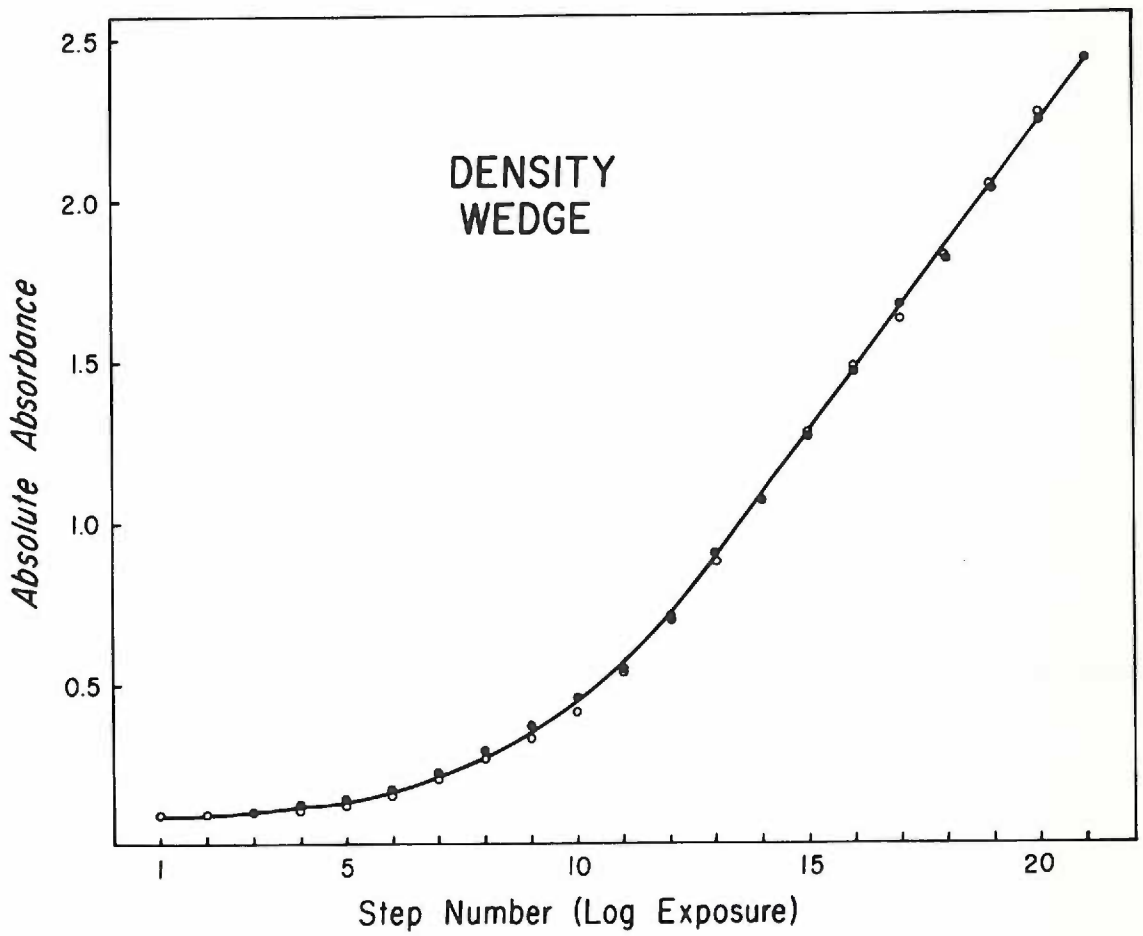
DENSITY
WEDGE
Absolute Absorbance
2.5
2.0
1.5
1.0
0.5
1
5
10
15
20
Step Number (Log Exposure)

relationship between the two images will be dependent upon $\gamma$ which is the slope of the straight portion of the characteristic curve. Thus, if fluorescence intensity is substituted for exposure in the photographic equation, the darkness of fluorescent bands on the negative will be logarithmically related to the amount of DNA contained within those bands:

O.D. (film) $\alpha$ log (F). Thus, O.D. (film) $\alpha$ log (DNA).

Pulleyblank, et al. (12) have addressed this problem with photographic quantitation of fluorescent bands and have devised two methods for exponentially integrating peak areas as required by the above equation. These methods involve densitometric scanning of negatives followed by extensive mathematical manipulation of the data. A simpler way to quantitate DNA is to measure the fluorescence emitted from the gel directly using a sensitive electronic detector. Peaks obtained can then be linearly integrated since fluorescence is directly proportional to DNA concentration.

In this report we compare photographic and direct densitometric methods for DNA quantitation and found them to give nearly identical results with respect to their sensitivity, range of linearity, and overall reproducibility. The direct fluorescent method was then utilized to examine preferential site dependent cleavage by the restriction enzyme Bgl I. The preferences of this endonuclease were of special interest because it cuts at a large (11 bp) recognition site which contains a 5 bp neutral region; thus individual sites can vary markedly in sequence. In this analysis the frequencies of Bgl I cutting at the three well separated sites on pBR322 were calculated by precisely

quantitating DNA restriction fragments generated by partial digestion with Bgl I.

We have used the same methodology to investigate the effect of furocoumarin (psoralen) binding on the frequency of Bgl I cutting at these sites. Psoralen derivatives, such as hydroxymethyltrimethylpsoralen (HMT) intercalate into DNA, and in the presence of long wavelength UV light, form covalent adducts to pyrimidines of the DNA. If two pyrimidines are adjacent and on opposite DNA strands, psoralen diadducts can form that will covalently cross-link the two strands. One previous report has indicated that psoralen adducts can block restriction enzyme sites in a differential manner, but no correlation was made between DNA sequence at or near the sites and the cutting frequency observed (2). Here we show that HMT blockage of Bgl I cutting is due to adducts within the recognition sites and suggest that preferential inhibition at one site is related to the presence of a DNA sequence favored for HMT photoaddition.

## MATERIALS AND METHODS

Enzymes and Chemicals. All restriction endonucleases (Hind III, Hpa II, Hinf I, Eco RI, Bam HI, Bgl I) were purchased from Bethesda Research Laboratories, Inc. Agarose (standard low $M_f$), acrylamide, N,N'-methylene-bisacrylamide, ammonium persulfate, TEMED, and bromphenol blue were electrophoresis quality reagents obtained from Bio-Rad Laboratories. CsCl was purchased from Beckman, Trizma base from Sigma, ethidium bromide from Calbiochem and all other analytical reagents were obtained from J.T. Baker Chemical Co. Tritiated

4'-hydroxymethyl-4,5',8-trimethylpsoralen (HMT) was generously provided by S. Isaacs and J. Hearst, and had a specific activity of $3 \times 10^7$ cpm/μg as determined by methods previously described (14).

Purification of pBR322 and SV40 DNA. Supercoiled SV40 DNA was isolated from infected CV-1 cells by Hirt extraction (5) and CsCl-ethidium bromide equilibrium density banding as described (14). Plasmid pBR322 DNA was obtained from E. coli strain RRI by standard procedures (3). SV40 and pBR322 DNAs were CsCl banded twice to obtain greater than 90% supercoiled molecules.

$^3$H-HMT Photoaddition. Samples containing 10-15 μg of Bam HI-linearized pBR322 DNA (prepared as described below) were diluted into 450 μl TE-buffer (10 mM Tris-hydrochloride-1 mM EDTA, pH 8.1) in 1.5 ml polyethylene microcentrifuge tubes. Various amounts of $^3$H-HMT (range: 3.5-1000 ng) from an aqueous dilution were added and reaction volumes were adjusted to 500 μl with distilled water. Samples were irradiated for 2 hrs at 4°C by suspending the tubes between two General Electric F15T8 BLB fluorescent tubes (2.2 mW/cm$^2$/tube) spaced 7 cm apart. Finally, the salt concentration was raised to 0.3 M with sodium acetate, each sample was extracted three times with chloroform-isoamyl alcohol (24:1) to remove noncovalently bound HMT, and ethanol precipitated.

Restriction Enzyme Digestion. Purified pBR322 or SV40 DNA samples in TE-buffer were digested with restriction enzymes according to the manufacturer's recommendations except that all digests contained 10 mM $MgSO_4$, 10 mM dithiothreitol, and 100 μg/ml sterile gelatin. SV40 DNA was digested with Hpa II and Hind III in sequential reactions in low and high salt buffer, respectively. The enzymes Hinf I and Eco RI were used together to digest pBR322 DNA in a buffer containing 25 mM Tris

hydrochloride, pH 7.4 and 75 mM NaCl. All reactions were terminated by addition of tracking dye (40% sucrose, 10 mM Tris-hydrochloride, pH 8.1, 200 µg/ml bromphenol blue, and 75 mM EDTA).

Bam HI-linearized pBR322 DNA was prepared by digestion with enzyme for 4 hrs at 37°C. Digestion was stopped by addition of EDTA to 5 mM, sodium acetate was added to 0.3 M, the sample was phenol extracted once, ether extracted three times, ethanol precipitated at -20°C overnight and resuspended in TE-buffer. Time course digestions with Bgl I were carried out by incubating approximately 21 µg of linear plasmid DNA with 60U Bgl I in a 0.2 ml reaction mixture and at times indicated 25 µl aliquots were removed and the reaction terminated.

Bam HI-linearized pBR322 DNA that had been photoreacted with $^{3}$H-HMT to various extents was also digested with Bgl I. For these samples 1 µg of photoreacted DNA was incubated with 20U Bgl I in a 25 µl reaction mixture containing 75 mM NaCl for 3 hr then the reaction was terminated. These conditions were sufficient to completely digest four fold higher amounts of non-photoreacted DNA present in control digestions.

Gel Electrophoresis. Hind III-Hpa II and Hinf I-Eco RI DNA fragments were separated by electrophoresis in vertical 4.5% polyacrylamide slab gels as previously described (14). Gel slots were 8 mm and 19 mm in size, respectively. Vertical gels used for electrophoresis of Hpa II-linearized SV40 DNA were made of 0.75% agarose in TBE buffer (89 mM Trizma base, pH 8.1, 89 mM boric acid, and 2.5 mM EDTA) gels were stained for 20 min in buffer with fresh ethidium bromide at a concentration of 2 µg/ml. This amount gives the high background fluorescence required in the photographic method of quantitation so that the subthreshold region of the film response curve is exceeded.

All DNA samples that were digested with Bgl I were electrophoresed on horizontal (Canalco HSG Apparatus) 0.75% agarose gels (34 by 18 by 0.3 cm) in TBE buffer containing 1 µg/ml ethidium bromide. The gel was run as a submarine (3 mm buffer overlay) at 90 V for 16 hrs. Horizontal gels were photographed with a Polaroid camera, using a short-wave UV-transilluminator (Ultra-Violet Products, Inc., San Gabriel, Calif.) then scanned by direct densitometry.

Direct Densitometric Analysis. Ethidium bromide stained gels were scanned in fluorescence mode using a Helena Quick Scan R and D densitometer, equipped with an extended red-range photomultiplier. Gels were supported in the instrument on a quartz tray (SDA 324, Schoeffel Instruments) above a mercury lamp (254 nm peak emission) that contained a cobalt blue filter (to screen out wavelengths $>$ 400 nm) and an excitation slit (7 mm by 0.7 mm). Ethidium bromide fluorescence was detected by the photomultiplier positioned directly over the gel, which bore another slit and a Wratten 23A filter (to screen out wavelengths $<$ 585 nm). A black masking tray was used to prevent stray UV light from exciting gel lanes other than the one of interest. Individual gel lanes were aligned in the scanning path using a UV spot lamp (366 nm peak emission, UVL-56, Ultra Violet Products, Inc.) in a darkened room then scanned twice, beginning at the top of the gel. Peak areas from the chart paper were integrated using an electronic planimeter (Numonics, Lansdale, Pa).

Photographic Analysis. Ethidium bromide stained gels were photographed for quantitative analysis by the method of Pulleyblank et al (12). A fluorescence intensity scale was constructed using a 21-step density wedge (Kodak Cat. #152-3393) and a strip of 1/32 in thick

fluorescent plexiglass (Rohm and Haas, Amber 2422). A layer of Saran wrap under the gel but not the fluorescence scale reduced the fluorescence intensity from the gel and brought it into the same range as that issuing from the fluorescence scale.

Photographs of gels and the fluorescence scale were taken with a Linhoff-Technikoff camera fitted with a 5 in. close-up lens and a Wratten 23A filter. Exposed 4 x 5 in. Kodak Tri-X panchromatic sheet film (320 ASA) was developed for 5 min at 21°C in Kodak D-11 developer with continuous agitation. The characteristic curve of each negative was determined by measuring the absolute density of the steps on the fluorescence scale using a Macbeth TD500 spot densitometer. Negatives used for further analysis were those in which both the background gel absorbance and the maximum peak absorbance fell within the linear region of the film's characteristic curve which, under our conditions was between 0.55 and 2.50 O.D. Individual lanes of the negatives were traced in absorbance mode at 520 nm using the Helena densitometer described above. Peak area was integrated by the use of the parabolic approximation method (12).

## RESULTS

Comparison of photographic and densitometric methods for fluorescence quantitation. Initially we compared the sensitivity and linearity of direct densitometric and photographic methods for the fluorescent quantitation of DNA fragments. Supercoiled SV40 DNA was linearized by digestion with Hpa II, and nine serial dilutions (2-fold) were prepared that contained from 500 to 2 nanograms of material. After

electrophoresis on an agarose gel and staining with ethidium bromide, the DNA was examined using the two procedures described in Materials and Methods. In the densitometric method lanes 1-4 and lanes 4-9 were scanned at two different sensitivity settings and normalized using lane 4 values. In the photographic method only one negative was used. The results of this analysis are shown in Figure 2, where integrated peak areas (arbitrary units) were plotted versus the amount of DNA applied to the gel. Using either method a linear relationship was obtained over the entire 250-fold range of DNA.

This comparison was extended to the case where multiple bands were present. For this purpose SV40 DNA was digested to completion with the enzymes Hind III and Hpa II to produce seven fragments. Quantities of this digest containing 0.5, 1.0, and 2.0 μg DNA were electrophoresed on 4.5% polyacrylamide gels (Fig. 3) and analyzed as described. The results of these analyses are listed in Table 1. In column 1 is shown the distribution of DNA, expressed as a percent of the total analyzed, that was expected based on the published DNA sequence of SV40 (13). In columns 2 and 3 are listed the DNA distributions determined using the photographic and direct densitometric methods respectively. Use of a statistical test, the chi square goodness-of-fit analysis, confirms what visual inspection suggests; both sets of determinations yield DNA distributions that closely approximate the expected DNA distribution. Both methods are biased slightly toward the two largest DNA fragments and underestimate the four smaller fragments. Some of this bias in the photographic method may be the result of difficulty in measuring peak dimensions accurately for the smaller fragments. A possible source of bias in the direct densitometric method may result from difficulty in

Figure 2. Linearity and Sensitivity of Two Methods for Fluorescence Quantitation.

Amounts of SV40 DNA ranging from 500 to 2 nanograms were examined on an agarose gel using the photographic method (●) or the densitometric method (○) as described in Materials and Methods. Points were fit to the lines by linear regression analysis and had r-values of 0.996 and 0.999 respectively.

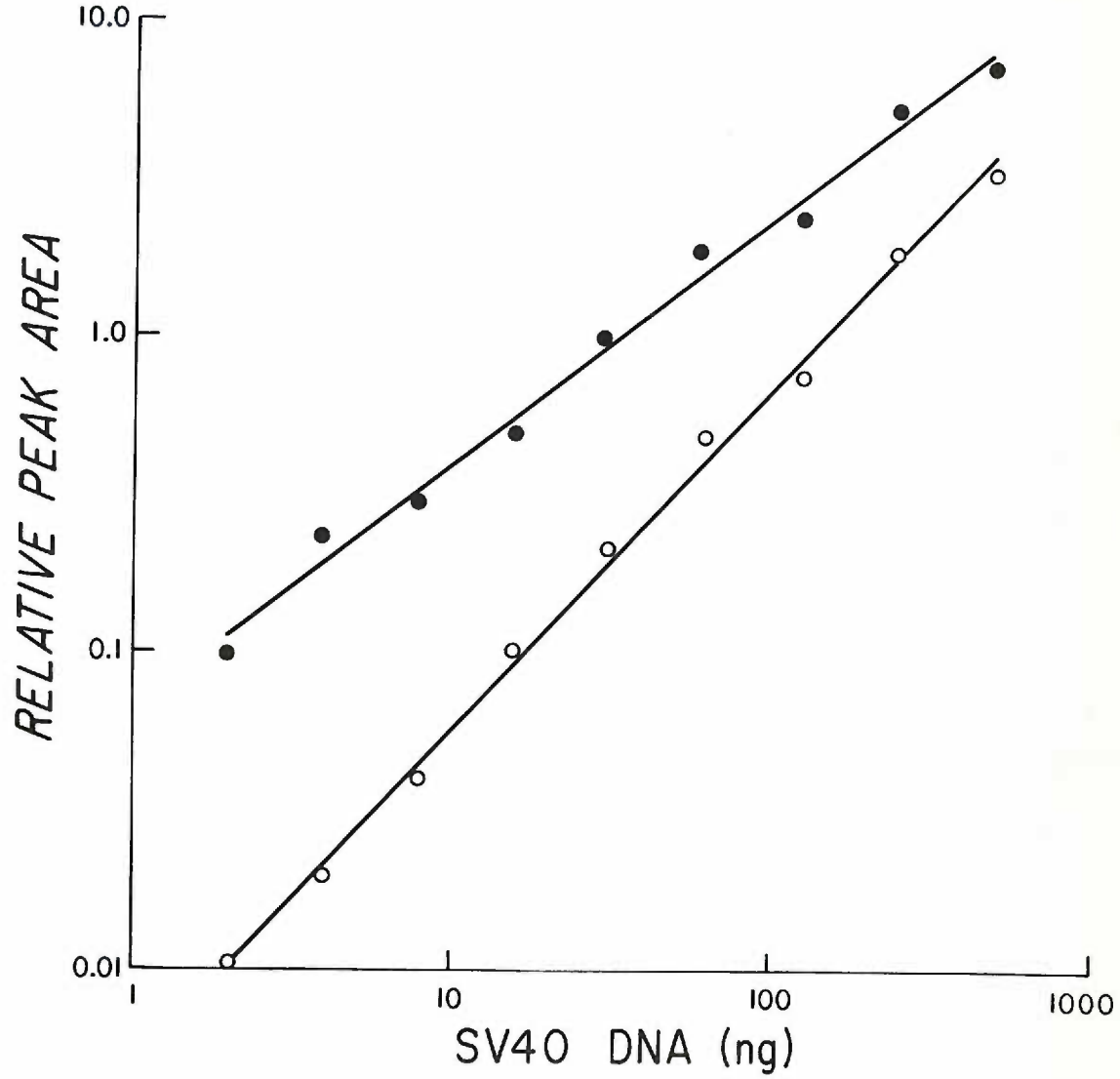
10.0
1.0
0.1
0.01
RELATIVE PEAK AREA
1
10
100
1000
SV40 DNA (ng)

Figure 3. Hind III-Hpa II Cleavage Pattern of SV40 DNA.

The amount of DNA indicated at the top of each lane was digested with Hind III and Hpa II and electrophoresed on a polyacrylamide gel as described in Materials and Methods. An image of the density scale is visible to the right of the gel.

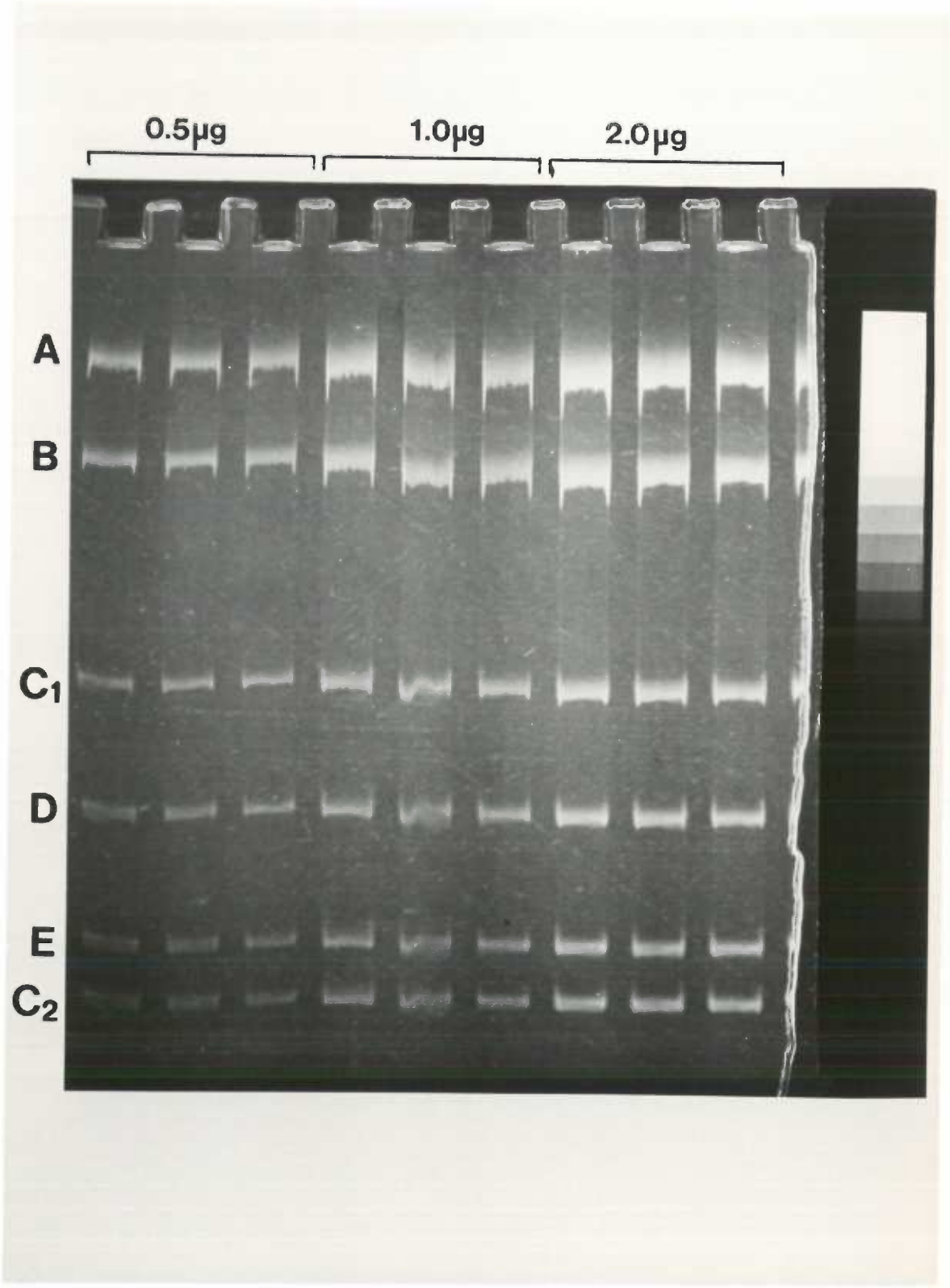
0.5µg
1.0µg
2.0µg
A
B
C1
D
E
C2

# TABLE 1 LEGEND

* Expected based on percentage of the total base pairs determined from the DNA sequence; fragment F was run off the gel during electrophoresis.

+ Determined by procedures described in Methods; averages ± standard errors of the mean are presented that are based on measurements of 17 separate lanes from two polyacrylamide gels. Chi square comparisons between Expected and Photographic or between Expected and Densitometric distributions yielded confidence values of 0.995, 0.950, & 0.990 and 0.975, 0.950 & 0.975, respectively, for 2, 1, & 0.5 µg lanes.

TABLE 1 Comparison of Methods for Fluorescence Quantitation of SV40 Hind III-Hpa II Restriction Fragments

| Fragment | Percent of Total DNA Analyzed | | |
|---|---|---|---|
| 2 µg total (N=5) | Expected* | Photographic+ | Densitometric+ |
| A | 35.2 | 36.1 ± 0.5 | 36.7 ± 0.6 |
| B | 23.3 | 24.0 ± 0.4 | 25.8 ± 0.3 |
| $C_1$ | 13.9 | 12.5 ± 0.3 | 12.6 ± 0.4 |
| D | 10.5 | 9.9 ± 0.1 | 9.8 ± 0.2 |
| E | 8.9 | 8.8 ± 0.4 | 7.9 ± 0.2 |
| $C_2$ | 8.3 | 8.7 ± 0.4 | 7.2 ± 0.3 |
| 1 µg total (N=6) | | | |
| A | 35.2 | 37.8 ± 0.5 | 37.5 ± 0.3 |
| B | 23.3 | 24.9 ± 1.0 | 25.6 ± 0.3 |
| $C_1$ | 13.9 | 11.6 ± 0.2 | 12.3 ± 0.3 |
| D | 10.5 | 9.7 ± 0.1 | 9.9 ± 0.2 |
| E | 8.9 | 8.2 ± 0.4 | 7.6 ± 0.2 |
| $C_2$ | 8.3 | 7.7 ± 0.5 | 7.0 ± 0.3 |
| 0.5 µg total (N=6) | | | |
| A | 35.2 | 37.4 ± 0.7 | 37.3 ± 0.6 |
| B | 23.3 | 23.9 ± 0.3 | 25.1 ± 0.5 |
| $C_1$ | 13.9 | 11.7 ± 0.3 | 12.7 ± 0.6 |
| D | 10.5 | 10.2 ± 0.2 | 10.4 ± 0.3 |
| E | 8.9 | 8.9 ± 0.2 | 7.7 ± 0.5 |
| $C_2$ | 8.3 | 8.0 ± 0.5 | 6.8 ± 0.2 |

TABLE 2 Densitometric Fluorescence Quantitation of pBR322 Hinf I-Eco RI Restriction Fragments

| Fragment 4 µg total (N=5) | Percent of Total DNA Analyzed | |
|---|---|---|
| | Expected* | Densitometric+ |
| A | 23.3 | 22.5 ± 0.4 |
| B | 14.7 | 15.6 ± 0.2 |
| $C_1 + C_2$ | 23.9 | 24.1 ± 0.2 |
| D | 9.2 | 9.2 ± 0.2 |
| E | 8.0 | 8.2 ± 0.1 |
| F | 7.0 | 6.8 ± 0.2 |
| $G_1 + G_2$ | 10.3 | 10.2 ± 0.2 |
| H | 3.6 | 3.4 ± 0.2 |

* Expected based on percentage of the total base pairs determined from the DNA sequence (8); fragment I was run off the gel during electrophoresis.

+ Same as described in Table 1, except that data is based on measurements of 5 double-width lanes from two polyacrylamide gels.

where Y = site I, II or III. From Fig. 4 it can be seen that Bgl I digestion of pBR322 DNA linearized by Bam HI treatment can produce 10 possible fragments, 4 of which are limit digest fragments. Molar amounts for all fragments were determined by scanning the gel, integrating the area under the curve representing each band and dividing by the number of base pairs in that DNA fragment. The numerator for the formula above was then calculated separately for each of the Bgl I sites by using the following summations:

(site I) CD + CDA + CDAB

(site II) CDA + DA + DAB + CDAB

(site III) AB + DAB + CDAB

Thus noncutting at site I (which lies between fragments C and D) will be represented by the molar sum of all fragments generated by a "noncutting" event between C and D. The denominator for the above formula was the same for each of the sites and was calculated by taking the average of the four summations:

C + CD + CDA + CDAB

D + CD + DA + DAB + CDAB

A + AB + CDA + DA + CDAB

B + AB + DAB + CDAB

Each total represents the molar amount of a different limit digest fragment on the gel. These sums should be the same for all fragments since equimolar amounts of each fragment are theoretically present.

The percent of DNA cleaved was obtained by subtracting the calculated % uncut from 100. Formulas similar to those described above could have been used to calculate directly percent DNA cut, but these

Figure 4. Schematic of DNA Fragments Possible following Bgl I Cleavage of Bam HI-linearized pBR322.

Indicated are the four limit (*) and six non-limit digest fragments possible following Bgl I cleavage of Bam HI linearized pBR322. The three cutting sites of Bgl I are designated I, II and III. All DNA fragments are lettered according to the limit digest fragments they contain, and are numbered to indicate base pairs of DNA, so that linear pBR322 is fragment CDAB and contains 4363bp.

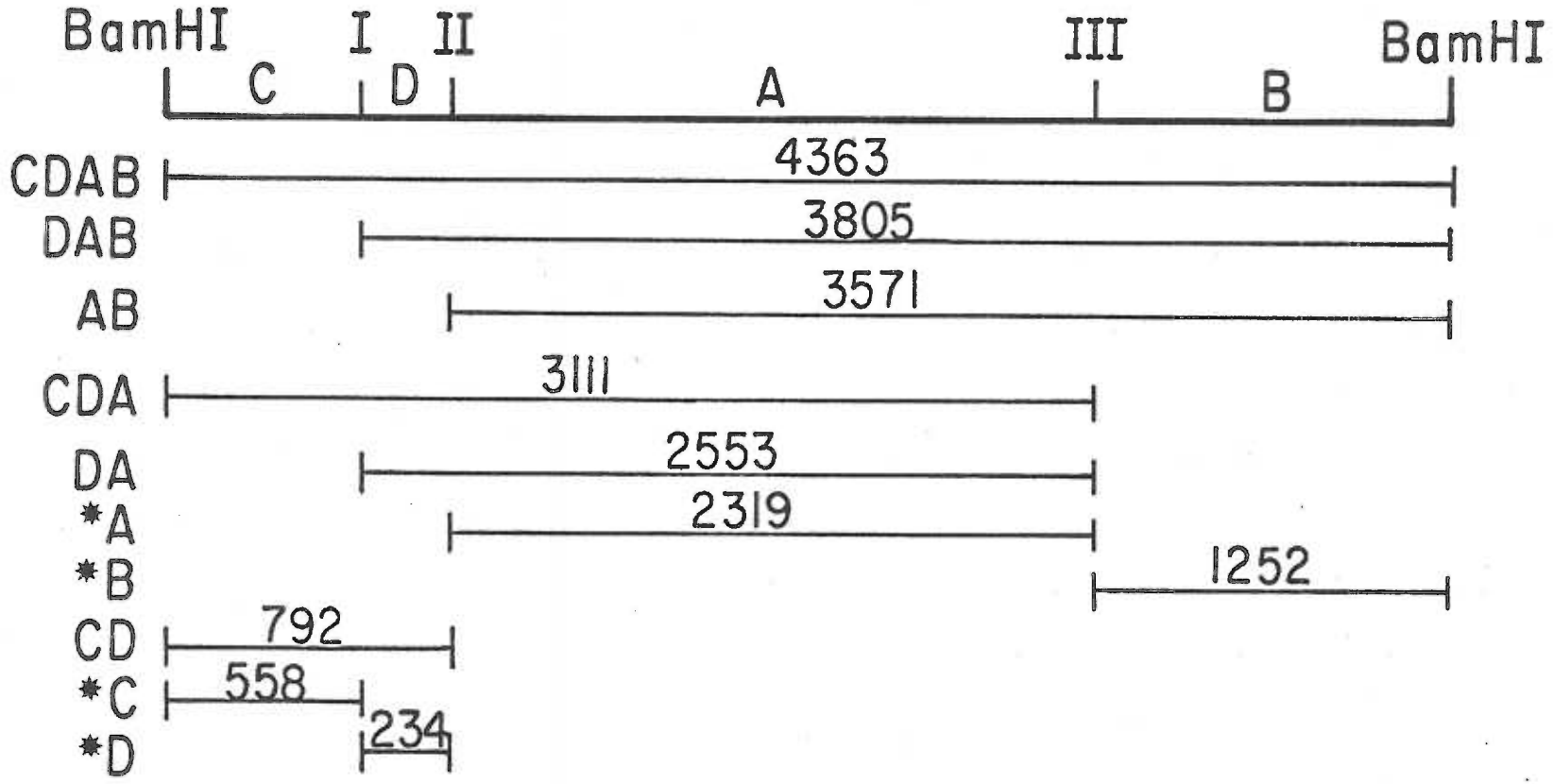
BamHI
I
II
III
BamHI
C
D
A
B
CDAB
4363
DAB
3805
AB
3571
CDA
3111
DA
2553
*A
2319
*B
1252
CD
792
*C
558
*D
234

computations would have depended heavily on information derived from the small DNA fragments (CD, C and D) that are preferentially lost from the gel during electrophoresis.

In the first series of experiments, a large amount of Bam HI linearized pBR322 DNA was cut with an excess of Bgl I. At the time points indicated, small aliquots of the digestion mixture were removed, the reaction was stopped, and these samples were electrophoresed as described in Materials and Methods and shown in Fig. 5. The semi-logarithmic plots of the calculated percent cut values for each site are depicted in Fig. 6. The rate of cutting by Bgl I was practically identical at sites I and II, but slightly faster at site III.

In a second set of experiments we investigated the inhibition of Bgl I cleavage by psoralen photoadducts on the DNA. The reaction conditions and analyses were similar to those described above for the kinetic experiments with non-photoreacted DNA. Samples were prepared with increasing ratios of the psoralen derivative HMT per base pair. Following digestion with Bgl I, the samples were electrophoresed, gels were scanned and the percent of DNA molecules uncut at each site was calculated. As can be seen from Figures 7 and 8, cleavage at all sites was inhibited as the number of psoralen adducts per DNA molecule increased. The rate of inhibition was very similar for sites II and III, but was dramatically higher for site I. In DNA samples with saturating levels of psoralen (1 per 4 base pairs), cleavage at site I was completely blocked, whereas it was only 50% inhibited in sites II and III. To ascertain that complete cutting actually occurred under these digestion conditions, particularly in the samples containing high

Figure 5. Time-course of Bgl I Digestion of Bam HI-linearized pBR322 DNA.

At the times indicated 3µg aliquots of the Bgl I diestion mixture were removed, the reactions terminated, and 1.5µg samples were electrophoresed in duplicate on agarose gels as described in Materials and Methods. The 120 minute sample was a limit digest sample from this reaction. Lettered fragments refer to those of Figure 4.

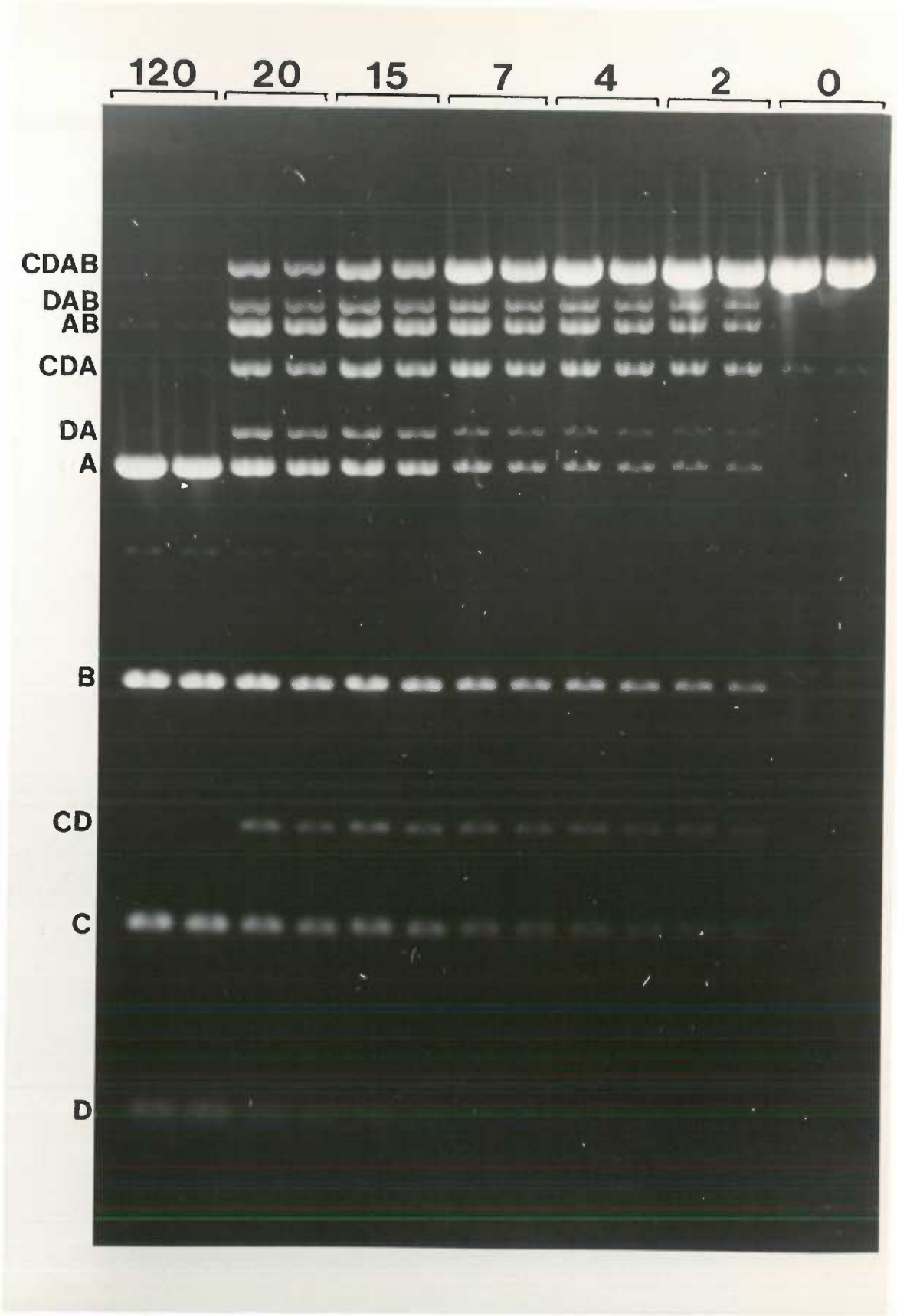
120
20
15
7
4
2
0
CDAB
DAB
AB
CDA
DA
A
B
CD
C
D

Figure 6. Kinetic Analysis of Bgl I Cleavage at the Three Cutting Sites on pBR322 DNA.

The percent of sites uncut by Bgl I at different times was determined by measuring amounts of DNA present in different bands from an agarose gel (Fig. 5) and by applying the formulas described in Results. Bgl I sites I(Δ), II(●), and III(○) are indicated. Points represent averages of two determinations and were fit to the lines by linear regression analysis and had r-values of 0.999, 0.999, and 0.998 respectively.

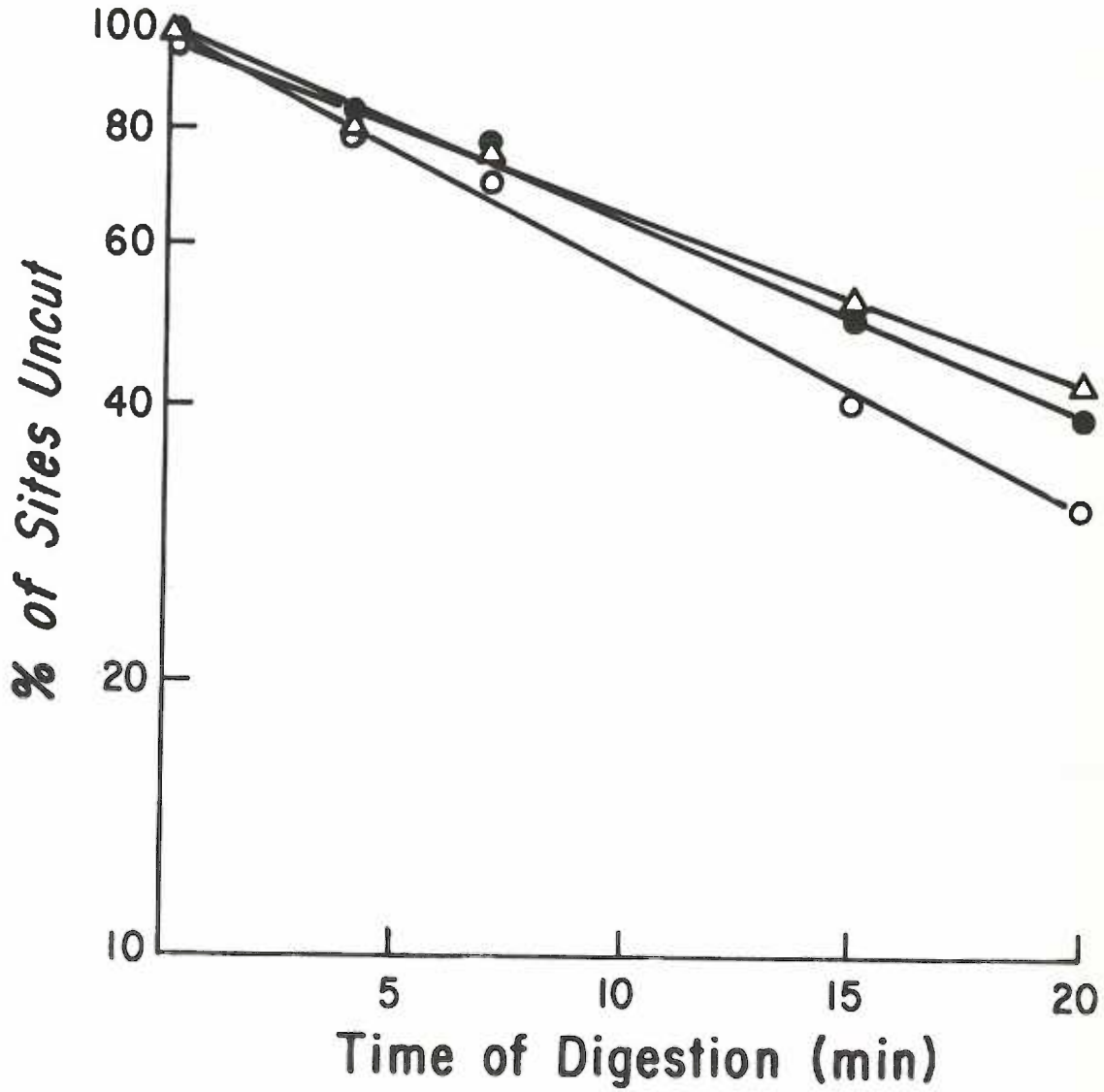
100
80
60
40
20
10
% of Sites Uncut
5
10
15
20
Time of Digestion (min)

Figure 7. Inhibition of Bgl I Cleavage by HMT Photoadducts Present on Bam HI-linearized pBR322 DNA.

Plasmid DNA samples that contained covalently bound HMT to the extent of a)0; b)4; c)8; d)10; e)24; f)42; g)83; h and i)250 molecules per 1000 bp of DNA were exhaustively digested with Bgl I and electrophoresed on agarose gels as described in Materials and Methods. Two samples on non-psoralen reacted pBR322 DNA digested with one-fourth the enzyme used above are also shown (a,j). Lettered fragments refer to those in Fig. 4.

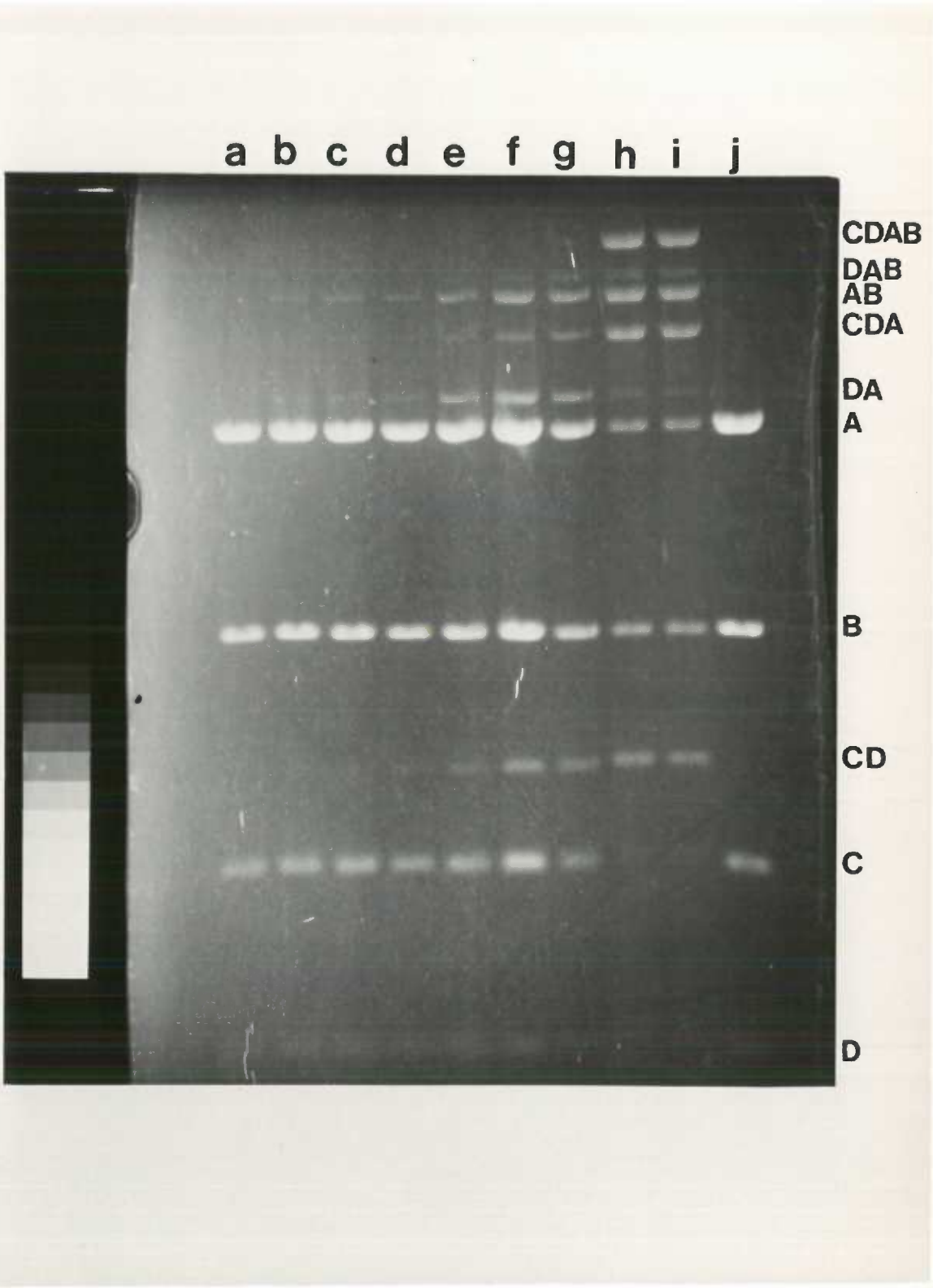
a b c d e f g h i j
CDAB
DAB
AB
CDA
DA
A
B
CD
C
D

Figure 8. Inhibition Profiles for Bgl I Cleavage at the Three Cutting Sites on HMT-photoreacted pBR322 DNA.

Data plotted was that obtained from fluorescence analysis of an agarose gel (Fig. 7) as described in Results. Bgl I sites I (Δ), II(●), and III(O) are indicated. Points were fit to the lines by linear regression analysis and had r-values of 0.999, 0.995, and 0.996 respectively.

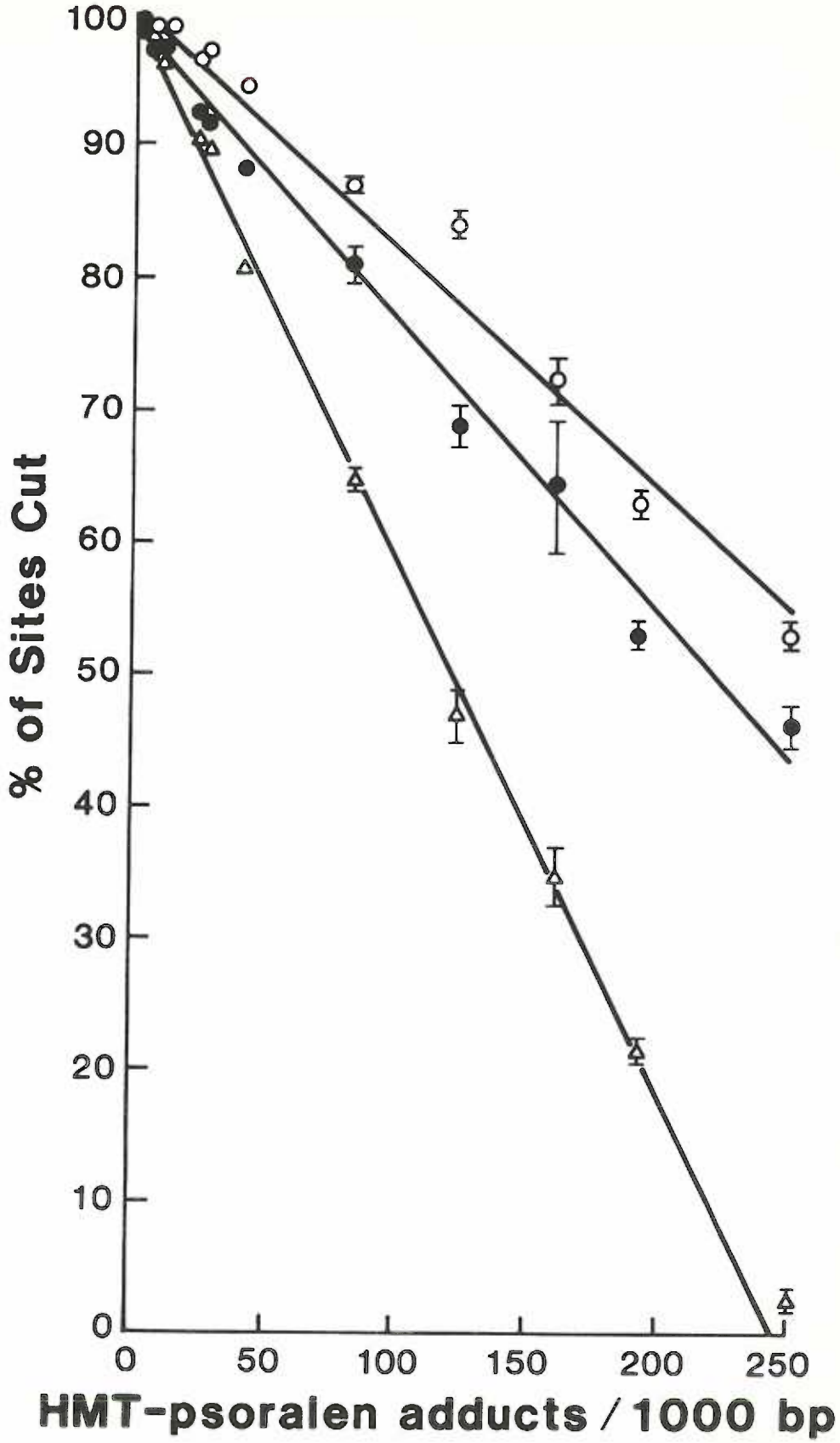
100
90
80
70
60
50
40
30
20
10
0
% of Sites Cut
0
50
100
150
200
250
HMT-psoralen adducts / 1000 bp

levels of psoralen adduct, a control experiment was carried out in which samples of linearized pBR322 containing 1 HMT molecule per or 4 base pairs were reacted with Bgl I for both 3 hours (the normal time of digestion) and 6 hours. When the results were compared it was found that no additional cutting occurred after the first 3 hours (data not shown).

## DISCUSSION

We have employed two different methods for the quantitation of restriction fragments using DNA-enhanced ethidium bromide fluorescence. The physical arrangement of excitation sources, gels, filters, and detectors was remarkably similar in both cases; the major difference was the type of detector employed. Both direct densitometry and photographic quantitation yielded a completely linear relationship between integrated peak area and DNA concentration over a 250-fold range. When a series of restriction fragments were examined, both methods accurately quantitated the distribution of DNA present in gel lanes, with reasonable standard errors. In terms of cost, the photographic method is clearly to be preferred although required items include a scanning absorbance densitometer, sheet film (4 x 5 in) with good response characteristics (not Polaroid film), and a camera capable of using this film. In contrast to Pulleyblank et al.(12), we find it unnecessary to use a quartz tray as a UV diffuser. With the photographic method we initially had difficulty providing enough illumination for the step wedge and recommend using a 300 or 366nm UV transilluminator. By placing layers of a UV absorbant plastic sheet

beneath the gel, but not the step wedge, fluorescence from the gel and step wedge can be brought within the same range. In the direct densitometric method, a densitometer containing fluorescence circuitry, a red-sensitive photomultiplier and quartz tray are all required. The time required for both the actual measurements and the data analysis is of course considerably less in the direct densitometric method. Clearly the choice of which method to employ depends on the specific requirements of each laboratory.

Utilizing the direct fluorescent method for DNA quantitation described above, we have measured the relative cutting by the enzyme Bgl I at the three recognition sites of pBR322. Bam HI pretreatment of the plasmid allows the initial Bgl I cut on the plasmid to be assigned unambiguously to one of the three sites, a feature that would not have been possible if a circular plasmid had been used. In the first experiment we followed the kinetics of cutting for the first 20 minutes of digestion, and found a slight but reproducible preference for cleavage at Site III. Much greater site preferences have been observed by others using the enzymes Pst I on pSM I DNA (1), Eco RI on λ DNA (17), and Hinc II on pBR322 DNA (9) where the cutting ratios of most to least preferred sites were 10, 10, and 4 respectively.

In the second experiment, linearized pBR322 DNA was photoreacted with the psoralen derivative HMT to different levels before exhaustively digesting it with Bgl I. After analyzing the amount of DNA present in different bands it was observed that sites II and III displayed comparable inhibition profiles, whereas site I was more strongly inhibited. Carlson, et. al. (2) have also looked at the effect of psoralen adducts on restriction site inhibition using the psoralen

derivative trimethylpsoralen. They report that the enzyme Hind III is extremely sensitive to low numbers of adducts (approximately 50% inhibition at 5 adducts/1000bp) relative to the enzyme Eco RI, which they claim has average sensitivity compared to other enzymes. In their analysis individual Hind III sites also exhibited different rates of inactivation which were ascribed to variations in the DNA sequences adjacent to the recognition sites. We suggest, however, that the enhanced sensitivity of Bgl I site I is due to sequences within the recognition site, as will be discussed in a following paragraph. We have used much higher levels of psoralen photoaddition in our analysis than those used by Carlson et al. because of the relative resistance of Bgl I cutting to psoralen inhibition. Although quantitative comparisons are problematic given the different psoralen derivatives and labeling conditions used, it is clear that the relative order of sensitivity to psoralen adducts for these three enzymes is: Hind III > Eco RI > Bgl I. This order is surprising because target inactivation theory would predict that the larger (11 bp) Bgl I site would be hit before the smaller (6 bp) Eco RI site. However, psoralen derivatives have been shown to bind to DNA with some sequence specificity. With synthetic DNA polymers the order of preference was determined to be poly d(A-T):poly d(A-T) > poly d(C-G):poly d(C-G) >> poly dA:poly dT ≈ poly dC:poly dG (4). Analyses of nucleotide photoadducts obtained following psoralen reaction with random sequence DNA have shown that greater than 90% of binding occurs with thymine (7, 8, 15), the remainder occurs with cytosine residues. Eco RI has the recognition sequence:

5' GAATTC 3'

3' CTTAAG 5'

The canonical Bgl I recognition sequence and the actual Bgl I sites of pB322 are shown in Table 3. It is apparent that based on thymidine content, the Eco RI site actually represents a larger target than do any Bgl I sites.

Another consideration which is relevant is that Bgl I does not require a specific DNA sequence for the 5 internal bases of its recognition site. It seems possible that an enzyme which requires little uniformity in its recognition sequence may tolerate one psoralen-modified base among these sequences. This could further account for the relative resistance of Bgl I to inhibition.

Target theory is not sufficient to explain the differential psoralen inhibition of the Bgl I sites that we have observed. Instead, a much more interesting interpretation is possible. Both sites II and III have similar inhibition profiles, yet site II has one and site III has two thymidine residues. Sites I and III both contain two thymidine residues at nearly the same location but their inhibition profiles are very different. In the latter situation, the relative DNA strand positions (opposite or same, respectively) of the two thymidines within the recognition site may be very important for determining high frequency intercalation or for the formation of a special type of psoralen adduct. Psoralen cross-links are in fact only favored in the thymidine configuration found in site I (8) where two thymidines are in adjacent and opposite positions. We are currently employing the psoralen derivative, 5-methylangelicin which only forms monoadducts, to explore the possibility that differential inhibition of Bgl I sites is a result of psoralen crosslink formation.

TABLE 3. Nucleotide Sequences Adjacent to Bgl I Sites of pBR322 DNA

| Site Number | Nucleotide Sequence |
|---|---|
| Canonical | 5'-GCCNNNNNGGC-3' |
| | 3'-CGGNNNNNCCG-5' |
| I | GGCCATTATC-GCCGGCATGGC-GGCCGACGCG |
| | CCGGTAATAG-CGGCCGTACCG-CCGGCTGCGC |
| II | GGCGATTTAT-GCCGCCTCGGC-GAGCACATGG |
| | CCGCTAAATA-CGGCGGAGCCG-CTCGTGTACC |
| III | AAACCAGCCA-GCCGGAAGGGC-CGAGCGCAGA |
| | TTTGGTCGGT-CGGCCTTCCCG-GCTCGCGTCT |

REFERENCES

1. Armstrong, K. and Bauer, W. R. (1982). Preferential site-dependent cleavage by restriction endonuclease Pst I. Nucl. Acids Res. 10, 993-1007.

2. Carlson, J. O., Pfenninger, O., Sinden, R. R., Lehman, J. M. and Pettijohn, D. E. (1982). New procedure using a psoralen derivative for analysis of nucleosome associated DNA sequences in chromatin of living cells. Nucl. Acids Res. 10, 2043-2063.

3. Clewell, D. B. (1972). Nature of Col E1 plasmid replication in E. coli in the presence of chloramphenicol. J. Bacteriol. 110, 667-676.

4. Dall'Acqua, F., Terbojevich, M., Marciani, S., Vedaldi, D. and Recher, M. (1978). New chemical aspects of the photoreaction between psoralen and DNA. Chem. Biol. Interact. 21, 103-115.

5. Hirt, B. (1967). Selective extraction of polyoma DNA from infected mouse cell culture. J. Mol. Biol. 26, 365-369.

6. Hoopes, B. C. and McClure, W. R. (1981). Studies on the selectivity of DNA precipitation by spermine. Nucl. Acids. Res. 9, 5493-5504.

7. Kanne, D., Straub, K., Rapoport, H. and Hearst, J. E. (1982). Psoralen-DNA photoreaction. Characterization of the monoaddition products from 8-methoxypsoralen and 4,5',8-trimethylpsoralen. Biochem. 21, 861-871.

8. Kanne, D., Straub, K., Rapoport, H. and Hearst, J. E. (1982). Isolation and characterization of pyrimidine psoralen diadducts from DNA. J. Am. Chem. Soc. 104, 6754-6764.

9. Malcom, A.B.D. and Moffatt, J. R. (1981). Differential reactivities at restriction enzyme sites. Biochim. Biophys. Acta. 655, 128-135.

10. Oliver, S. G. and McLaughlin, C. S. (1977). An apparatus for the fluorescence scanning of ethidium bromide-stained gels. Anal. Biochem. 82, 271-277.

11. Prunell, A. (1980). A photographic method to quantitate DNA in gel electrophoresis., pp. 353-358., in L. Grossman and K. Moldave (eds.), Methods in Enzymology, Vol, 65. Academic Press, N. Y.

12. Pulleyblank, D. E. Shure, M. and Vinograd, J. (1977). The quantitation of fluorescence by photography. Nucl. Acids Res. 4, 1409-1418.

13. Reddy, V. B., Thimmappaya, B., Dahr, R., Subramanian, K. N., Zain, B. S., Pan, J., Ghosh, P. K., Celma, M. L. and Weissman, S. M. (1978). The genome of SV40. Science 200, 494-502.

14. Robinson, G. W. and Hallick, L. M. (1982). Mapping the in vivo arrangement of nucleosomes on SV40 chromatin by the photoaddition of radioactive hydroxymethyltrimethylpsoralen. J. Virol. 41, 78-87.

15. Straub, K., Kanne, D., Hearst, J. E. and Rapoport, H. (1981). Isolation and characterization of pyrimidine-psoralen photoadducts from DNA. J. Am. Chem. Soc. 103, 2347-2355.

16. Sutcliffe, J. G. (1979). Complete nucleotide sequence of the E. coli plasmid pBR322. pp. 77-90., in Cold Spring Harbor Symposia on Quantitative Biology, Vol. XLIII, Cold Spring Harbor Laboratory, N.Y.

17. Thomas, M. and Davis, R. W. (1975). Studies on the cleavage of bacteriophage lambda DNA with Eco RI restriction endonuclease. J. Mol. Biol. 91, 315-328.

## IV. SUMMARY AND DISCUSSION

We have developed a simple non-disruptive method with which to examine the positioning of nucleosomes on intracellular SV40 chromatin complexes. Using radioactive psoralen-labeling we have determined, in agreement with others using complementary in vitro approaches (1-4), that nucleosomes are arranged randomly on the SV40 genome except for a 300-400 base pair region to the late side of the replication origin. This region appeared from our analysis and from those of others to be devoid of nucleosomes, although not necessarily devoid of all bound protein. Electron microscopic analyses demonstrated that only a fraction of the extractable SV40 chromatin possessed this structure (3,4). The nucleosome-free region identified on SV40 spans the replication origin, the tandem T-antigen binding sites, the 5' cap sites for early and late mRNA, and the putative transcriptional control elements (5), making it probable that this structure is involved in viral DNA replication, transcription, or both. Numerous research groups were motivated by this finding to examine various subpopulations of intracellular minichromatin for one that was enriched in molecules possessing this structure. To date none of these efforts have been successful. We chose to examine the structure of SV40 chromatin within the virus particle for several reasons. First, unlike transcribing or replicating minichromosomes, virions were available in quantity during a lytic infection and could be purified to homogeneity. The virion minichromatin also represents the template for viral early transcription and DNA replication in a newly infected cell and might therefore require a highly accessible origin region. Finally, because virions are

permeable to psoralen derivatives (6), the minichromatin within the virus particle could be analyzed by psoralen photoaddition without prior disruption of the capsid. This step is required in analyses of virion minichromatin by nucleases and electron microscopy, and leaves open the possibility of nucleosome rearrangements.

Using the methods developed in Paper 1 we examined the chromatin structure in intact SV40 virions (Paper 2) and found that the nucleosomes were positioned randomly on the virion DNA. We concluded that the "open region" near the SV40 origin was either eliminated during maturation, or that minichromatin molecules lacking this region were preferentially packaged. Consistent with the first hypothesis are results obtained by nuclease digestions of minichromatin from virions or provirions which suggest that in these complexes the nucleosomes have become redistributed on the DNA (7,8). We are currently engaged in a direct test of the two hypotheses using a "psoralen pulse-chase" approach, which will involve photoaddition to intracellular SV40 chromatin followed by isolation of virus and analysis for an "open region."

Our psoralen saturation studies with intact virions (Paper 2 and unpublished electron microscopic data of E. Ostrander and M. Stenzel-Poore) and other studies of SV40 nucleoprotein derived from gently disrupted virions (9, 10) have led to the conclusion that virion "minichromatin" may totally lack normal nucleosomes. When examined directly by electron microscopy the DNA extracted from virions was found to be covered with minibeads of protein and its length was condensed only half as much as SV40 DNA packaged in normal minichromatin (10). Curiously the level of condensation was similar to what has been

observed for actively transcribed rDNA genes from several organisms (11). If this chemically disrupted complex resembles a biologically uncoated virion particle, the overall "accessibility" of this structure may contribute to its efficient transcription in vivo.

Investigation of the nucleosome-free region at the SV40 origin has proceeded rapidly, and it now appears likely that the multiple DNase I hypersensitive sites located there are involved in viral transcriptional control. Very recently, deletion mapping has been employed to define the DNA sequences within this region which are responsible for its nuclease sensitivity (12). These experiments show that no single DNA element (i.e. TATA box, 72bp repeat, 21bp repeat) can totally account for the accessibility of this region. Clearly further work will be required to decipher the confusing picture that currently exists, and to clarify the relationship between "enhancer" sequences and DNase I hypersensitive sites.

As a first step toward the development of a technique for mapping the location of psoralen adducts at the nucleotide level, we examined in Paper 3 the inhibition of the restriction enzyme Bgl I by psoralen photoadducts. Because the recognition site of this enzyme contains a five base-pair neutral region, it was possible to compare the effect of different sequences on this inhibition. The site on pBR322 that contains the sequence most favored for cross-link formation (AT) could be blocked almost completely (98% inhibition) whereas the other two Bgl I sites were inhibited to a lesser extent. These findings give us confidence that it should be possible to find exonucleases that can also be efficiently blocked by psoralen adducts on DNA.

The results in Paper 3 and our experience with other exo- and endonucleases have been used to design and test a procedure for the fine structure mapping of psoralen photoadducts. The procedure shown in Figure 1 is based on a scheme that was previously used to define the locations of pyrimidine dimers and cis-platinum adducts on DNA fragments of known sequence (13). This scheme uses the 3'-specific exonucleolytic action of exonuclease III to degrade unmodified regions of DNA fragments that were $^{32}$P-labeled on one 5'-end. Progressive digestion ceases whenever the exonuclease encounters a modified base. After denaturing the DNA and electrophoresing it on a urea-polyacrylamide sequencing gel, the positions of base modifications can be deduced from the length of incompletely digested fragments (i.e. length = distance from the $^{32}$P-labeled end to the modified base).

In our procedure for mapping psoralen adducts we have started by lightly photoreacting (1 adduct/DNA molecule) a 311bp restriction fragment from the SV40 origin with the psoralen derivative angelicin, which forms monoadducts but not crosslinks (14). Angelicin was employed in these preliminary experiments to facilitate the separation of DNA strands required in a later step of the analysis. A control DNA that is carried through all subsequent steps is irradiated in the absence of drug. Then one or two $^{35}$S-α-phosphorothioate residues are added to each 3' end by a filling-in reaction with DNA polymerase. This has the effect of end-labeling the fragment and also protecting both the 3'-ends from exonuclease III digestion since the α-phosphorothioate bonds are known to resist cleavage (15). A small DNA fragment (27bp) is then removed from one end by digestion with Ava II, giving a 285bp fragment that has only one 3'-end blocked and $^{35}$S-labeled. Finally the large

Figure 1. Procedure for Nucleotide-level Mapping of Psoralen Adducts.

The recombinant plasmid pSV07 is cut with Eco RI, which excises the three tandem copies of the SV40 origin region (0.631-0.691 map units) which are purified free of vector DNA. The 311bp origin fragment is photoreacted with angelicin in the presence of UV light to form psoralen monoadducts on the DNA. The 3'-ends of the fragment are then extended one or two nucleotides by synthesis with Klenow DNA polymerase in the presence of dATP$\alpha^{35}$S (X). One end of the fragment is removed by cutting with Ava II to give an approximately 285bp piece that has only one 3'-end blocked and $^{35}$S-labeled. This 285bp fragment is digested with exonuclease III to give molecules that are shortened at the 3'-end of the unlabeled DNA strand, and terminated by a psoralen-modified base. The SS-tails on the $^{35}$S-labeled DNA strand are removed by S1 digestion. Finally, the DNA is denatured, run on a sequencing gel, treated for fluorography and exposed to X-ray film.

# SV40 Origin DNA (311bp)

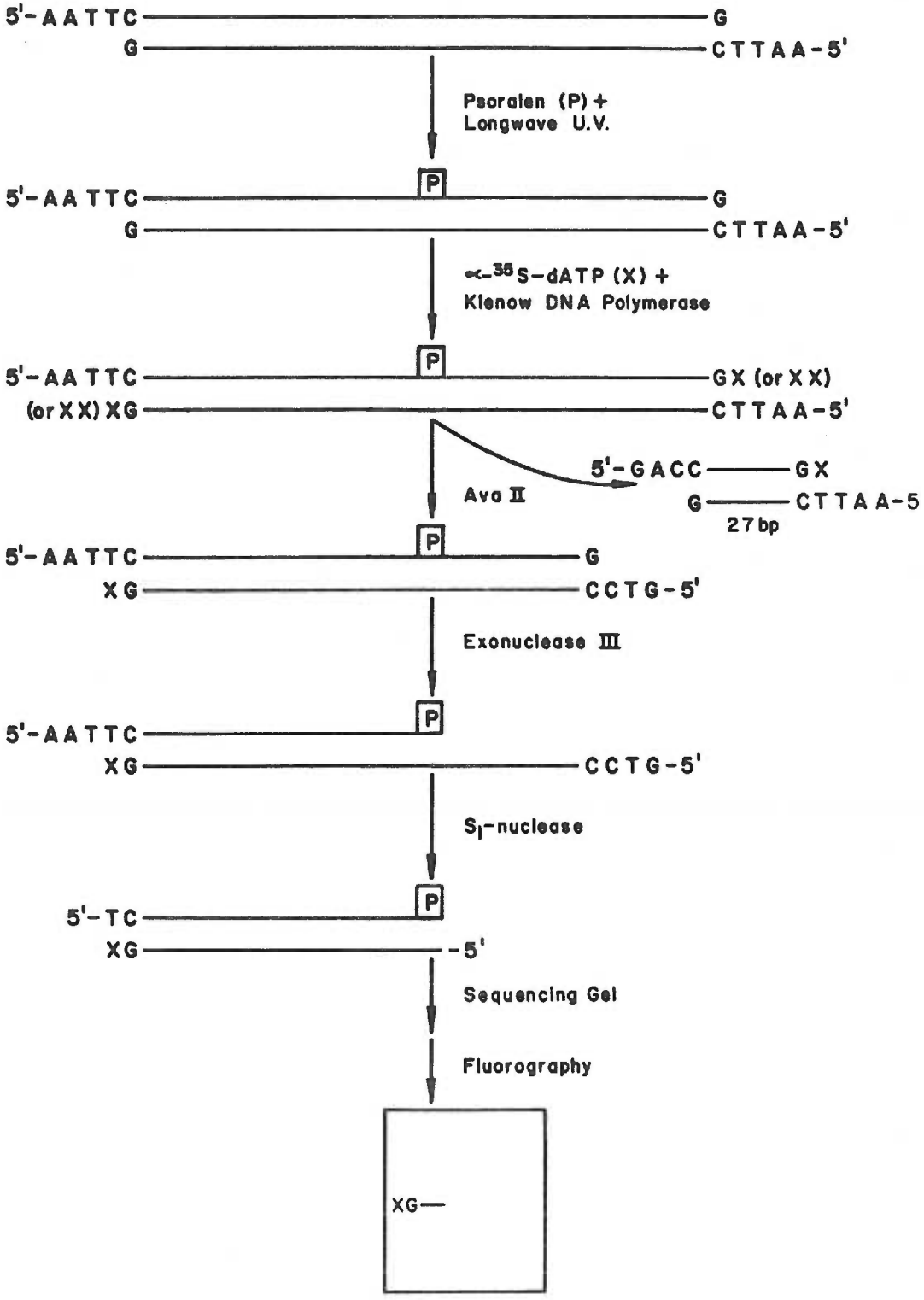

fragment is digested in sequential reactions with exonuclease III and S1-nuclease (to remove single-stranded DNA tails). The resulting DNA fragments (which hopefully have an angelicin adduct on the unlabeled 3' end) are then denatured in formamide buffer, electrophoresed on a sequencing gel, treated for $^{35}S$-fluorography and exposed to X-ray film. An example of such an experiment is shown in Figure 2.

As is apparent from the figure, angelicin-treated DNA remains of high molecular weight following exonuclease III digestion. Unfortunately, exonuclease III shows many artifactual terminations or pauses on the control DNA which are not eliminated by adding more enzyme (from 5 to 50 units). The apparent width of the bands in the angelicin treated but not the control lanes is actually due to the presence of "half-bands" that result from bound angelicin adducts:

$$\frac{\text{MW angelicin}}{\text{MW nucleotide}} = \frac{172}{326} = 0.53.$$

This interpretation is strongly supported by the finding of "half-bands" in the size markers, which were generated by Bgl I and Hind III restriction enzyme cleavage of $^{35}S$- labeled 311 bp DNA previously reacted with angelicin. We believe that the "82b" marker bands correspond to fragments bearing 0, 1, and 2 (light upper band) angelicin adducts. We have repeated the above experiments under a variety of exonuclease III and S1 conditions and have been able to visualize, upon longer exposure, bands and "half-bands" in the angelicin treated samples, particularly in the region of the gel separating fragments from 30-80 nucleotides in length. However, the background band pattern in the unreacted DNA is too great to analyze the preferred fragments in the angelicin reacted samples.

Figure 2. Fluorogram of $^{35}$S-labeled, Exonuclease III-Resistant DNA Fragments

$^{35}$S-labeled 285bp DNA fragments digested sequentially with exonuclease III (5 to 50 units) and S1 nuclease as described in Figure 1 were denatured and electrophoresed on 8.3M urea-polyacrylamide gels. Gels were then fixed in 5% TCA, soaked in Enhance, dried, and exposed to X-ray film for 2.5 days. Lanes containing angelicin-photoreacted DNA (Ps) and control DNA (C) irradiated in the absence of angelicin are indicated. Molecular weight markers (M) were produced from $^{35}$S-DNA photoreacted with angelicin, then digested with Hind III and Bgl I (in separate reactions). $^{35}$S-labeled fragments with 5'-ends terminating in the "TATA" box and 21 bp repeat sequences are bracketed.

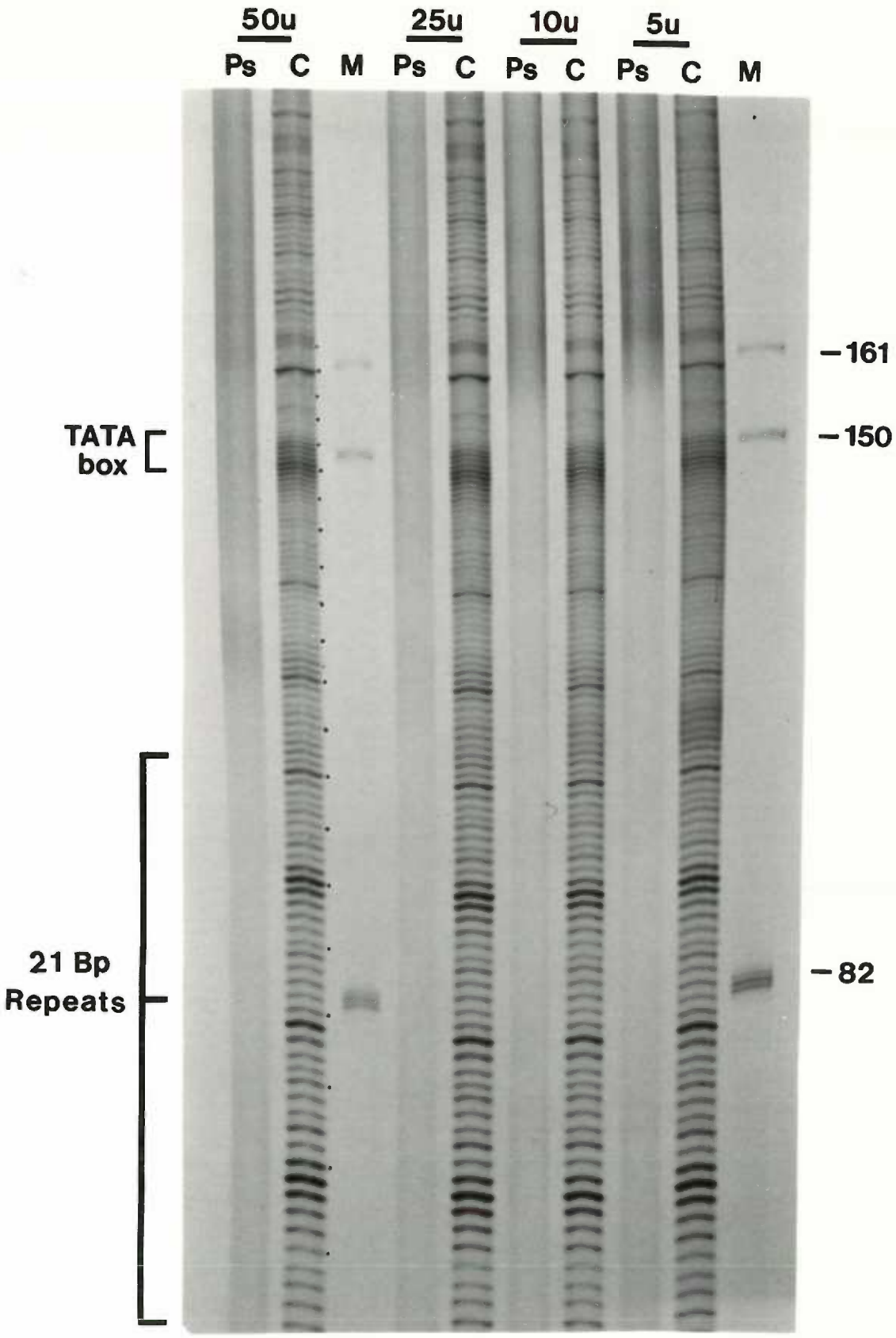
50u
25u
10u
5u
Ps
C
M
Ps
C
Ps
C
Ps
C
M
TATA box
21 Bp Repeats
161
150
82

Although the mapping experiments to date have not been totally successful, we feel that with slight modifications the procedure outlined will allow us to map psoralen adducts to the nucleotide in the near future. Very recent results (E. Ostrander, personal communication) have shown that 5-methylangelicin (which forms only monoadducts) does not inhibit Bgl I restriction endonuclease in the system described in Paper 3. Although there may be differences between the effects of psoralen monoadducts on inhibition of an endonuclease (Bgl I) and an exonuclease (exonuclease III) it would probably be wise to switch to an alternative derivative in future mapping experiments. In addition, the 3'-exonucleolytic activity of T4 DNA polymerase appears less inclined to "pause" on the control DNA, and may be a more suitable enzyme for these experiments. A psoralen mapping technique will dramatically expand the range of experiments that are feasible with psoralens. In particular it should enable the sequence-specificity of psoralen photoreactions to be determined in greater detail than is currently possible. Finally, it should be possible to look for "psoralen-hypersensitive" sites on SV40 chromatin or next to cellular genes for which a cloned probe is available.

REFERENCES

1. Scott, W. A. and Wigmore, D. J. (1978). Sites in SV40 chromatin which are preferentially cleaved by endonucleases. Cell 15, 1511-1518.

2. Varshavsky, A. J., Sundin, O. and Bohn, M. (1979). A stretch of late SV40 viral DNA about 400 bp long which includes the origin of replication is specifically exposed in SV40 minichromosomes. Cell 16, 453-466.

3. Jakobavits, E. B., Bratosin, S. and Aloni, Y. (1980). A nucleosome-free region in SV40 minichromosomes. Nature (London) 285, 263-265.

4. Saragosti, S., Moyne, G. and Yaniv, M. (1980). Absence of nucleosomes in a fraction of SV40 chromatin between the origin of replication and the region coding for the late leader RNA. Cell 20, 65-73.

5. DePamphilis, M. L. and Wassarman, P. M. (1982). Organization and replication of papovavirus DNA., pp. 37-114., in A. S. Kaplan (ed.), Organization and Replication of Viral DNA, CRC Press, Boca Raton, Fl.

6. Hallick, L. M., Yokota, H. A., Bartholomew, J. C. and Hearst, J. E. (1978). Photochemical addition of the cross-linking reagent 4,5',8-trimethylpsoralen (trioxalen) to intracellular and viral SV40 DNA-histone complexes. J. Virol. 27, 127-135.

7. Hartmann, J. P. and Scott, W. A. (1981). Distribution of DNase I-sensitive sites in SV40 nucleoprotein complexes from disrupted virus particles. J. Virol. 37, 908-915.

8. Coca-Prados, M., Yu, H. Y.-H. and Hsu, M-T. (1982). Intracellular forms of SV40 nucleoprotein complexes. IV. Micrococcal nuclease digestion. J. Virol. 44, 603-609.

9. Brady, J., Radonovich, M., Lavialle, C. and Salzman, N. P. (1981). SV40 maturation: Chromatin modifications increase the accessibility of viral DNA to nuclease and RNA polymerase. J. Virol. 39, 603-611.

10. Moyne, G., Harper, F., Saragosti, S. and Yaniv, M. (1982). Absence of nucleosomes in a histone-containing nucleoprotein complex obtained by dissociation of purified SV40 virions. Cell 30, 123-130.

11. Lewin, B. (1980). Chromatin under transcription, pp. 404-408., in B. Lewin (ed.), Gene Expression 2: Eucaryotic Chromosomes, 2nd ed., John Wiley, and Sons, N.Y.

12. Gerard, R. D., Woodworth-Gutai, M. and Scott, W. A. (1982). Deletion mutants which affect the nuclease-sensitive site in SV40 chromatin. Mol. Cell Biol. 2, 782-788.

13. Royer-Pokora, B., Gordon, L. K. and Haseltine, W. A. (1981). Use of exonuclease III to determine the site of stable lesions in defined sequences of DNA: the cyclobutane pyrimidine dimer and cis and trans dichlorodiammine platinum II examples. Nucl. Acids Res. 9, 4595-4609.

14. Bordin, F., Marciani, S., Baccichetti, F., Dall'Aqua, F. and Rodighiero, G. (1975). Studies on the photosensitizing properties of angelicin, an angular furocoumarin forming only monofunctional adducts with the pyrimidine bases of DNA. Ital. J. Biochem. 24, 258-267.

15. Putney, S. D. Benkovic, S. J. and Schimmel, P. R. (1981). A DNA fragment with an α-phosphorothioate nucleotide at one end is asymmetrically blocked from digestion by exonuclease III and can be replicated in vivo. Proc. Natl. Acad. Sci. U.S.A. 78, 7350-7354.

## V. ACKNOWLEDGEMENTS

I would like to express my sincere appreciation to my thesis advisor, Dr. Lesley M. Hallick, for the excellent direction she has provided throughout the work on this thesis. Her friendship and encouragement during the past four and a half years has helped make the effort enjoyable.

I would also like to acknowledge the collaboration of my co-workers, Sophia Kondoleon and Elaine Ostrander in carrying out the experiments described in this thesis. My gratitude to numerous laboratories in the Biochemistry and Microbiology departments for use of special equipment is acknowledged. I also thank James Fendrick for preparing the excellent graphics and Elaine Ostrander for typing this thesis.

Thanks to all my bench-buddies, Sophia Kondoleon, Elaine Ostrander, James Fendrick, Mary Stenzel-Poore, Peter Stenzel, and Gary Wiesehahn for their interest and friendship. A special thank you goes to Chuck Faust for his friendship and willingness to act as my alternate advisor on many occasions.

To the punkins-of-my-heart, Marilyn and Will, I owe a special debt for their love, support, and perspective during these years of graduate work. Finally, I thank my parents for their faith and generosity.

DONALD A ROBINSON
2301 St. Clair, Brentwood, MO 63144
(314) 962-8045

February 26, 1983

Dear Marilyn & Gordon,

Some day not far away you'll look at each other and say "well, by gum, that's it!" Then that evening or the next you'll want to go out to dinner at a nice place, have a drink, a good steak, a bottle of wine from your new home state--maybe a Robert Mondavi, etc.

I wish it were possible for us to join you on this occasion, but we'd like to help pick up the check, hence the attached.

We're very proud of our Portland family.

Regards and Congratulations,

Don R. + Kathy

Kathy & Don R.